



MAG2POL

Navid Qureshi, ILL 2016 - 2026

USER MANUAL

Version 8.0

Navid Qureshi
Institut Laue-Langevin



Contents

1	Preface	1
1.1	About the program	1
1.2	Purpose of the program	1
1.3	Disclaimer	1
2	Getting started	3
2.1	Installation	3
2.1.1	Windows	3
2.1.2	MacOS	3
2.1.3	Linux	3
2.2	Setting up a structure model	3
2.3	Visualizing crystal and magnetic structures	9
2.4	Atom and spin info	10
2.5	Bonds and polyhedra	11
2.6	Rigid bodies	12
2.6.1	Creating a rigid body model	12
2.6.2	Boundaries and constraints	14
2.6.3	Model vs. instance vs. fit instance	15
2.7	Saving and loading input files	16
2.8	Calculation of structure factors and polarization matrices	17
3	Further parameters	19
3.1	Global settings	19
3.1.1	General	19

3.1.2	Refinement	20
3.1.3	Plot	20
3.1.4	Labels	21
3.1.5	Render	21
3.2	Scale factor and $\lambda/2$ contamination	22
3.3	Extinction	22
3.4	Domains and twins	24
3.5	X-ray and magnetic form factors	26
3.5.1	Built-in form factors	26
3.5.2	User-defined form factors	27
3.6	User-defined basis vectors	29
3.7	Mixed irreducible representations	30
3.8	Magnetic form factor models	30
3.8.1	Sum of radial integrals	31
3.8.2	Multipole expansion	31
3.8.3	Orbital expansion	33
3.9	Orientation matrix	33
3.10	Instrument	36
4	Fitting	39
4.1	Loading raw data	39
4.2	Absorption correction	44
4.2.1	Simple sample shapes	44
4.2.2	Special sample shape	44
4.2.3	On-the-fly absorption correction	48
4.3	Correction for the spin-filter efficiency	50
4.4	Refinement flags and constraints	52
4.5	Powder patterns	57
4.5.1	Plot controls	57
4.5.2	Geometry	58
4.5.2.1	Instrument resolution function (IRF)	58

4.5.3	Background	60
4.5.4	Excluded regions	61
4.5.5	Pattern and phase parameters	61
4.5.6	Constraints	63
4.6	Refinement and results	63
4.7	Batch fitting	67
4.7.1	Single-pattern	67
4.7.2	Multipattern batch fitting	69
4.8	Fit macros	70
5	Reflection lists, powder patterns and maps	75
5.1	Reflection lists	75
5.2	Intensity maps	75
5.3	Powder pattern	76
5.4	Magnetization density maps	80
6	Tools	83
6.1	Sample information	83
6.2	Space group tables	84
6.2.1	Space group transformations	85
6.2.2	Magnetic space group transformations	87
6.2.3	Magnetic superspace group transformations	89
6.3	Data converter	90
6.4	Irreducible representations	92
6.5	Spin correlations	96
6.6	Multi- \mathbf{q} magnetic structures	97
6.7	L ^A T _E X export	98
6.8	Pattern editor	99
6.9	Indexation of powder patterns	101
6.10	Propagation vector finder	104
6.11	Guides to the eye	108

6.12	Phase transitions	109
6.13	Crystal calculator	111
6.14	Cell animation	113
6.15	Bond distances	114
6.16	Polarization matrix plot	116
7	Mathematical information	119
7.1	Basic equations	119
7.2	Polarization matrices	120
7.3	Flipping ratios	122
7.4	Multipoles	123
7.5	Orbitals	124
7.6	Spin correlations	125
7.7	Powder patterns	126
7.7.1	Calculated profile	126
7.7.1.1	Lorentz and polarisation factor	127
7.7.1.2	Asymmetry	127
7.7.1.3	Preferred orientation	127
7.7.1.4	Absorption and extinction	128
7.7.1.5	Profile functions	130
7.7.1.6	Offsets / Time of flight	135
7.7.1.7	Background	136
7.7.1.8	Size/strain broadening and microstructure analysis	137
7.8	Local susceptibility tensor	137
7.9	Standard deviations and agreement factors	138
	Bibliography	141

1 Preface

1.1 About the program

The MAG2POL source code is entirely written in C++ and can be downloaded in compiled form for the main platforms Windows, MacOS and Linux. The program is based on the Qt5, QCustomPlot, Eigen and OpenGL libraries.

1.2 Purpose of the program

MAG2POL was developed to supply an easy-to-use tool for analyzing spherical neutron polarimetry data obtained from single-crystal neutron scattering experiments using the Cryogenic Polarization Analysis Device (CRYOPAD). In addition it can treat flipping ratios in combination with a multipole expansion of the magnetic form factor. The analysis of nuclear and magnetic structures based on integrated intensities is of course also possible. Since version 2.4 multiple-wavelength integrated intensity data as well as X-ray data can be treated. Version 2.4.1 introduces the calculation of Schwinger scattering flipping ratios. Rietveld refinement of powder data was introduced in version 4.0. The refinement of nuclear/magnetic structures to time-of-flight data was introduced for powders and single crystals in versions 5.0 and 8.0, respectively.

Crystal and magnetic structure models can easily be introduced via the graphical user interface (the latter also with the help of the Irreducible Representation and Space Group Tables tool) and viewed in 3D in an OPENGL widget. Those models can then be refined to experimental data within a least-squares refinement. Hereby, spherical neutron polarimetry data, integrated intensities from a standard single-crystal diffraction experiment and powder/x-ray diffraction data can be simultaneously analyzed in any combination.

1.3 Disclaimer

MAG2POL is distributed under the GNU Lesser General Public License v. 3 (LGPLv3). The complete Qt5 source code of the used Qt5 libraries can be downloaded from the MAG2POL download page (note that the original code was not modified). The program

1 Preface

is distributed with dynamically linked libraries which can be rebuilt by the user, if they wish to use a different Qt version. A copy of the LGPL license text can be viewed in the *About* window accessible from the main menu.

2 Getting started

2.1 Installation

2.1.1 Windows

In order to run under Windows Qt5 depends on Microsoft Visual Studio. The Visual Studio Redistributable Packages are included in the download of MAG2POL and have to be installed by running `vc_redist_x64.exe`. Afterwards, MAG2POL can be started from its executable, which should stay in its folder with all necessary libraries.

2.1.2 MacOS

Open the downloaded `dmg` image and drag the application to your Applications folder or directly download MAG2POL from the Mac App Store. Once the prompt appears saying that the application cannot be opened (after the first attempt of starting the application downloaded from the MAG2POL website), cancel it and launch *System Preferences*. Navigate to the *Security & Privacy* section, and under the *General* tab you'll see the blocked program. Simply click *Open Anyway* to launch it.

2.1.3 Linux

- AppImage (only 64 bit Linux versions)

Download and launch the AppImage.

- Debian package (only up to MAG2POL version 3.0)

Download `gdebi` from a terminal by typing `sudo apt-get install gdebi`. Then install the debian package with `sudo gdebi mag2pol_3.0.0-1.amd64.deb`, which will download the necessary libraries from the internet. Start the program by typing `Mag2Pol`.

2.2 Setting up a structure model

The main window contains a toolbar for the most frequently used menu entries and dockable widgets, which can be reorganized to one's individual taste. Moving a widget on top

of another will automatically create a tab widget and single tabs can be extracted to form new widgets. All the settings related to the toolbar and the dock widgets can be found in the *View* menu. Six different presets of different window dispositions can be accessed with the shortcuts CTRL/CMD + 1-6. Note that the exact position and size of the individual widgets are saved, when the program is closed and restored at the next start.

The first step for a meaningful use of MAG2POL is the parametrization of a nuclear and eventually magnetic structure model in the main window. This is done in the tab widget on the upper left part of the main window, when MAG2POL starts up (shown in red in Fig. 2.1) or by loading a *.cif or *.mcif file.

The crystallographic space group (CSG) of the underlying nuclear structure has to be entered in Hermann-Mauguin notation in the corresponding field under the *Symmetry* tab. It is also possible to enter a magnetic space group (MSG) or a magnetic superspace group (MSSG), see also Sec. 6.2 for more information about space groups. Note that all information related to MSGs and MSSGs is based on the tables available at the ISOTROPY SOFTWARE SUITE [1], and in particular ISO-MAG [2] and ISO(3+D)D [3–6]. The entry of a CSG, MSG or MSSG is case dependent, i.e. the first letter should be upper case and any following letters lower case. Eventual additional spaces will be removed. Note that for MSGs and MSSGs lower-case symbols need to be preceded by an underscore (e.g. $P2_1'$ in order to distinguish $P2_1'$ from $P21'$) in order to avoid ambiguity, while this is not necessary for CSG. For MSGs having the same label as a CSG an underscore should be added (e.g. $Pmna_.$ for the MSG and $Pmna$ for the CSG). The symbol will be shown in green, if the space group has been recognized, and in red in the contrary case. In the case of CSGs, all alternative monoclinic settings are included as well as space groups with different origin choices or trigonal space groups with different axes settings (hexagonal or rhombohedral). For MSGs and MSSGs the following conventions are chosen by default: monoclinic unique axis b , monoclinic cell choice 1, hexagonal axes for trigonal groups and origin choice 2 for groups with more than one origin choice. Alternatively, the space group can be entered by its number or its numerical label in case of a MSG or MSSG. If the entry is followed by # the numerical entry will be replaced by the space group label (e.g. 139# for space group $I4/mmm$). Note that an MSG or MSSG can be changed and the structure regenerated even while refining a magnetic structure in the fit window as long as the atomic positions remain the same (i.e. the parent CSG needs to be the same, e.g. a change from $Pnm'a$ to $Pn'ma'$). This allows for a quick testing of different magnetic models.

If an entered CSG has origin or axes setting choices a combo box will appear next to the space group field, in which the corresponding choice can be entered. For cell transformations the *Space group tables* tool has to be used (see Sec. 6.2).

The lattice parameters should be given in Ångströms and degrees. If a CSG was entered

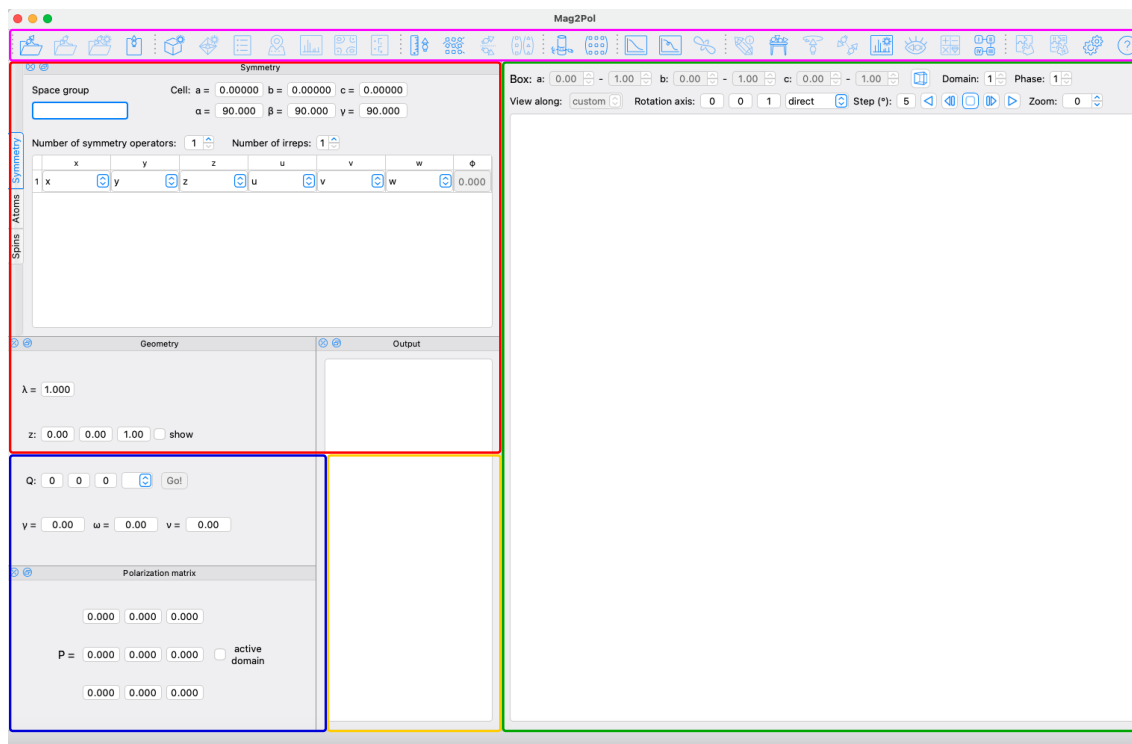


Figure 2.1: MAG2POL main window at the program start (in the *Compact 1* preset). The cyan box shows the toolbar from which most of the menu entries can be triggered. The crystal and magnetic structure information are entered in the tab widget marked by the red box. The green box contains the OpenGL widget for the 3D visualization of the nuclear and magnetic structure and the drawing box given in relative lattice coordinates. The blue box is devoted to the experimental geometry including wavelength and sample orientation. Individual calculations for a given (hkl) reflection can be triggered from here. The calculated angles corresponding to the instrument geometry are shown in the respective boxes. The results of the calculations (nuclear/magnetic structure factors, flipping ratios, etc.) are shown in the orange output box.

the magnetic symmetry can be given manually by a number of symmetry operators (generators) which can be constructed from the drop-down menus. It is also possible to use the smart copy-paste feature, i.e. copy the text corresponding to a symmetry operator (e.g. in the *Irreducible representations* or *Space group tables* windows) and paste it into the symmetry table of the main window by right-clicking the vertical header number (starting from the second row, since the first operator is always the identity). The first part featuring xyz refers to the symmetry operator which is applied to the atomic position, whereas the second part featuring uvw is the corresponding symmetry operation acting on the magnetic moment. Each symmetry operator can be combined with a magnetic phase. Note that the magnetic symmetry can be obtained from calculating the irreducible representations through the menu item *Generate→Irreducible representations* (see Sec. 6.4). In that case it is not necessary to enter the magnetic symmetry operators by hand. Similarly, the use of a MSG or MSSG will automatically set the magnetic symmetry. MAG2POL supports the loading of *.mcif files for MSGs and MSSGs together with the appropriate transformations.

Under the tab *Atoms* the different sites can be entered by adjusting the corresponding number. Each site needs an atom label which corresponds to the element symbol in case of a purely nuclear scatterer. For a magnetic atom, the label starts with an M or J followed by the element symbol and the oxidation state, e.g. MCo3 or JHo3. The M refers to the magnetic form factor containing only spherical Bessel functions $\langle j_0 \rangle$, while J denotes a magnetic form factor of rare-earth elements approximating $\langle j_0 \rangle + c_2 \langle j_2 \rangle$. For the calculation of Schwinger flipping ratios the exact x-ray form factor is needed for which the oxidation state should be given as e.g. Co2 for a non-magnetic atom. Contrarily to the space group symbol, the entry is case independent, however, no spaces can be used.

The atomic positions should be entered as fractional coordinates, where fractions like $1/3$ or $2/3$ need to be rounded to the 5th digit, i.e. 0.33333 or 0.66667, respectively. It is also possible to right-click the atom label in order to choose from the list of Wyckoff sites and respective positions within the given space group. If the atomic position is already entered, the occupied Wyckoff site will be shown in bold and can be converted to any other position within this list.

An isotropic temperature factor B and an occupation factor (1 for a fully occupied site) can be entered for each site. Anisotropic temperature factors can be chosen by right-clicking the isotropic value, which opens a pop-up menu for activating and setting the values. Depending on the site symmetry certain entries of the anisotropic temperature tensor may be 0 or constrained. In MAG2POL this is handled automatically by determin-

ing the site-symmetry group. As stated in [7] one should choose the first atomic position of an equivalent set given in the International Tables Vol. A [8] in order to obtain the correct restrictions. When the tensor is the zero matrix it will be initialized as isotropic according to the isotropic temperature factor following [9]. The inverse operation is also possible: the isotropic temperature factor can be set as an *equivalent* one from the anisotropic tensor by evoking the previously mentioned pop-up menu. Anisotropic displacement ellipsoids can be visualized in the unit cell by checking the corresponding checkbox in the settings menu (see [this](#) demo video).

If a magnetic ion has been recognized, it will be displayed in the *Spins* tab, where its complex Fourier components and a phase factor can be entered (in the case of user-defined basis vectors or basis vectors of irreducible representations or magnetic (super) space groups, the coefficients of those basis vectors should be entered here, see Sec. 3.6 and Sec. 6.4). When a CSG and no basis vectors are used, the description of the complex Fourier components can be switched between Cartesian and spherical coordinates, by right-clicking the *Spin* header in the spin table. For analyzing flipping ratio data it is convenient to set the magnetic moments parallel to the applied magnetic field direction (typically the vertical diffractometer axis) which can be done by right-clicking the *z* label in the *Geometry* window and selecting *set moments parallel*. Note that this automatically adds the generators of the used CSG as magnetic symmetry operators in order to generate the magnetic unit cell with parallel spins.

It is also possible to describe the magnetic moments using the local susceptibility approach [10], for which the 6 entries of a symmetric anisotropic tensor (see Sec. 7.8) need to be given together with the magnetic field value (the direction of the field is the vertical direction of the diffractometer, either given by the orientation matrix or the *z* axis shown in the *Geometry* window). Site symmetry relations between the tensor coefficients are automatically set depending on the point symmetry. Note that the local susceptibility ellipsoids need to be activated as plot objects in the settings menu.

In addition to the magnetic moment coefficients, the propagation vector can be entered in the *Spins* tab, which relates the translational symmetry of the magnetic cell to the nuclear one. The checkbox $+q \neq -q$ is automatically set when the propagation vector or the space group is changed. It should be activated, when $\mathbf{q} - (-\mathbf{q})$ does not correspond to a vector of the reciprocal lattice. The automatic setting can always be overridden, e.g. if the reflections were measured with a component 0.501 which in fact should be commensurate. The propagation vector can also be set by right-clicking the *Propagation vector: q =* label which opens a context menu. Under the menu entry *Brillouin zone*

label all symmetry-inequivalent propagation vectors—with respect to the currently used space group—and their labels are listed from which one can be chosen by clicking it. The label of the currently active propagation vector is shown in italic and is only updated after re-generating the structure. Note that the labels are given with respect to the standard space group setting, i.e. the effect of an eventual basis transformation on the propagation vector is not taken into account.

A generated crystal structure can be converted to any of its maximal non-isomorphic subgroups of type I (translationengleich), IIa (klassengleich, loss of centering translations), IIb (klassengleich, enlarged unit cell) or maximal isomorphic subgroups of type IIc (klassengleich, enlarged unit cell). This can be achieved by right-clicking the label *Space group* and selecting the appropriate subgroup from the context menu. The eventual basis transformation and splitting of atomic positions will be applied automatically. Any structure (except *P1*) can directly be converted to space group *P1* by selecting *convert to P1* from the context menu. This will add all atoms (formerly generated by the space group symmetry) to the list in the *Atoms* tab, which can be useful if one wants to treat the nuclear/magnetic structure without symmetry constraints. If a structure is already expressed in *P1* symmetry, an additional menu entry *create supercell* is visible in the context menu. When clicked, the supercell can be given in the form of $n_a \times n_b \times n_c$ (note that the \times are optional, spaces work as well), which will then be applied to the lattice parameters and to all atomic positions.

It is possible to set up multiple phases. When treating single-crystal data, this feature can be useful in the presence of co-existing magnetic structures which have the same propagation vector and therefore contribute to the same magnetic reflections. Multiple phases may also be used to generate or analyze a powder pattern.

In order to create an additional phase simply right-click the *Phase* label above the OPENGL widget and under the *Add phase* menu choose either *New phase*, *Duplicate current phase* or *Load from file*. In the second case a copy of the present phase will be generated which can then be modified. When a new phase is loaded from a file, **.xml* or **.cif* formats are supported, while for multi-phase **.xml* files all phases are added. The different crystal and magnetic structures can be visualized by modifying the phase number through the arrow buttons. A volume fraction is associated to each phase which can be set in *Structure*→*Phases, domains and twins*.

Different example videos are available for [setting up a structure model](#), [setting up a simple magnetic structure](#) or [setting up a complex magnetic structure](#).

2.3 Visualizing crystal and magnetic structures

Once all necessary parameters have been entered, the crystal and magnetic structures can be visualized by triggering the menu entry *Generate*→*Unit cell* or using its shortcut (CTRL/CMD + U). In case of a missing or erroneous input, the corresponding error message should pop up. MAG2POL can optionally check, if the atomic positions entered by the user are not too close to a special position of the space group. This would lead to generated atoms which are too close to each other and trigger a warning. This option and also the shortest allowed distance between generated atoms can be set in *Settings*→*Symmetry*. The perspective can be modified by dragging within the OPENGL widget. A rotation around the axis vertical to the viewing plane can be achieved by dragging within the upper or lower left corner of the widget. Zooming in and out is done via the mouse wheel, whereas the original zoom can be restored with a right click. Rotations around a user-definable axis can be achieved by entering vector components of the rotation axis, selecting the type of vector (direct cell, reciprocal cell or viewport), the single step value and then by using the play-stop buttons. Zooming in and out can also be done stepwise by clicking on the up and down buttons next to the zoom value (right-clicking this value allows to set the single step). The view can be shifted by keeping the SHIFT key pressed while dragging. The perspective or orthographic view can be toggled by clicking the icon above the play-stop buttons. When the perspective view is activated, the depth of the projection can be modified by holding down the CMD/CTRL button and zooming. After a change using the mouse wheel, the *Zoom* spinbox is replaced by the *Depth* value which can be modified stepwise (depth values between -20 and -40 usually give satisfying results). After a normal zoom the *Zoom* spinbox is restored. The bounding box of the volume to plot can be modified in the spin boxes corresponding to relative units of the lattice constants. In some cases, the bounding box values cannot be adjusted appropriately to show an intended selection of atoms. For such cases, undesired atoms can be masked by selecting them (either by a single click, a shift click showing the bond, are two shift clicks showing the angle, see next section) and then hitting ALT+M. Masked atoms can be cleared with ALT+C.

If more than one phase or magnetic domain is present, each individual structure can be viewed by selecting the respective phase/domain number in the spin box. The position of the light source can be modified by dragging the scene while pressing the ALT key. The default position is restored by ALT+rightclick.

The appearance of every atom/spin site can be modified with the plot options shown at the right of the atomic position. A site can be turned invisible by removing the tick below *plot*. A right-click on either of the *plot* check boxes opens a context menu from which it can be chosen whether all, only nuclear or only magnetic atoms will be plotted. The color

can be chosen by clicking on the colored square and then by setting the *RGB* values in the pop-up window, either for the atom or for the spin (if the atom is magnetic). The color boxes also provide convenient shortcuts through a context menu: a selected color can be applied to all atoms, all nuclear atoms, all magnetic atoms or all atoms with the same label. The sizes of the atoms and spins can be defined in the boxes *size a* and *size s*, respectively. If the Fourier components are imaginary and the imaginary part is perpendicular to the real part (within 1°) then an envelope will be drawn automatically emphasizing the rotation plane of the spin.

The objects to be plotted can be chosen from the *Settings* menu together with the quality and resolution of the objects. The coordinate axes can be plotted in the lower-left corner instead of the colored unit cell axes. Also, a smart legend can be added in the upper-left corner, which will automatically adjust the legend entries depending on repeated elements with the same appearance (such sites will automatically be numbered, e.g. O1, O2, O3...). Furthermore, multiple unit cell edges can optionally be plotted as well as multicolored atoms representing the respective occupation of shared sites. Furthermore, MAG2POL features antialiasing by using multisampling per pixel and the objects' distance to the viewer is calculated for each view which allows for a correct back-to-front rendering of transparent objects. Those features massively increase the quality of the rendered picture. The OPENGL objects have been designed in order to minimize the calls to the frame buffer, for which the improved graphics don't come alongside with slower performance.

Via *File* \rightarrow *Export* the crystal/magnetic structure plot can be exported into a *.png file or into a binary GL Transmission Format *.glb file for further use in POWERPOINT presentations or in 3D rendering programs like BLENDER. When creating a *.png file, an input dialog will open up in which the zoom factor can be entered. This factor is proportional to the image size and quality. Upon export of a 3D model, three dialogs will pop up which serve to modify the object material with respect to its basis color, metallicity and roughness.

2.4 Atom and spin info

Once a (magnetic) structure is drawn in the OPENGL widget the user can visualize atomic positions, magnetic moment values, bond distances, angles between 3 atoms and angles between two spins. In order to get information concerning the position of an atom or the Fourier components of a magnetic moment, just click on the atom (sphere) or on the cone of the spin, respectively. The information will be shown in the status bar of the main window, the object will be drawn with a different lighting/material (depending

on the rendering settings, see Sec. 3.1.5 and highlighted in the respective atom or spin table. After highlighting an atom or spin in that way, its components can be inverted by pressing ALT+I, or individual components can be flipped by using ALT+X, ALT+Y or ALT+Z. Atom and spin info can alternatively be shown, when the atom or spin label in the respective table is clicked, which will also highlight the object in the unit cell plot. In order to get distances between 2 atoms click the first atom and then SHIFT-click a second one, which will show the distance in the status bar and will draw the bond between those 2 atoms. The same procedure has to be done to get the angle between 2 spins. For the angle made up by 3 atoms simply SHIFT-click the 3 atoms. Note that you can rotate the perspective in between SHIFT-clicks if necessary.

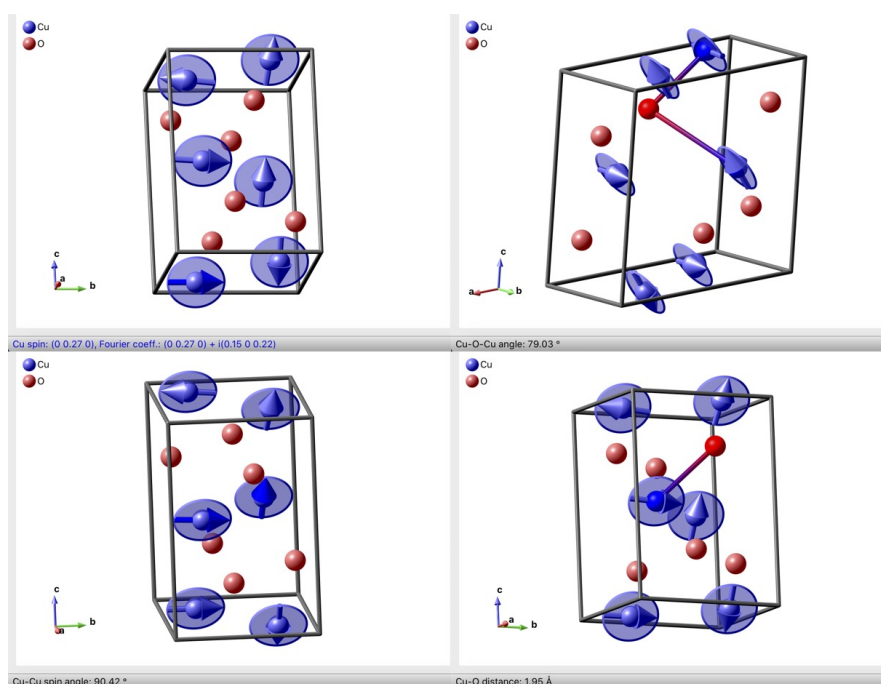


Figure 2.2: Geometry options in MAG2POL.

2.5 Bonds and polyhedra

MAG2POL features the plotting of bonds and polyhedra. After a structure has been generated this can be done via the *Generate*→*Bonds* menu or the toolbar icon. A control window will open up, which is shown in the upper part of Fig. 3.1. Here the number of bond types to search and generate can be entered which creates the according number of rows in the *Bonds* and *Polyhedra* tables. The center (atom1) and ligand (atom2) atoms can be chosen from the combo boxes. Note that the content of these boxes is a list of

elements followed by the list of sites. In the example shown in Fig. 3.1, the structure contains two Co sites, so in order to plot all possible Co-O bonds, irrespective of the specific site, the elements have been chosen from the first (element) list. A number of parameters can be adjusted in order to control the bond distances and the appearance of the rendered objects. The meaning of these parameters are explained when hovering the mouse over the horizontal header items. Note that the minimal distance between the center atom and the polyhedron faces should be increased, if the resulting polyhedra look unexpected. This can be the case for heavily distorted polyhedra. The information about bonds created in the OpenGL widget can be retrieved by clicking on the center of the bond. This will show the two connected atoms, their positions and the bond length in the status bar of the window.

The parameters for the bond search as well as for the appearances of bonds and polyhedra are saved in the *.xml file.

2.6 Rigid bodies

Rigid bodies can be used when the relative position of a group of atoms is known and the deformation of the rigid body is zero or negligible, e.g. when a molecule occupies a specific Wyckoff position. Before using a rigid body by placing it in the atom table of the main window, the *Rigid body window* (Fig. 2.4) has to be used in order to construct one or several rigid body models.

2.6.1 Creating a rigid body model

When the *Rigid body* window is first entered, one has to click the *New* button which will create a new model labeled *Rigid body 1*. The name of the model can be changed by modifying the *Label* line edit. The next step is to define the number of atoms, which can of course also be done step-wise during the process of construction. The atoms and spin tables are where the rigid body information will be entered and the result is automatically visualized to the right-hand side of the window (the visualization options are the same as for the unit cell in the main window). The rigid body models are created using the Z-matrix, where each line gives the internal coordinates for one of the atoms within the molecule. The first atom is the center of the rigid body and any further atoms have specific relations to the previously defined ones. An atom is created in the same way as explained in Sec. 2.2 including the possibility to create magnetic atoms (note that in addition to choose between Cartesian and spherical coordinates by right-clicking the *Spin* header of the spin table it is also possible to choose between local and cell reference). Note that the center can be displaced by using the offset values Δx , Δy and Δz . The

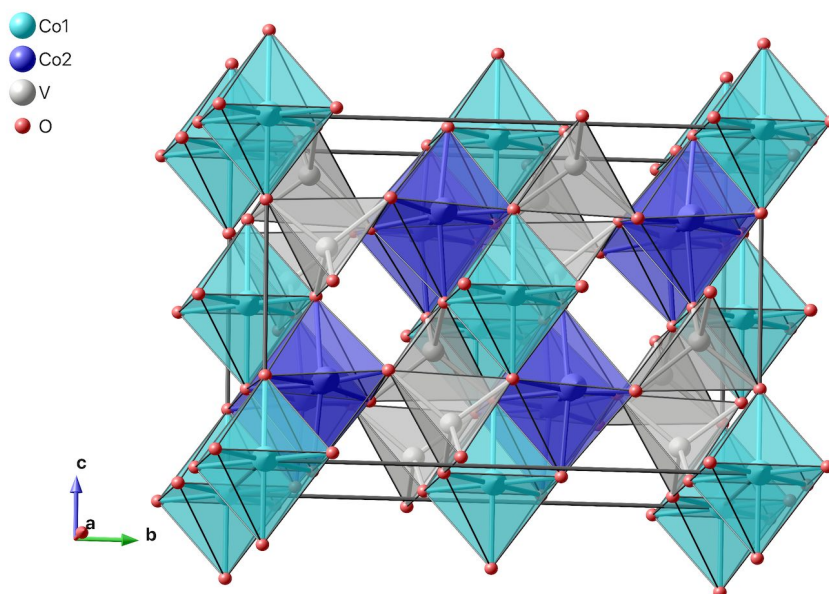
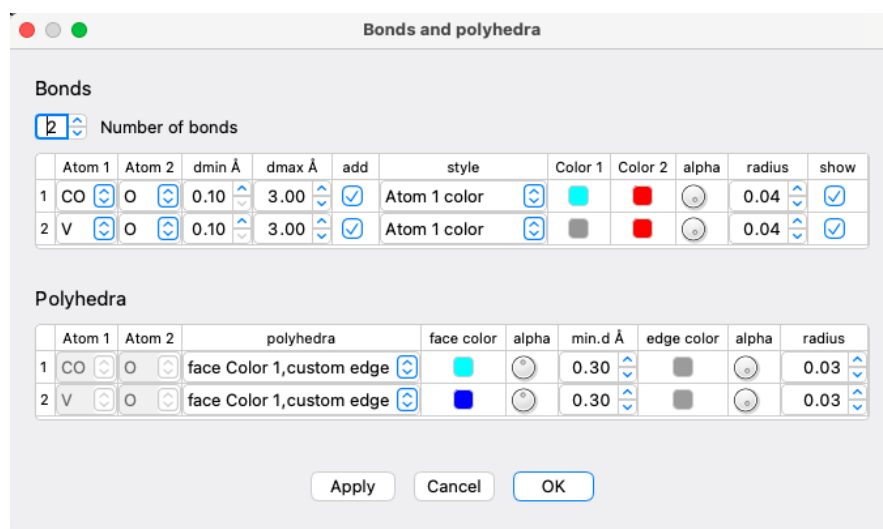


Figure 2.3: Bonds and polyhedra plotting in MAG2POL.

orientation of the rigid body, given by the local orthogonal reference xyz is given by the three angles θ (angle between the z and the unit cell's c axis, measured towards the positive a axis), ϕ (counterclockwise rotation around the c axis when viewed from above) and χ (counterclockwise rotation around the z axis when viewed along $-z$). The second atom is given by a bond distance in relation to the first atom: *ref1* is *A1*. The third atom (and any atom onwards) has a choice for *ref1* and can be set to any of the previously defined atoms. Additionally, it needs a bond angle which is formed between *ref1*, *ref2* and the new atom. Starting from the fourth atom the dihedral angle has to be entered which defines the angle between the two half planes containing *ref1*, *ref2*, *ref3* and *ref2*, *ref3* and the new atom, respectively. Bonds are automatically created between the newly entered atom and the *ref1* atom, where the bond style can be customized as in Sec. 2.5. Note that dummy atoms can be used, which can be advantageous for creating specific molecule geometries. A dummy atom has the label X and will not be taken into account for structure factor calculations. Depending on the geometry of the created rigid body it might be necessary - for the sake of visualization - to create additional bonds, which can be done at the bottom of the window by increasing the number of additional bonds and defining it between two atoms (numbered as in the atoms table).

Further rigid bodies can be defined by clicking the *New* button and it can be switched between them using the combo box. A right-click on the rigid-body label evokes a context menu showing a small library of molecules which can be used as a starting point or for understanding the Z-matrix formalism.

2.6.2 Boundaries and constraints

Boundaries and constraints can be defined in order to provide a more robust structural model in the refinement process. Constraints are especially useful in order to maintain a specific molecule symmetry and thereby reduce the number of refinable parameters. Both features refer to the bond distance, the bond angle and the dihedral angle (depending on the number of the atom) and can be accessed by right-clicking the label of an atom which opens a context menu allowing to choose either *Set boundaries* or *Constrain*. The default boundaries are 0 and 10 Å for the bond distance, 0 and 180° for the bond angle and -180 and 180° for the dihedral angle, and a click on *Clear boundaries* restores these values. The bond distance and angle as well as dihedral angle of an atom can be constrained to any of the atoms above in the list. While the bond distance and angle are defined to be positive, the dihedral angle can also be constrained to be -1 times the reference value. In the spin table the constraints are also set by right-clicking the magnetic moment label and by choosing from a list of options (whole moment, module, real/imaginary part only etc.). Constrained values will be grayed out in the atom and spin tables and automatically

updated when the reference value is changed.

2.6.3 Model vs. instance vs. fit instance

All models created in the *Rigid body* window can be used in the main window and they will also be saved to the project XML file. Regardless of the label chosen for a particular rigid body model, the symbol to be used in the atoms tab corresponds to the position of the rigid body model in the list, i.e. the first one will be identified as *R1*, the second one as *R2* and so on. The fractional *x*, *y* and *z* positions define the position of the rigid body center to which the eventually defined offset will be added. The (an)isotropic temperature factor applies to all atoms of the rigid body. Special attention needs to be paid to the occupation factor. While for conventional atomic position the occupation defines the actual occupation of this Wyckoff site (1 for a fully occupied site, 0.5 for a half-occupied site), rigid bodies will be - depending on the space group and on the Wyckoff site symmetry - generated *on top* of each other, no matter if the rigid body symmetry matches the Wyckoff site symmetry or not. As an example: a benzene molecule has a main *C*6 axis which would fit, for example, perfectly fit on the site 6.. symmetry of Wyckoff position *1a* in space group *P*6. Nevertheless, the molecule will be generated six times, rotated by 60°, which is not visible in the unit cell plot, but can be easily seen by activating the *Dummy atom as rigid body* in the settings and by verifying the atomic positions in the *Sample info* window. Therefore, in such a case the user is responsible to enter the correct occupation factor, i.e. for a fully occupied *1a* site in the present example the occupation factor would be 1/6. This also applies to molecules whose symmetry is lower than the site symmetry of the Wyckoff position they are placed on. In that case, multiple molecules will be seen at the same position and the occupation factor has to be adjusted accordingly.

By using a rigid body model in the atom table a new instance will be created, which is a one-to-one copy of the model. In the instance, the molecule geometry can be changed within the constraints and boundaries defined by the model. In order to do so, right-click on any of the *x*, *y* or *z* value of the rigid body in the atom list and choose *edit rigid body* from the pop-up menu. This will open the *Rigid body* window in the *instance* mode, where the unconstrained values can be changed, but the constraints and boundaries as well as the offsets and all appearances (atom colors, bond styles, etc.) are fixed. In addition, the orientation of the rigid body can be set (note that a quick way to set the orientation is to choose *set orientation* from the pop-up menu mentioned previously). If the geometry, constraints or boundaries are changed in the rigid body model, all instances used in the structure model will be updated. The individual atom parameters can also be changed from within the fit window (by either right-clicking the positional parameters, or - in the case that the nuclear structure is not refined - by right-clicking the magnetic moment

2 Getting started

parameters). In addition, each of those parameters will have a check box to signal it as a refined parameter. Fit flags can also be conveniently set by choosing *Fit flags* from the pop-up menu.

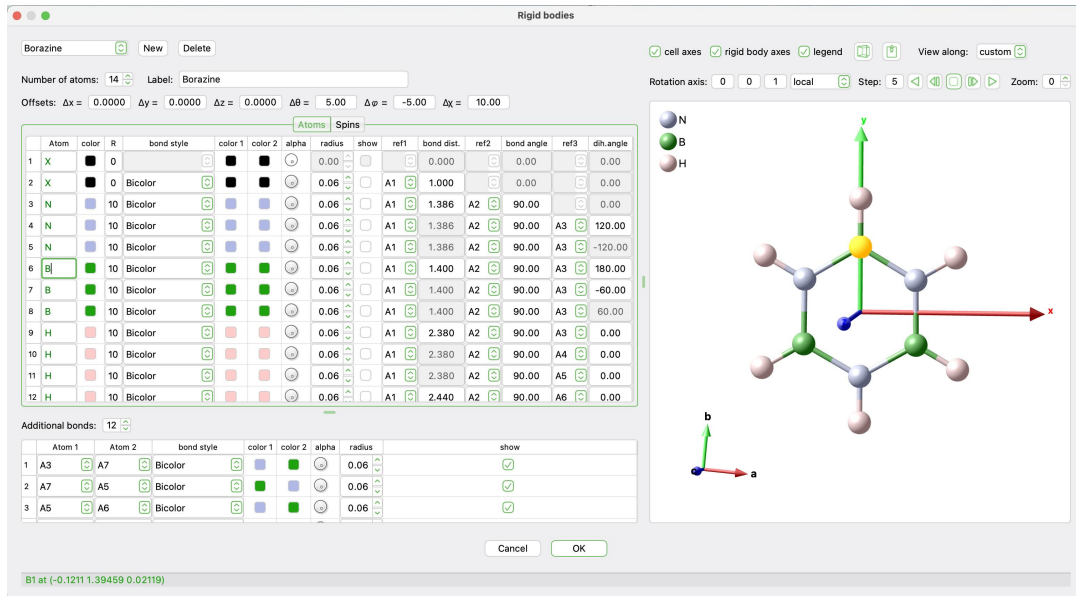


Figure 2.4: *Rigid body* window for the construction of rigid bodies.

2.7 Saving and loading input files

All parameters which have been entered or modified can be saved into an input control file in XML format from the menu entry *File*→*Save/Save as*. Additional information concerning scale and extinction factors, magnetic domains, fit parameters and constraints, user-defined magnetic form factors, powder patterns, plot parameters like the cell range, the perspective and the zoom are saved as well. Note that if a magnetic (super) space group is used after having calculated irreducible representations, the latter will not be saved in the XML file. The respective parameters will be explained in Sec. 3. Saved input files can be loaded via *File*→*Load*. The MAG2POL main window can also be reset by *File*→*Reset*.

Crystal and magnetic structures can also be exported in *.cif or *.mcif format. When the propagation vector is 0, the magnetic symmetry will be exported either using the user-defined magnetic symmetry operators or that given by an irreducible representation. Note that only 1-dimensional irreps can be exported and that for mixed representations only the first will be considered. For non-zero propagation vectors the magnetic moments

(real vectors) will be calculated for all atomic sites and the structure will be exported in $P1$ symmetry.

2.8 Calculation of structure factors and polarization matrices

Besides the correct description of a magnetic structure, MAG2POL needs information concerning the experimental geometry in order to calculate the nuclear/magnetic structure factors and the polarization matrices. Herefore, the wavelength should be given in Ångströms, which already allows the calculation of structure factors. The calculation of the polarization matrix depends on the orientation of the sample, which can be given either by defining the vertical sample axis (reciprocal lattice vector) or by supplying the orientation matrix of the experiment in the menu *Geometry*→*Orientation matrix*. In the latter case the instrument angles are automatically calculated and shown in the respective boxes. For the 4-circle geometry a ψ value can be given, which is the rotation angle around the scattering vector, where $\psi = 0$ refers to bisecting geometry. From any given angles the corresponding (hkl) indices can be calculated by right-clicking any angle value and selecting *calculate hkl*.

Note that the flipping ratio geometry requires the use of the vertical axis (not Cryocradle). The vertical axis will automatically be calculated and set after setting the normal-beam orientation matrix. Since in a flipping ratio experiment one usually assumes the magnetic moments to be aligned parallel to the vertical direction (magnetic field direction) one can align the moments automatically by right-clicking the label *z axis* and choosing *set moments parallel*. If the UB matrix is not given the program will calculate the moment direction from the values given for the vertical axis. Note that the uvw components of the magnetic moments will have to be constrained in a refinement. Another option is to use user-defined basis vectors before aligning the moments vertically, which requires the refinement of only one parameter.

With MAG2POL it is possible to calculate flipping ratios due to Schwinger scattering [11–14], which is automatically done in the absence of magnetic ions in the unit cell (e.g. use **Fe2** instead of **MFe2**). Note that the polarization axis of the neutrons is taken to be parallel to $\mathbf{k}_i \times \mathbf{k}_f$.

The calculations are done for the Bragg reflection $(hkl)\pm\mathbf{q}$ entered by the user by pressing *Go!* (see also [this](#) demo video). If the propagation vector is 0, there is no difference concerning the combo box. When more than one propagation vector was entered in the *Domain* window (see Sec. 3.4), they will all be shown in this combo box and by selecting e.g. $(hkl)-\mathbf{q}_2$ the program will automatically check if a contribution from another configuration domain is present at the \mathbf{Q} position.

If the checkbox *show* is activated, the local coordination system (see Sec. 7) and the mag-

netic interaction vector \mathbf{M}_\perp are drawn.

The results of the calculation are shown in the output text window (orange box in Fig. 2.1) and the individual polarization matrix entries are shown in their respective boxes in the Geometry section of the window (blue box in Fig. 2.1).

Whole lists of reflections can be generated under *Generate*→*Reflection list* for given criteria like *hkl* range, intensity, polarization and diffractometer angles. This can be useful as a preparation for an experiment e.g. by selecting those magnetic reflections which show a large chiral component in the P_{yx} term. The reflections which fulfill the given criteria are shown in a table after clicking *Create hkl list*. By right-clicking on a respective horizontal header the list can be ordered according to that parameter, either ascending or descending. The reflection list can be saved in ASCII format which is directly readable by MAD or NOMAD due to the comments marked by '!'.

3 Further parameters

In addition to simple calculations as shown in the previous section, scale/extinction parameters and magnetic domains can be defined, which obviously affect the observed intensities and polarization values. In case of a crystallographic site being shared by multiple magnetic ions, user-defined magnetic form factors can be created, plotted and saved.

3.1 Global settings

The global settings of the application can be evoked from the *Settings* or *Preferences* menu (depending on the platform).

3.1.1 General

General parameters concerning the application, the instrument, symmetry and the view can be found in the *General* tab. Most of the settings are self-explaining, however, a short notice on the use of p_0 and the cell efficiency is necessary. The sign of p_0 depends on the instrument's neutron beam polarization and is positive (negative) if the neutron beam is polarized *up* (*down*). While in the fitting procedure the cell efficiency is always taken as a positive value, the use of a negative value in the settings only effects single calculations of polarization matrices in the main window, where the sign of the cell efficiency defines the direction of the analysis vector. Therefore different combinations ++, +-, -+ and -- can be calculated, while when analyzing data, this information is extracted from the data file. Note that the theme colors and the dark mode can also be set via the shortcuts ALT + 1 to ALT + 8 from within the main window.

In the *Symmetry* section, the option *Check special atomic positions* assures that the user does not define an atomic position (by mistake) which is too close to a special Wyckoff position. If after generation of the unit cell, atoms of the same site reveal a distance shorter than the one defined under *Shortest allowed distance*, the program will show a warning. The option *Constrain lattice parameters in powder fit* will automatically add constraints concerning the lattice parameters during Rietveld refinement depending on the space group. The setting *Constrain propagation vector in powder fit* constrains e.g. $q_y = q_x$ for a tetragonal, trigonal (hexagonal setting) or hexagonal space group or e.g. $q_z = q_y = q_x$ for a cubic or trigonal (rhombohedral setting) space group. Note that

when using a space group or magnetic (super) space group with a lattice system of lower symmetry, it is still possible to maintain the original constraints of the parent structure by right-clicking on the *Cell* or *Propagation vector* q label and then clicking *override* in the *symmetry* menu. Afterwards, the lattice system can be chosen by evoking the context menu once more.

The setting *Extract observed F_M using model* refers to flipping ratio data, where the magnetic structure factor F_M is extracted from the observed flipping ratio R by solving an equation of order 2. If this option is checked, the solution being closer to the calculated F_M value (based on the underlying magnetic structure model) will be selected. Otherwise, the solution with smaller $|\gamma|$ will be chosen, where $\gamma = F_M/F_N$ (as in SORGAM from the CCSL).

3.1.2 Refinement

Under the *Refinement* tab different least-squares fit parameters can be set. The convergence criterium is defined as the maximum parameter shift divided by its standard deviation. The range in multiples of the peak FWHM can be defined for which the peak profile will be calculated in a powder pattern. When the *Calculate pattern in excluded regions* option is disabled, only the peak positions will be calculated and shown, but no intensities will be calculated. This can be a convenient choice for low-symmetry structures with hundreds (thousands) of reflections in the high- Q region of the powder pattern. The setting *Ignore secondary phases for single crystal* should be unchecked when those secondary phases are only present in a powder diffraction pattern. It should be checked when two nuclear and/or magnetic phases are actually present in the single-crystal sample and contribute to the same reflections.

Usually, the magnetic form factor is refined against flipping ratio data, but if a refinement against integrated intensity data is desired, then the *Refine magnetic form factor with INT data* should be checked which enables the necessary tabs in the fit window. The option *Automatically constrain split sites* is useful for atoms sharing the same site and sets reasonable constraints when entering the fit window for the first time (position, temperature factor, split occupation, magnetic parameters).

3.1.3 Plot

All settings concerning the unit cell plot in the OpenGL widget can be found under the *Plot* tab. Here the objects to be rendered can be chosen as well as the mouse sensitivity for zooming and rotating the plot. Note that a right-click on the *Spins, cone radius* label opens up a context menu that allows to restore the default values for the spin vector geometry.

The powder pattern plot in the (batch) fit window can be fully customized regarding the marker, line and plot background colors (a click on *Reset* restores the default values). In addition, the color gradient of 2D maps can be defined here. Note that in the intensity maps and magnetization density maps windows, the shortcuts ALT + +, ALT + - and ALT + I can be used to cycle through the different gradients and to invert the color scale, respectively.

3.1.4 Labels

Under the *Labels* tab the position, scale and font size of the coordinate axes and legend can be customized. It is also possible to enter individual translation values for the axes labels. These settings are also saved in the *.xml file.

3.1.5 Render

In the *Lighting and material* section different profiles can be defined in which the lighting and material properties of (un)selected objects in the unit cell plot can be modified with respect to their ambient, diffuse and specular values. A click on the light color tool button opens the color selection dialog, while the horizontal slider next to it increases/decreases the 3 RGB values simultaneously, e.g. to quickly move between black and white over different gray tones. The shininess can also be defined for selected and unselected objects. These settings can be saved into different profiles. Four built-in profiles are included in MAG2POL and can be recovered by clicking *Reset all*.

Several options exist to adjust the rendering quality which affect the fluidity with which you can manipulate the drawing. The level of multisampling can be set by the number of samples per pixel, which affects the rendering of edges (smoother edges for increasing multisamples). The object resolution is a measure of the number of vertices which are calculated for the creation of an object. The minimum number is 3 and corresponds to a triangle in comparison to a circle with higher resolution.

Crystal and magnetic structures can be visualized with a depth effect, like fading or blurring, and the customizable factor regulates the intensity of this effect. For the blur effect a pixel-by-pixel post-processing step is necessary, which can be slow depending on the computing power. It is therefore recommended to use a low *Quality* setting for a fluid movement of the drawing and eventually a higher setting for the export to file. The focus for the blur effect can be modified by holding down the OPT/ALT key while zooming.

In order to correctly render transparent objects, when they are aligned one behind the other, the order is crucial. Since the perspective is constantly changed by the user, the order of the transparent objects is automatically recalculated on-the-fly. For a large number of transparent object this means a lot of calculation cost, of course. Therefore, the

3 Further parameters

threshold for continuous reordering can be adjusted, the default value being 1000 objects, e.g. 100 octahedra (each containing 8 transparent planes) and 200 spin envelopes. Above this threshold, the order will only be recalculated when the mouse button is released after dragging the perspective. In order to avoid too long calculation times when a very large supercell with a lot of transparent objects is plotted, the automatic reordering can be turned off with the second threshold value (default is 5000).

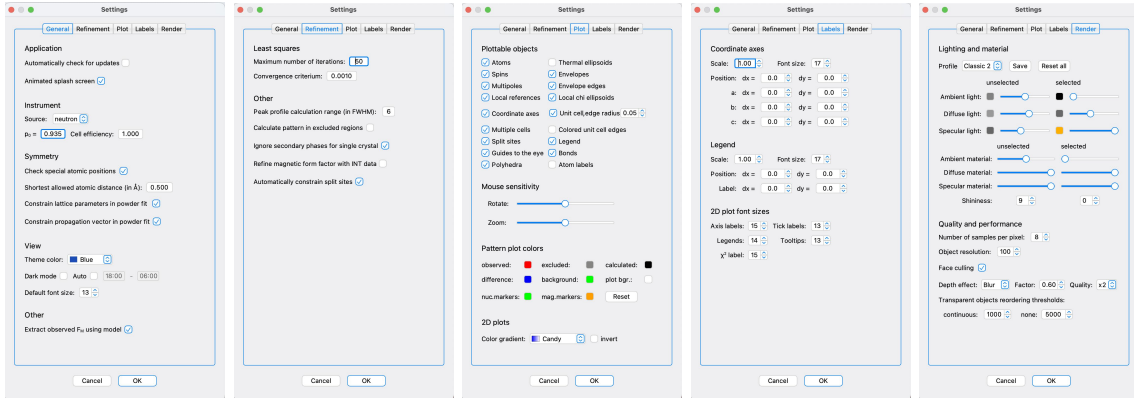


Figure 3.1: Global settings in MAG2POL.

3.2 Scale factor and $\lambda/2$ contamination

The scale factor and the fraction of $\lambda/2$ contamination can be set via the menu entry *Structure* \rightarrow *Scale factor*. The scale factor is multiplied to the calculated intensities of Bragg reflections in order to be compared with the observed ones. If the $\lambda/2$ contribution is greater than 0, the calculation of nuclear and magnetic structure factors as well as flipping ratios and polarization matrices of a reflection (hkl) will include the higher-order contamination of $(2h\ 2k\ 2l)$ by $\lambda/2$. For a zero propagation vector the nuclear and magnetic intensities will have their respective higher-order contamination, whereas for an incommensurate propagation vector, no $\lambda/2$ contribution will be calculated. For half-indexed propagation vectors, the $\lambda/2$ contamination of nuclear nature is added to the magnetic intensity of (hkl) . Note that this contamination is not calculated, when *purely magnetic* is chosen in the fitting procedure.

3.3 Extinction

The extinction parameters can be set via the menu entry *Structure* \rightarrow *Extinction*. The extinction parameters x_{ij} build up the tensor \mathbf{x} which allows the treatment according to

an empirical model which represents a compromise to treat both primary and secondary extinction. It is also implemented in FULLPROF [15] and in SHELX [16] and has shown to work well in practice. The extinction correction is given by

$$y = \left(1 + \frac{px_{\text{aniso}}F_c^2\lambda^3}{4\sin(2\theta)(\sin\theta/\lambda)^2} \right)^{-\frac{1}{2}}$$

where x_{aniso} is the anisotropic extinction parameter and F_c is the calculated structure factor. p is $1e^{-3}$ for neutrons and $1e^{-6}$ for x-rays. x_{aniso} is obtained by operating the tensor \mathbf{x} subsequently on the scattering vector (hkl) :

$$x_{\text{aniso}} = \begin{bmatrix} \begin{pmatrix} x_{11} & x_{12} & x_{13} \\ 0 & x_{22} & x_{23} \\ 0 & 0 & x_{33} \end{pmatrix} \begin{pmatrix} h \\ k \\ l \end{pmatrix} \end{bmatrix} \begin{pmatrix} h \\ k \\ l \end{pmatrix} = x_{11}h^2 + x_{22}k^2 + x_{33}l^2 + x_{12}hk + x_{13}hl + x_{23}kl$$

The isotropic version of this model only requires a single parameter x and the extinction is corrected according to

$$y = \left(1 + \frac{pxF_c^2\lambda^3}{\sin(2\theta)} \right)^{-\frac{1}{2}}$$

A more physical model based on the highly oversimplified concept of an ideally imperfect crystal takes into account the size of structural domains and the mosaicity and was developed by P. J. Becker and P. Coppens [17–19]. The same implementation as in the CCSL and FULLPROF is featured in MAG2POL and corrects secondary extinction effects by

$$y_s = \left(1 + 2x_s + \frac{A_s x_s^2}{1 + B_s x_s} \right)^{-\frac{1}{2}},$$

where x_s is given by

$$x_s = \frac{2}{3}Q\alpha\bar{T} \cdot 1e^3$$

with \bar{T} being the mean beam path length given in mm and

$$Q = \frac{F_c^2\lambda^3}{V^2\sin(2\theta)}$$

with the sample volume V in mm^3 and the wavelength λ in \AA . The coefficients A_s , B_s and α depend on the mosaicity distribution which can be assumed to be Lorentzian (L) or Gaussian (G):

$$A_{s,L} = 0.025 + 0.285 \cdot \cos(2\theta)$$

$$B_{s,L} = \begin{cases} -0.45 \cdot \cos(2\theta), & \text{for } 2\theta \geq 90 \\ 0.15 - 0.2 \cdot [0.75 - \cos(2\theta)]^2, & \text{for } 2\theta < 90 \end{cases}$$

$$\alpha_L = \bar{\alpha} \left(1 + \frac{2\bar{\alpha}}{3\omega_D} \right)^{-1}$$

$$A_{s,G} = 0.58 + 0.48 \cdot \cos(2\theta) + 0.24 \cdot \cos^2(2\theta)$$

$$B_{s,G} = 0.02 - 0.025 \cdot \cos(2\theta)$$

$$\alpha_G = \bar{\alpha} \left(1 + \frac{\bar{\alpha}^2}{2\omega_D^2} \right)^{-\frac{1}{2}}$$

Finally, $\bar{\alpha}$ is given by

$$\bar{\alpha} = \frac{3}{2} r_D \sin(2\theta) / \lambda$$

where the domain radius r_D (in nm) and the mosaicity distribution ω_D (in inverse radians) are refinable parameters. Note that - due to the dependence on the sample shape - this model can only be chosen after designing a convex-hull model of the single crystal (see Sec. 4.2.2). In that case, the beam path lengths are calculated for each (hkl) reflection and, therefore, this model should be used on a data set without averaging equivalent reflections. MAG2POL offers the possibility to create a corrected data set after refining a structural model with Becker-Coppens extinction correction in which the intensities are corrected by y . The corrected data set (which is also corrected for eventual $\lambda/2$ contamination and absorption effects, see also Sec. 4.2.3) can then be merged and re-analyzed without extinction correction.

3.4 Domains and twins

An unlimited number of magnetic domains and structural twins can simply be added via the menu *Structure*→*Domains and twins* (see [demo](#) video). The program differentiates between S -domains and k -domains, see [20] for a review. For k -domains at least two propagation vectors have to be set to which the magnetic domains (see below) can be attributed.

For magnetic domains, first the number of different domains has to be set, which automatically applies an even population between the domains. Then, the symmetry operators (usually the ones from the paramagnetic space group which have been lost in the magnetic phase transition) have to be entered using the combo boxes. This can also be done using the smart copy-paste feature, i.e. copy the text corresponding to a symmetry operator (e.g. in the *Irreducible representations* or *Space group tables* windows) and past it by right-clicking the vertical header number (starting at the second row, since the first is always the identity). In addition, check boxes can be activated to define inversion or chiral domains. The first simply reverses every magnetic moment, whereas the latter takes the complex conjugate but keeps the phase shift of the user-given Fourier components describing the magnetic structure. If a symmetry operation is not included in the little group, i.e.

it transforms $+\mathbf{q}$ into $-\mathbf{q}$, the program calculates the complex-conjugate and inverts the phase. That means that if a magnetic structure breaks inversion symmetry and therefore two magnetic domains are related by the inversion center, the *chiral* checkbox should not be checked. When only one propagation vector is present, then all magnetic domains are considered as *S*-domains. When more than one propagation vector is entered, then each of the magnetic domains can be attributed to a specific *k*-domain by choosing the arm of the propagation vector star through the combo box with q_1 , q_2 , etc.

Structural twins are set up in the same way, however, in this case the matrix relating the (*hkl*) reflections of the different twins has to be given. For the calculation of structure factors those rotations matrices will be multiplied to the observed (*hkl*) values and if the result corresponds to integer indices (\pm the propagation vector) it will be considered as a contribution from another twin. Note that in the presence of multiple magnetic domains it is possible to reorder their sequence for each structural twin, which can be necessary in order to retrieve the same kind of domain in each twin for some particular cases. The sequence is simply entered by typing n integer numbers from 1 to n (with n being the number of magnetic domains defined), e.g. 4 2 3 1, when 4 magnetic domains are present.

The structural twins and their relation to another can be visualized in the *Twin Q-space viewer* by clicking on the icon on the right of the tolerance value. A new window opens which is divided into two parts separated by a horizontal splitter: on the left a 3D plot of each twin's reciprocal lattice and on the right side several plot options for each of the previously defined twins. The options apply to the twin that is selected at the top.

In the *Orientation* section the matrix relating the twins' (*hkl*) is repeated and is further expressed as the rotation axis and angle around the direct/reciprocal axis of the 1st twin from which the reciprocal lattice of the n^{th} twin is obtained. Here, both the matrix and the rotation axis/angle are synchronized, i.e. one is always recalculated from the other when any value is modified.

Under the *Plot settings* it can be specified for each twin, if the reciprocal lattice edges and points are shown and in which color or size. Nuclear reflections are represented by spheres, whereas magnetic reflections are depicted by cubes. The *beyond tolerance* appearance is used for reciprocal lattice points of twins different from the selected twin that would not be measured using the selected twin's reciprocal lattice (plus and minus the propagation vector). This is a very useful visual feedback in order to define the tolerance value in accordance with the observed reflections. It can further be selected, if forbidden, nuclear or magnetic reflections should be hidden in the plot.

The reciprocal lattice points of nuclear and magnetic origin can be clicked and selected in the 3D plot, which shows their respective (*hkl*) values in the status bar and also in the *Output* section. If the *colored* checkbox is activated, the output is given using the colors as shown in the plot legend. It is further possible to carry out structure factor calculations

3 Further parameters

of a given (hkl) Bragg peak (in the reference of the 1st twin) by entering the respective values of the scattering vector \mathbf{Q} and clicking on *Go!*

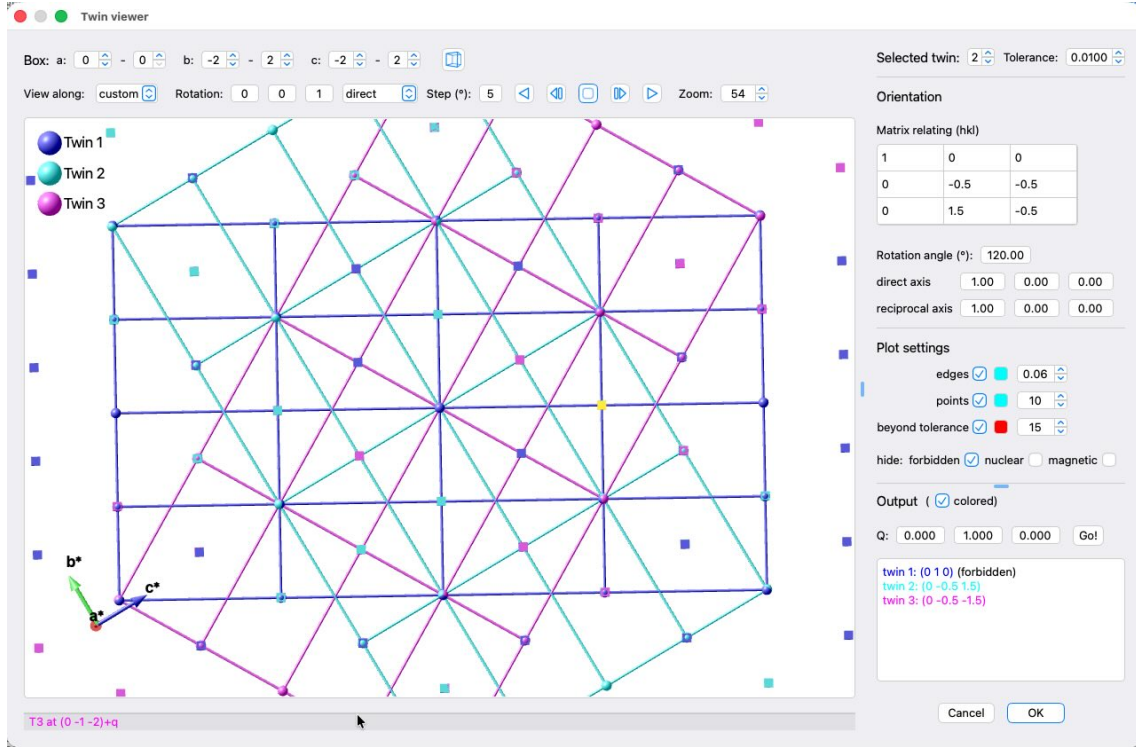


Figure 3.2: Twin Q-space viewer showing the reciprocal lattices of three structural twins.

3.5 X-ray and magnetic form factors

3.5.1 Built-in form factors

In the present version of MAG2POL the scattering length, absorption cross section, incoherent cross section and X-ray form factor of all elements and the magnetic form factors of the 3d, 4d and actinide ions are implemented. The latter are described by the analytical expression

$$f_M(\mathbf{Q}) = A \exp(-as^2) + B \exp(-bs^2) + C \exp(-cs^2) + D \quad (3.1)$$

with $s = \sin(\theta)/\lambda$. The magnetic form factors marked with the letter M (e.g. MCo2 for Co^{2+}) consist of only spherical Bessel functions $\langle j_0 \rangle$. For the rare-earth elements additional magnetic form factors are implemented which are marked with the letter J (e.g. JHo3 for Ho^{3+}) which approximate $\langle j_0 \rangle + c_2 \langle j_2 \rangle$.

The atomic or X-ray form factor is given by

$$f(\mathbf{Q}) = \sum_{i=1}^4 a_i \exp(-b_i s^2) + c \quad (3.2)$$

The form factor is then corrected for anomalous dispersion which modifies it to

$$f(\mathbf{Q}) = f_0 + f' + if'' \quad (3.3)$$

where the real and imaginary part of the anomalous dispersion f' and f'' are stored wavelength-dependent in MAG2POL. The complete list of built-in scattering lengths and (magnetic) form factors can be accessed under *Form factors*→*View list* (see [this](#) demo video). The list can be ordered either by element name, by atomic number or alphabetically by right-clicking on the combo box and selecting the appropriate menu entry. By selecting an element from the combo box the scattering lengths, cross sections and the (magnetic) form factor coefficients will be displayed as well as a plot of the x-ray and magnetic form factor as a function of $\sin(\theta)/\lambda$. Multiple form factors can be plotted by clicking *Keep* before selecting another element (see Fig. 3.3). Parts of the plot can be zoomed in by the usual controls of clicking and dragging, while the original view is reset by a right click. The plot can be cleared by clicking *Clear*.

3.5.2 User-defined form factors

In some cases it is desirable to use a custom magnetic form factor, e.g. if the magnetic form factor under question is not tabulated or if one crystallographic site is shared by different magnetic ions. In this case MAG2POL offers a simple method to add user-defined magnetic form factors which can then be saved in the input control file. In order to add (or delete) custom magnetic form factors, open the respective window under *Form factors*→*Manage user-defined* (or the corresponding toolbar icon), where you will find two tabs for the respective actions. Under *Add* either enter the form factor coefficients and the scattering length manually or type in a linear combination of built-in magnetic form factors. The number of elements is unlimited, however, the weights have to sum to 1. Interstitial sites can be handled through the occupation factor in the main window. Fig. 3.4 shows an example of a compound in which Co and Fe ions in bi- and trivalent oxidation state share the same crystallographic site. The corresponding input is `0.19*MCo2+0.27*MCo3+0.31*MFe2+0.23*MFe3`, which is case-independent. A correct entry, i.e. the sum of weights is 1 and the (magnetic) ions have been recognized, is signalled by green text (red otherwise). Note that you can only mix either only magnetic or only non-magnetic ions. Instantly, the weighted magnetic and atomic form factor coefficients and scattering length will be displayed as well as the plot of the form factors as a function of $\sin(\theta)/\lambda$. In order to save the new element a symbol has to be given. Any name

3 Further parameters

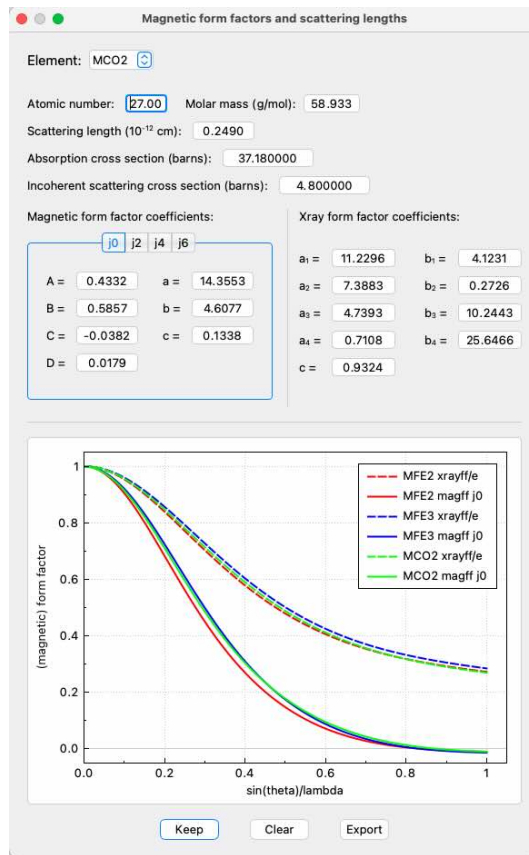


Figure 3.3: Example of the comparison of multiple form factors.

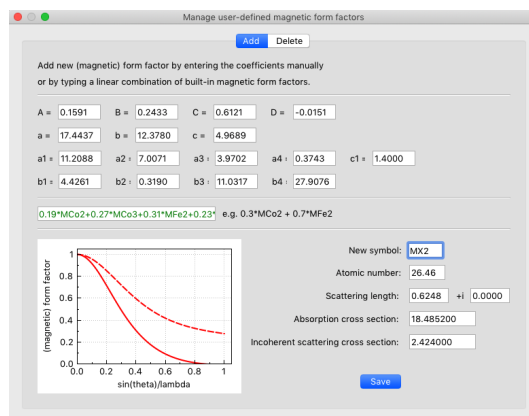


Figure 3.4: Example of a user-defined magnetic form factor.

(different from any built-in element) can be used for the new element. Upon clicking *Save* a pop-up window will inform the user, if the new element has been saved as magnetic or non-magnetic ion.

Built-in form factors can be viewed in the complete list as well as under the *Delete* tab. In the latter you can remove the selected one by clicking the button *Delete*.

3.6 User-defined basis vectors $\begin{pmatrix} \alpha \\ \beta \end{pmatrix} \begin{pmatrix} \lambda \\ \mu \end{pmatrix}$

For magnetic structures with higher symmetries it may be of advantage to use symmetry-adapted basis vectors instead of manually putting constraints between the individual components before refining the structure. Therefore, under *Structure* \rightarrow *Basis vectors* up to 6 basis vectors can be defined (see Fig. 3.5). Once the *use basis vectors* check box is activated MAG2POL will interpret the values under the *Magnetic structure* tab as well as in the *Fitting* window as coefficients to be multiplied to the basis vectors. This is signalled by the label *<- BVs ->* between the first and last 3 basis vector coefficients. Note that symmetry-adapted basis vectors can be deduced with the Irreducible Representation tool which is described in Sec. 6.4.

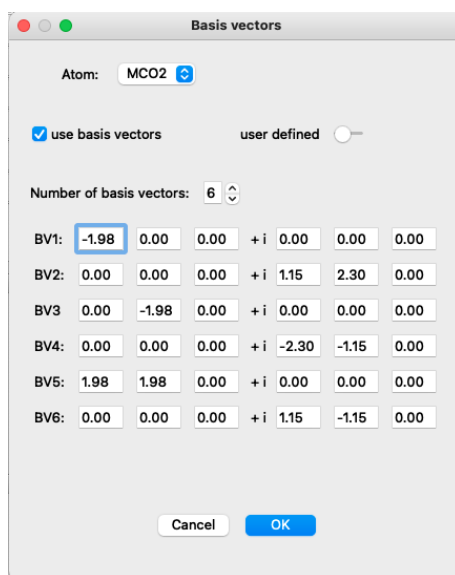


Figure 3.5: Example of a user-defined basis vectors.

3.7 Mixed irreducible representations

Two one-dimensional representations can be combined to a two-dimensional one. This can be achieved by setting the number of representations to 2 under the *Symmetry* tab of the main window. This will duplicate the symmetry operations where the first half corresponds to representation 1 and the second half to representation 2. The nuclear symmetry can obviously not be changed, however, the magnetic symmetry should be set by adjusting the (uvw) combo boxes according to the individual representations. Under the tab *Magnetic structure* you can now attribute the individual real and imaginary parts of the Fourier components to a respective representation by right-clicking on its value, which will open a context menu. Here you can select either *irrep1* or *irrep2* as shown in Fig. 3.6 (if the magnetic moments are described by spherical coordinates, the attribution still concerns the x , y and z directions of the Fourier components, for example: the context menu on the value $R\theta$ applies to Ry in Cartesian coordinates). Note that symmetry-adapted basis vectors of the irreducible representations can also be mixed using the Irreducible Representation tool (see Sec. 6.4).

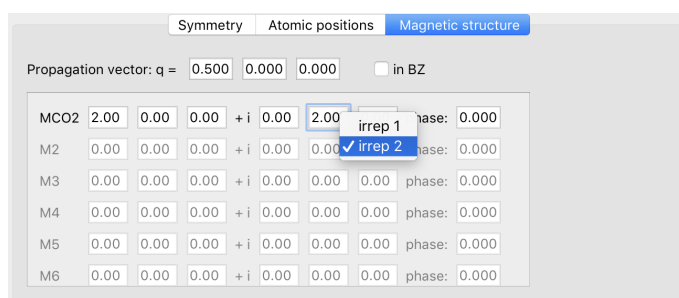


Figure 3.6: By right-clicking on the value of the Fourier component it can be defined according to which irreducible representation it transforms.

3.8 Magnetic form factor models

When defining a magnetic ion the default magnetic form factor corresponds to a spherical magnetization density which is expressed by the radial integral $\langle j_0 \rangle$. Further magnetic form factor models can be chosen for each magnetic ion individually by entering the *Form factor models* window via *Form factors* → *Form factor models* (or its toolbar icon). Note that those parameters (not belonging to the default model) can be refined in the fitting procedure by activating the *Refine magnetic form factor* checkbox when the refinement is done on flipping ratios. When integrated intensities are analyzed the checkbox *Refine magnetic form factor with INT data* should be activated in the settings.

3.8.1 Sum of radial integrals

This model still yields a spherical magnetization density and the magnetic form factor is given by

$$f_M(\mathbf{Q}) = \langle j_0 \rangle + w_2 \cdot \langle j_2 \rangle + w_4 \cdot \langle j_4 \rangle + w_6 \cdot \langle j_6 \rangle \quad (3.4)$$

with the $\langle j_n \rangle$ being spherical Bessel functions and the w_n refinable parameters. The coefficients of the analytic approximation of the $\langle j_n \rangle$ integrals are stored inside the program and can be looked up in the form factors window (*Form factors* → *View list*). The analytical approximation of the different spherical Bessel functions is given by

$$\langle j_0 \rangle = A \exp(-as^2) + B \exp(-bs^2) + C \exp(-cs^2) + D \quad (3.5)$$

with $s = \sin(\theta)/\lambda$ and

$$\langle j_n \rangle = (A \exp(-as^2) + B \exp(-bs^2) + C \exp(-cs^2) + D) \cdot s^2 \quad (3.6)$$

for $n \neq 0$.

The resulting magnetic form factor is plotted together with the spherical $\langle j_0 \rangle$ in order to point out the differences and can be exported as a PDF or ASCII file.

3.8.2 Multipole expansion

If the data allows for a more sophisticated description of the magnetic form factor, the deviation of the magnetization density from the spherical symmetry can be achieved by a linear combination of basis functions. In MAG2POL those basis functions are the real spherical harmonics which describe the angular dependence of the magnetization density. The radial dependence is calculated according to a Slater-type function (see Sec. 7.4 for a complete description). The description of each combination of multipoles is always in relation to a orthogonal local reference system, where for $\theta = \varphi = \chi = 0$ the local x axis is parallel to the unit cell's a axis, y is within the a - b plane and z is perpendicular to a and b . By selecting the multipole expansion for a particular magnetic ion the coefficients of the different basis functions (multipoles) can be set together with the Slater-type function coefficients and the local reference angles for each magnetic ion. Non-magnetic ions, e.g. O^{2-} can in principle be treated by first creating a new magnetic ion as described in Sec. 3.5.2 and then using that ion in the multipole expansion.

The respective ion to which the local reference and the multipole/Slater coefficients apply can be chosen in the combobox. The tab widget then offers a clearly arranged representation of the coefficients C_l^m , the Slater exponent n and the parameter Z , divided into

3 Further parameters

monopole, dipoles, quadrupoles, octupoles and hexadecapoles. Note that the monopole coefficient C_0^0 represents the global magnetic moment of that ion and that the values in the magnetic structure tab are ignored. As soon as a coefficient C_l^m is different from zero the respective multipole can be plotted in the OpenGL widget (see Fig. 3.7, left panel). When using many multipoles it can be difficult to see the individual ones clearly, so in this case the tickboxes above the OpenGL widget can be used in order to only plot the ones of interest. Clicking on *color scale according to coefficients* changes the color code in dependence on the values of C_l^m . It is also possible to visualize the weighted sum of the individual multipoles, which plots the angular dependence of the magnetization density distribution (see Fig. 3.7, right panel). Since the magnetization density is non-spherical the magnetic form factor in the right panel can now be plotted along a user-defined reciprocal lattice vector. It can also be chosen to show the amplitude, the real or the imaginary part.

On clicking *OK* all parameters are saved for each atom. In the main window the (angular dependence of the) magnetization density distribution around the ion can be visualized in the unit cell, if the *Multipoles* and eventually the *Local references* check boxes are checked in the *Plot* tab of the settings window. Note that the scale can be modified by the spin and atom plot scales, respectively.

A demo video can be seen [here](#).

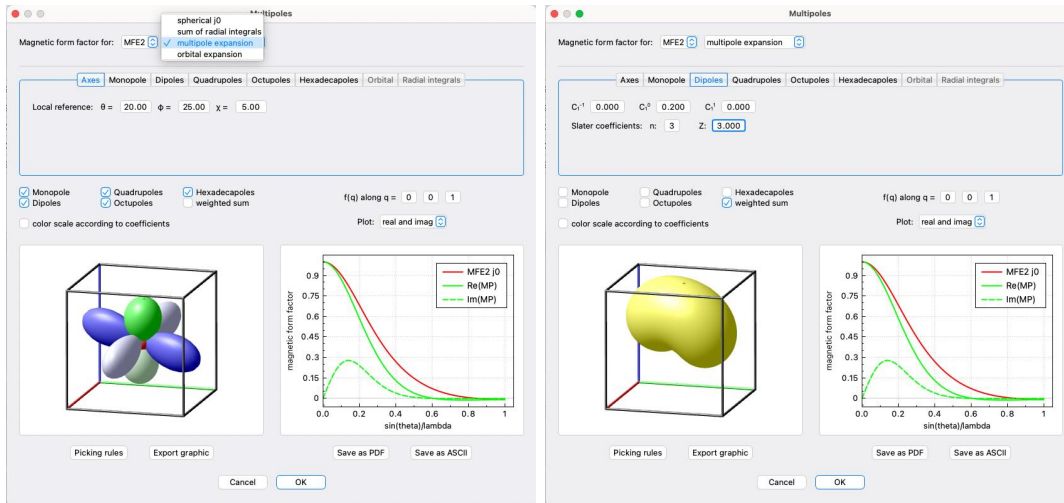


Figure 3.7: Multipole window allowing to set the coefficients of the multipole expansion of the magnetization density. Left: Visualization of the individual orbitals with positive and negative lobes. Right: Weighted sum of the individual orbitals.

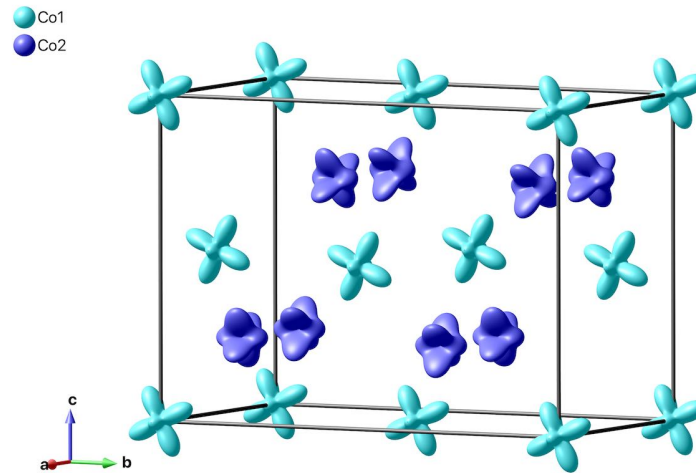


Figure 3.8: Multipole expansion of the magnetization density for each magnetic ion in the crystallographic unit cell (arbitrary population coefficients).

3.8.3 Orbital expansion

The relation between multipole population parameters and orbital occupancies can be generalized as shown in [21] for which the magnetization density distribution can be expressed in a similar way as in the previous section, but by using well-defined orbitals centered at the atomic position. The angular dependence can be chosen between $2p$, $3d$, $4f$ and a hybridized sp orbital, while the options for the radial dependence are the tabulated $\langle j_n \rangle$ values, a hydrogen-like orbital or a Slater-like orbital as in FULLPROF. Note that the coefficients C_l^m are normalized before being converted to the multipole population parameters (see Sec. 7.5) for which a single non-zero coefficient does not have any effect in a least-squares refinement.

3.9 Orientation matrix $\begin{pmatrix} \circ & \circ & \circ \\ \circ & \circ & \circ \\ \circ & \circ & \circ \end{pmatrix}$

As mentioned briefly in Sec. 2.8 the orientation matrix of a Cryocradle experiment is necessary to calculate the sample orientation for each (hkl) reflection. In other geometries the orientation matrix is necessary e.g. for calculating the absorption correction or the diffractometer angles. This UB matrix can either be entered manually or by using the smart copy-paste feature (right-click on the UB matrix which offers to paste a single value, a row, a column or the whole matrix depending on how many readable numerals have been copied to the clipboard) in the window which opens by clicking *Geometry* \rightarrow *Orientation matrix* or by selecting *Get UB* in that window. Here the individual observations with

3 Further parameters

their respective angle values after centering can be entered manually or a list of reflections can be loaded by clicking *Browse*. The program reads **.dat* files which are generated and filled by the MAD centering commands on the instrument D3. The refinement of the UB matrix is done according to the formalism presented by Busing and Levy and is based on the conventions of the instrument given in the *Geometry*→*Instrument* menu, see next section. The positioning of the sample with the Cryocradle setup does not correspond to the bisecting geometry as for standard four-circle geometries due to the fact that the angle ω is fixed. The positioning by using the angles χ and ϕ basically correspond to a non-zero ψ value (ψ being the angle around the scattering vector, which is 0 in the bisecting geometry). Fig. 3.9 shows the corresponding window for calculating and refining an experimental UB matrix after the centered reflections have been read from a file.

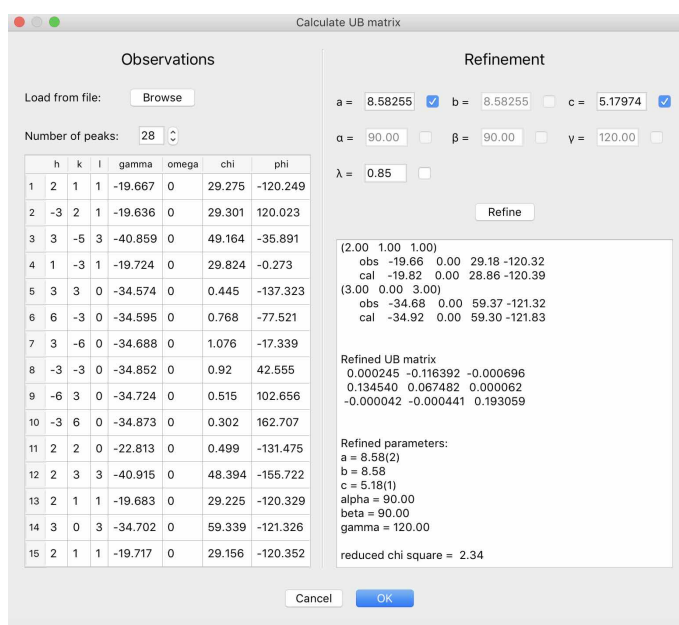


Figure 3.9: The experimental orientation matrix can be calculated and refined from a number of observed reflections.

The refinement is presently reserved for the lattice parameters only (by activating the respective check boxes), i.e. the wavelength cannot be varied. The symmetrical constrains, e.g. $a = b$ and $\gamma = 120^\circ$ are automatically set and fixed from the space group. By clicking the *Refine* button a least-square refinement will be started, where the initial orientation matrix is calculated from the first two reflections in the list and then refined on all observations.

The results of the calculation/refinement are shown in the text field and consist of the initially calculated UB matrix, a list of all observations and their observed and calculated

angles, the refined UB matrix, the refined lattice constants including their respective standard deviations and the reduced χ^2 . By clicking *OK* the refined UB matrix will be passed on to the previous window, which can then be saved by clicking *OK* on the latter.

Another possibility is to set the orientation matrix by choosing two vectors - either direct or reciprocal - pointing along the positive z axis and the positive x axis of the instrument (i.e. according to the definition of the instrument geometry), respectively. The corresponding UB matrix will be calculated by clicking on *Calc UB*. If the given vectors are not perpendicular (2-digit precision in reciprocal Å), the program will show a warning. It is possible to add an offset on ω (rotation around the vertical axis), χ (rotation around the beam axis for $\omega=0$) and φ (rotation around the vertical axis for $\chi=0$) which will automatically update the calculated UB matrix. Note that the rotation senses of the ω , χ and φ angles also follow the definition of the actual instrument geometry.

If a crystal model has been setup in the *Sample info* window (under *Absorption*) (or in the *Data reduction* window), it will be shown in a 3D plot on the right-hand side of the window (see Fig. 3.10). The usual OpenGL controls like rotating, zooming, panning and changing the light direction (ALT + rotating) are available. The plottable objects can be switched on/off using the checkboxes on top of the 3D plot, which can be exported to a *.png file by clicking on the export button. Recalculating the UB matrix from the given sample orientation (through the 2 definable vectors) or by moving the angle sliders will update the sample orientation in real time.

Furthermore, it is possible to visualize the successive rotations of the sample when posi-

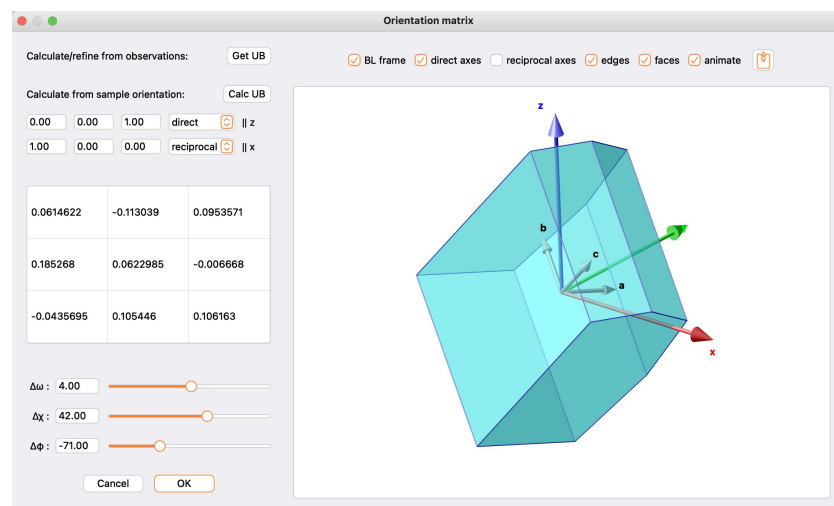


Figure 3.10: Orientation of the 3D sample model with respect to the Busing-Levy frame (colored axes). The instrument geometry definition is taken into account for the visualization.

tioning it for a particular Bragg reflection. In addition, the scattering vector, the incoming beam and the diffracted beam will be shown. This can only be achieved, when the UB matrices between the main window and the UB window are synchronized, i.e. the UB window was just opened without modifying the orientation matrix. Then, when calculating the angles and structure factors of a Bragg reflection \mathbf{Q} in the main window, the sample will be positioned in the 3D plot of the UB window. If one wishes to see the final orientation only, the *animate* checkbox can be unchecked before clicking *Go!* in the main window.

3.10 Instrument

All instrument angle calculations are based on the definitions given in the *Geometry*→*Instrument* menu (Fig. 3.11). On the one hand it is necessary for calculating the vertical sample axes for a given (hkl) reflection for polarization matrix calculations, on the other hand it is needed by the absorption correction module in order to calculate the beam path lengths in the sample (see Sec. 4.2).

Five ILL single-crystal diffractometers (D3, D9, D10, D19, D23) can be selected from the combo box and their axes definitions, angle rotation senses and standard angle limits will be automatically set. It is also possible to either change the definitions for another instrument or to choose a *Custom* instrument. The angle definitions are taken with respect to the conventions of Busing & Levy [22], i.e. the incident beam is directed along the positive y axis, z is the vertical axes and x completes the right-handed coordinate system. E.g. the definition $x: -x, y: +y, z: -z$ means that the x axis according to Busing & Levy is actually the $-x$ axis according to the instrument's definition. In this example the reference frame is rotated by 180 degrees around the y axis. In case the instrument axes definition does not coincide with the Busing & Levy convention the instrument orientation matrix is internally transformed before the calculation of the diffractometer angles. The scattering geometry can be chosen between *normal beam* and *4 circle* as well as *Cryocradle* for D3. In 4-circle geometry the chi quadrant in which the instrument performs should be given, but is automatically set to the standard value for the ILL diffractometers. The calculated angles are converted back to the instrument's convention with respect to the rotation senses and whether the neutrons are diffracted to the left or to the right. The diffraction direction is taken in the reference frame of the neutron, i.e. standing at the source and looking towards the sample. The rotation sense of the angles θ , ω and ϕ (ϕ for $\chi=0$) are called clockwise or anticlockwise when viewed from the top. The sense of χ is defined for $\phi=0$ and looking towards the source. These definitions are shown as tooltips when hovering the mouse above the respective combo boxes. The angle limits are used in order to calculate the exact position of the sample in case the bisecting scattering geome-

try cannot be achieved and/or another chi quadrant has to be tried. Note that the offsets are not yet used.

The screenshot shows a dialog box titled "Instrument" with the following settings:

- D10
- Axes definition with respect to Busing & Levy:
 - x: -x
 - y: +y
 - z: -z
- Scattering geometry:
 - 4 circle
 - Chi quadrant: 0 < chi < 90
 - Blind reflection: try -h-k-l
 - Neutrons diffracted to the: left
- Rotation senses:
 - 2θ: CCW
 - ω: CCW
 - χ: CCW
 - φ: CCW
 - v: CW
- Limits and offsets:

	Limits		Offsets
2θ	4.0	- 160.0	0.0
ω	-178.0	- 178.0	0.0
χ	-30.0	- 120.0	0.0
φ	-178.0	- 178.0	0.0
v	-20.0	- 5.0	0.0

Buttons: Cancel, OK

Figure 3.11: Instrument axes and angles definitions used for the calculation for the sample orientation at a particular (hkl) reflection.

4 Fitting

The main purpose of MAG2POL is the refinement of a nuclear and/or magnetic structure model to different kinds of data sets: spherical neutron polarimetry data, flipping ratios, integrated intensities from a monochromatic single-crystal diffraction experiment and powder diffraction patterns. Correlated refinements can be done in any combination of the previously mentioned data types. After the structural data, the magnetic structure model, magnetic domains, scale factor and extinction parameters have been entered and the unit cell has been successfully generated and visualized, one can proceed to the refinement module by clicking *Fit*→*Fit* or the icon in the toolbar.

4.1 Loading raw data

The raw data are loaded in the *Data* tab using the respective buttons. In the present version of MAG2POL the accepted data types are

- D3 *.fli files containing the polarization values of the individual polarization matrix entries and/or the flipping ratios
- D3 raw data Numors
- FULLPROF *.int files containing (a) integrated intensities of integer reflections plus eventually a list of propagation vectors corresponding to $+\mathbf{q}_n$ and $-\mathbf{q}_n$ both constant wavelength or time-of-flight (the latter is identified by $\lambda = 0$ and an additional column for the wavelength of each *hkl*) or (b) flipping ratios together with the beam polarization and the orientation matrix.
- *.col files as an output of a RACER integration [23] of two-dimensional detector data
- *.fsq files as an output of a COLL5 integration of single-detector data
- *.sf files as an output of a CCSL program
- *.bra files as an output of a D19 large-detector integration
- powder data in different formats (see below)

When data files have been successfully loaded a list will appear in the respective part of the *Data* tab of the fit window. By right-clicking on a list entry the wavelength, source and weight can be adjusted or the loaded data set can be deleted (note that the wavelength and source of powder patterns can be entered in the respective tab, which will be explained in Sec. 4.5). When loading *.fli files the program will detect if the data has been collected in polarimetry or flipping ratio geometry of D3 and will modify the GUI accordingly (e.g. enable/disable the spin-filter related information). In case of flipping ratio data the checkbox *Refine magnetic form factor* appears, which if set will add a corresponding tab to the fit window. If flipping ratio data were loaded from a *.fli file the data reduction window will open, which will be explained in more detail below for integrated intensity data. The loaded data can be viewed by clicking on *View data*. Right-clicking on a vertical header opens a context menu, which permits to delete a single reflection (*Delete*) or all reflections of the same (*hkl*) values (*Delete all*). This is useful to remove nuclear reflections, which have been measured to calibrate the efficiency of the ³He spin-filter cell, from a list of polarization matrices (note that polarization matrices from spherical neutron polarimetry data can be visualized in matrix form, both using numbers or colored dots, by clicking on the *Color plot* button at the end of the data list, see Sec. 6.16). Activating the checkbox *Refine nuclear structure* for any data type will add an *Atoms* tab containing the atomic positions, isotropic temperature factors and occupation factors as well as the scale and extinction factors. In the case of integrated intensities the checkbox *Purely magnetic scattering* should be checked, if the loaded data was obtained from a subtraction of a nuclear background.

When opening a *.col, *.fsq, *.sf, *.bra or a flipping ratio *.fli file a data reduction window will open (see Fig. 4.1), in which the user can merge the loaded data with respect to a given space group (at the beginning the space group from the main window is automatically set). The reflections will be shown regrouped and the R_{int} value will be printed together with reflection statistics (unique, symmetry inequivalent, forbidden reflections). The internal R value is calculated according to

$$R_{int} = \frac{\sum_n I_n - \bar{I}}{\sum_n I_n} \quad (4.1)$$

and the sum is taken over all n reflections without previously averaging repeated observations. Forbidden reflections can be excluded from the calculation. The reflection list is ordered by scattering angle by default, but it can be ordered with respect to h , k , l , I/R , dI/dR or 2θ by right-clicking on the corresponding horizontal header and by choosing either *ascending* or *descending* from the sort menu. A right-click on a column header to

the right of the individual (hkl) reflections allows to plot the data against 2θ , $\sin(\theta)/\lambda$ or d value. Hovering the mouse over the cell containing the integrated intensity or the flipping ratio shows the corresponding Numor as a tooltip. A particular reflection can be searched by opening a find dialog using the *Ctrl/Cmd+Shift+F* shortcut.

Among the equivalent reflections the weighted average of the observations y_i is calculated by

$$\bar{y} = \frac{\sum_i \frac{1}{\sigma_i^2} y_i}{\sum_i \frac{1}{\sigma_i^2}}$$

In the case of integrated intensities the error is given by the larger value between

$$\sigma_1 = \sqrt{\frac{\chi^2}{\sum_i \frac{1}{\sigma_i^2}}},$$

where

$$\chi^2 = \sum_i \frac{(y - \bar{y})^2}{\sigma_i^2},$$

and the arithmetical mean over the N equivalents

$$\bar{\sigma}_2 = \frac{\sum_i \sigma_i}{N}.$$

When flipping ratios are averaged among equivalent reflections, the error is calculated in a slightly different way (in MAG2POL) and corresponds to the larger value between the statistical error

$$\bar{\sigma}_S = \sqrt{\frac{1}{\sum_i \frac{1}{\sigma_i^2}}}$$

and the standard deviation reflecting the weighted distribution of the observations

$$\bar{\sigma}_D = \sqrt{\frac{\chi^2}{(N-1) \sum_i \frac{1}{\sigma_i^2}}}.$$

Furthermore, the flipping ratio statistics include the counting time T and the aimed counting time to achieve a certain error (aim value in %):

$$T_{\text{aim}} = T \cdot \left[\left(\frac{100 \cdot dR / |R - 1|}{\text{aim}} \right)^2 - 1 \right].$$

The aimed counting times are shown in color when the standard deviation is larger than the statistical error and an improvement of statistics by repeated measurements is improbable.

The (hkl) indices can be transformed by entering a transformation matrix and a precision setting (e.g. to round 5.998 to 6) in the upper-right part of the window and then clicking *Apply*. Any further application of different transformation matrices will be applied to the original indices and the applied changes can be reverted by clicking the corresponding button.

The data can then be transferred to the fit window or be exported in a format corresponding to a FULLPROF *.int file (this is also possible for flipping ratio data). Furthermore, for integrated intensity data a second data set can be subtracted from the first one by clicking on *Subtract dataset*, which is useful for removing the nuclear contribution from $\mathbf{q} = 0$ reflections. If the second data set lacks reflections which are present in the first data set, there are two options: either ignore (delete) the corresponding reflection or treating the missing reflection as $I = 0$. The latter can be convenient, if a low-temperature magnetic data set contains (hkl) reflections which are forbidden and have not been measured in the high-temperature nuclear data set. Note that before subtraction repeated reflections within each dataset will be merged.

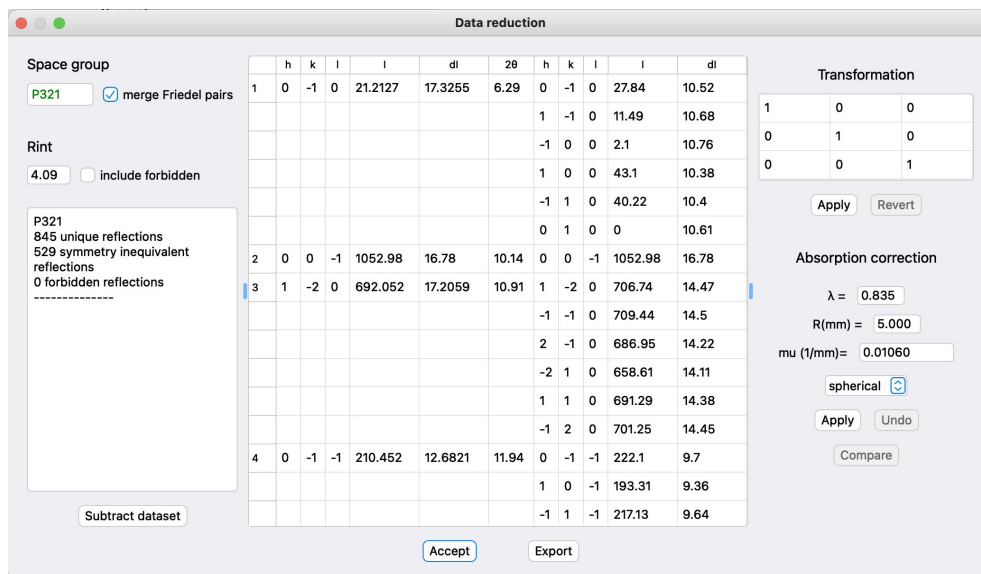


Figure 4.1: Data reduction window permitting to merge integrated intensities with respect to a given space group.

From within the data reduction window an absorption correction of integrated intensities can be applied for different sample shapes, see next chapter. Changing the wavelength automatically re-calculates the absorption coefficient and the scattering angles.

The integrated intensity or flipping ratio data transferred from the data reduction window

to the fit window as well as the data directly loaded from an `*.int` file will be shown as a list in the *Integrated intensities* or in the *Polarization data* section, respectively. Note that several data files can be loaded one after the other. A right-click on a data set offers different options in a context menu, e.g. deleting or replacing the data set. The *replace* option is useful if one wants to use the same structure including the scale factor for the refinement of another data set. Note that deleting a data set also deletes its corresponding scale factor. Other parameters which can be addressed from the context menu are the source, the wavelength and the weight of the data set in the least-squares algorithm. Polarization data sets have further options like the incident polarization, the sample orientation and the spin-filter efficiency (the latter only for polarimetry data).

Before loading powder patterns the corresponding format of the file has to be specified in the drop-down menu. The different options are

- MAG2POL format. It consists of a header with title, wavelengths, ratio and temperatures followed by the data in values of 2θ , counts and sigmas. Powder patterns in other formats can be exported in this format by clicking on *Save data* after successful opening.
- XYSIGMA corresponding to FULLPROF INS = 10
- D1A, D2B corresponding to FULLPROF INS = 6
- D1B, D20 corresponding to FULLPROF INS = 3
- FREE FORMAT corresponding to FULLPROF INS = 0
- DMC, HRPT corresponding to FULLPROF INS = 8
- GSAS TOF corresponding to FULLPROF INS = 12
- ISIS TOF corresponding to FULLPROF INS = 14

When a wrong format was specified an error message will be shown, otherwise, after successful opening a *Patterns* tab will appear in the tab widget in which the loaded data can be viewed and analyzed (see Sec. 4.5). A successfully opened diffraction pattern of any format can be exported into MAG2POL format with `*.m2p` extension. The data is stored in three columns - 2θ , counts and σ - and is preceded by a header containing the lines `TITLE`, `WAVE`, `TEMP`, `COMP` (composition parameter x , e.g. in A_xB_{1-x}) and the corresponding metadata. Further lines might be added in future versions while obviously maintaining compatibility. A pattern is exported by selecting it in the table of loaded

patterns and clicking *Save data*. Input dialogs will pop up in which the metadata can be entered. As for integrated intensity data, a right click on the data set evokes a context menu with the possibility to delete or replace the data set as well as to change the weight in the least-squares algorithm.

4.2 Absorption correction

4.2.1 Simple sample shapes

An absorption correction can be applied for spherical sample shapes and cylindrical sample shapes with normal-beam geometry, which is based on [24]. The linear absorption coefficient is automatically calculated based on the structure model and displayed in the according box, but of course, one is free to enter whatever value. The calculation is done according to:

$$\mu = \frac{\sum_i o_i(\sigma_{i,a} \cdot \lambda/1.798197 \text{ \AA} + \sigma_{i,inc})}{V} \quad (4.2)$$

where the sum is done over the atoms i of the unit cell with volume V . o_i is the occupation, $\sigma_{i,a}$ is the absorption cross section (at $\lambda = 1.798197 \text{ \AA}$) and $\sigma_{i,inc}$ is the incoherent scattering cross section of atom i . The incoherent scattering cross section is wavelength independent for most elements, with a notable exception being hydrogen for which it is given by

$$\sigma_{H,inc} = 19.2 \cdot \lambda + 20.6 \quad (4.3)$$

with λ given in \AA resulting in $\sigma_{H,inc}$ in barns [25].

After setting the radius of the sample in mm one only needs to click *Apply* to perform the absorption correction. The internal R value will directly be recalculated. The corrected, uncorrected and normalized uncorrected data can be verified under *Compare*. The button *Undo* permits to remove the applied correction.

4.2.2 Special sample shape

MAG2POL offers the possibility to index the bounding faces of a convex crystal shape based on a sequence of picture frames which can be loaded into the program (note that a crystal model can be set up *blindly* even without such frames, see hints below). This is done within an interactive OpenGL widget, which can be opened by selecting the *special* sample shape and clicking *Set faces*. When first opened the crystal model utility should show a red crosshair on a white or black background (for dark mode off/on, respectively). Depending on the platform (as seen for Linux and Windows) borders in a different color can be present, which should be removed by right-clicking within the widget and selecting ADJUST SIZE (furthermore Linux and Windows machines display a wrong aspect ratio of

the frames which is not a problem for the following treatment). The program assumes that the picture frames are taken during a successive rotation of the sample around the φ axis for 4-circle geometries or around the ω axis for normal-beam geometries. For the first, it is necessary to indicate the χ value at which the frames have been taken. Before opening the picture files the lower and upper angles spanned by the rotation should be entered in the corresponding boxes. When selecting the files in the file browser, they should be ordered according to angles with the first file selected corresponding to the lower angle. Since the camera position and rotation can be general, it should be stated to which diffractometer axes the right and up directions of the OPENGL widget refer to. The file names and camera parameters will automatically be saved in a `crystalFrames.info` file which can conveniently be chosen for the next time. The diffractometer axes should be given according to the convention of Busing & Levy, i.e. the incoming beam is along the positive y axis and the z axis is vertical, x completes the righthanded set. The orientation matrix will internally be transformed according to the instrument's definition (see Sec. 3.10). On the ILL instruments the camera is mounted on the omega table and is pointing upwards. With the neutrons entering from the top part of the taken picture the correct settings for this geometry are those which are loaded by default, i.e. right = $+x$, up = $-y$. The frames are then taken by rotating around the φ axis with $\chi = 90^\circ$ and the sense of rotation is calculated based on the instrument's definition.

Camera and sample offsets can be set in the *Offsets* tab on the right. x sample offsets should be set, when a picture close to $\varphi = 0$ is viewed, while y sample offsets can be seen for $\varphi \approx 90$. The buttons for ± 90 or ± 180 rotations can be used for finding the offsets conveniently. A z sample offset concerns the height along the sample pin. The camera offsets refer to the lateral misalignment of the camera and its rotation around the z axis. The goal is to have the crystal's center of mass in the center of the crosshair. In the *View* tab it is important to set the zoom factor so that the radius of the crosshair (in mm) corresponds roughly to the real crystal dimensions.

The frames can be viewed by dragging the horizontal slider below the OPENGL widget or by using the buttons below it. The play speed can be adjusted and the loop checkbox can be set, if you want to see a continuous rotation.

In order to add a plane to the crystal model, one has to rotate the crystal to a position in which the face is parallel to the view direction. In this position simply click and drag a line along the edge, which will add a plane (converted to hkl) to the table. The length of the line is not very important and only serves for drawing unbound planes as a square having the edge length according to the drawn line. By adding more planes in

different sample positions the program will redraw the bound volume and show the model on top of the picture. Note that it is of course possible to draw a sample model without having loaded any frames. In that case, it is recommended to change the plane color under the *View* tab to a different color than the background. First, one should draw e.g. four lines in the shape of a square around the crosshair, then move the φ slider by $+90^\circ$ or -90° and draw two horizontal lines above and below the center position, which should create a closed volume.

In order to highlight a plane simply click on it in the table or in the model. When a parameter in the table is highlighted, it can be adjusted using the horizontal slider or a new value can be entered directly. The crystal model will be updated instantaneously. If a plane is actually needed to draw the smallest possible volume will be shown with a *yes* or *no* in the last column of the table. Planes can be removed by right-clicking the vertical header and selecting *Delete*. Multiple planes can be deleted simultaneously. For very irregularly shaped crystals it may be more intuitive to uncheck the *Hide planes behind picture* option in the *View* tab. An example of a complex crystal shape is shown in Fig. 4.2 and a tutorial video can be seen [here](#). By clicking *OK* the created planes will be transferred to the Data reduction window. Note that the planes are only saved when at least 4 used planes are present. Unused planes are not saved. MAG2POL will automatically calculate the corresponding diffractometer angles for every measured reflection based on the instrument definition and will determine if a non-zero ψ angle or a different χ quadrant was necessary to measure a particular reflection. Furthermore, the number of integration samples should be given along the a , b and c axes of the sample by clicking on *Set grid*. The grid points will be distributed according to the Gaussian integration procedure described in [26].

Once all the necessary information are entered, the absorption correction is done like for simple sample shapes by clicking the *Apply* button. By clicking on any hkl index in the table the orientation of the crystal model and the integration points are shown together with the diffractometer axes and the incoming/outgoing neutron beams (see Fig. 4.3). The planes of the model which are intersected when diffracting from the origin are marked by orange edges. The diffractometer angles are shown below the OpenGL widget together with the average path lengths along the incoming (r_1) and outgoing beam (r_2). The

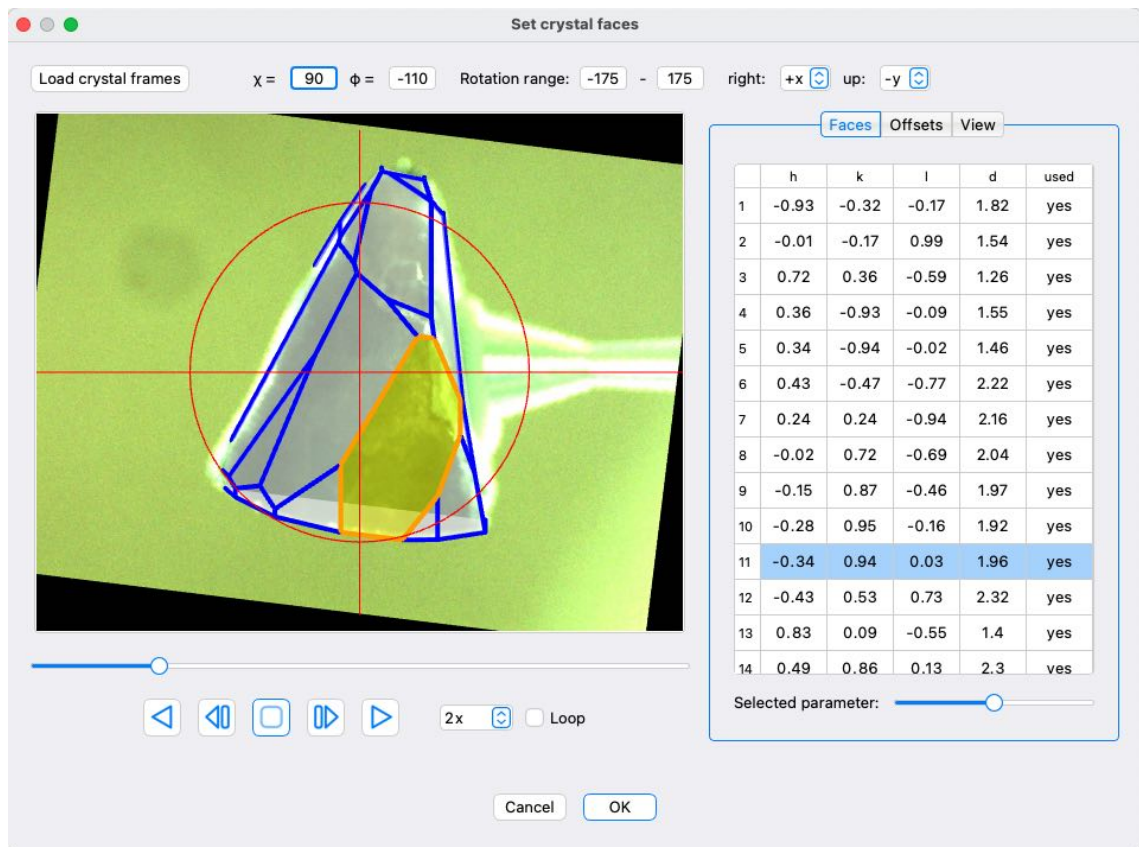


Figure 4.2: Complex crystal shape containing 19 limiting faces.

average transmission T is approximated by a Gaussian integration [26] according to

$$\begin{aligned}
 T &= \int_V \frac{1}{V} \exp[-\mu(r_1 + r_2)] dV \\
 &\approx \sum_{i=1}^{n_x} \sum_{j=1}^{n_y} \sum_{k=1}^{n_z} (b-a)[d(x_i) - c(x_i)][f(x_i, y_j) - e(x_i, y_j)] R_i R_j R_k 1/V \exp[-\mu(r_1 + r_2)],
 \end{aligned}
 \tag{4.4}$$

where the a, b, c, d, e, f are the corresponding limits of integrations and the R_i, R_j, R_k are the respective weights which are taken from [27]. The visualization of the scattering geometry is animated by default, i.e. the successive rotation of angles will be shown. By unchecking *animate* the final diffraction position will be shown immediately. For a more fluid rendering the grid points can be omitted in the rendering process. The absorption

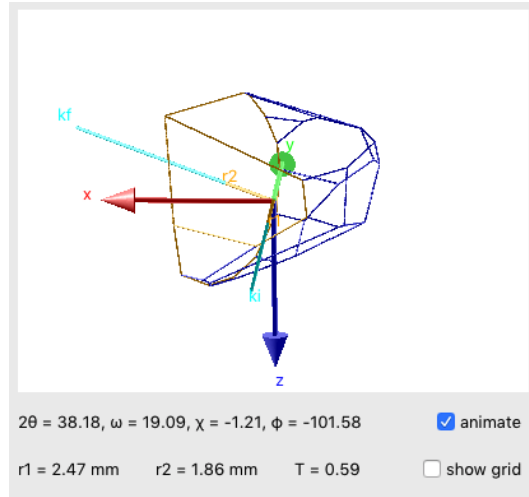


Figure 4.3: Orientation of the sample for a given (hkl) reflection within the Busing-Levy frame (colored axes). The diffractometer angles are give together with the average beam paths inside the sample and the transmission factor.

correction in MAG2POL has been compared to the subroutine AVEXAR of the CCSL subroutine library for normal beam and 4-circle geometries. The results are identical within rounding errors starting from $n_x = n_y = n_z = 3$ as can be seen in Fig. 4.4.

4.2.3 On-the-fly absorption correction

The absorption correction mentioned in the section above can be applied to correct the dataset of integrated intensities which was opened in the data reduction window. In that case the correction factors are applied to each measured (hkl) reflection before an eventual merging with respect to the given space group. The corrected data can directly be used

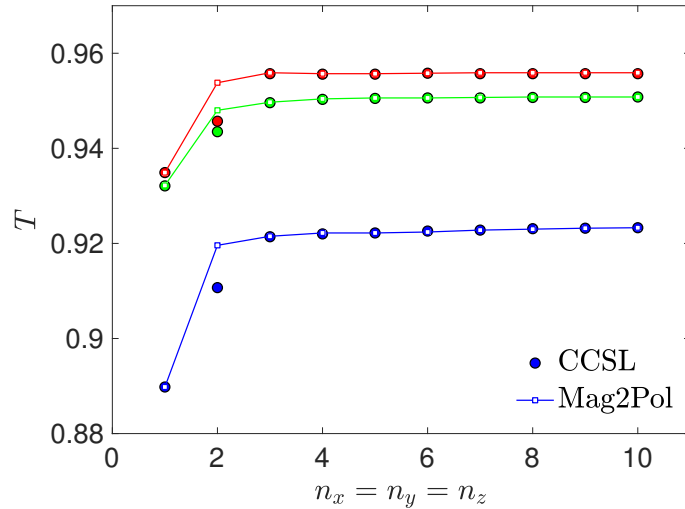


Figure 4.4: Transmission as a function of integration points $n_x = n_y = n_z$ for three different Bragg reflections calculated by MAG2POL and CCSL.

in the analysis or they can be exported into an `*.int` file.

It is also possible to use the convex-hull crystal model to do an *on-the-fly* absorption correction, which is useful if one wants to refine the occupation of a heavy absorber as it influences both the absorption through the linear absorption coefficient and the scattering potential through the scattering length (e.g. incomplete ^{11}B or ^{160}Gd substitution). This possibility allows for a self-consistent analysis of the data. In order to activate this feature a crystal model needs to be present before entering the fit window, which can be done by opening the *Sample info* window (see Sec. 6.1) and clicking *Edit* under the *Absorption* tab. In that case, when the fit window is entered the option *On-the-fly absorption correction* becomes visible below the loaded integrated intensity data. When it is activated the program will calculate the neutron beam path lengths for all the reflections only once before starting the refinement iterations. In each iteration the linear absorption coefficient may be different, if the atomic occupations are refined parameters. Note that the use of this feature is even possible for multiple integrated intensity files as long as the data were recorded in the same instrument geometry (e.g. different wavelengths).

If the occupation of a heavy absorber is uncertain and needs to be refined, the recommended procedure is the following:

In a first step, the integrated intensities should be reduced in $P1$ or $P-1$ symmetry (the beam path lengths are identical for Friedel pairs, however, small deviations may be possible in the calculation due to precision errors) and loaded for the refinement. After activating the *on-the-fly absorption correction* check box, the nuclear structure refinement can be

done as usual.

In a second step, the refined nuclear structure from the first step should be used to apply the absorption correction on the raw data which are then eventually merged and exported (as explained in Sec. 4.2.2). Alternatively, a corrected data set can be conveniently created after the refinement process by clicking on *Create corrected dataset* at the bottom of the *Fit* tab (note that in the presence of multiple data sets, a single one has to be selected first from the plot data combo box). This will subtract the $\lambda/2$ contamination from the observed intensities and then correct for absorption and extinction effects (the latter only in the case of the Becker-Coppens model which also depends on the beam path within the sample). The resulting intensities will be shown in a new data reduction window and can be merged, exported or directly used for the subsequent analysis (note that it may be necessary to change the wavelength either in the data reduction window or in the fit window using the right-click menu in the loaded data list, since the wavelength in the data reduction window is initially read from the main window).

The last step consists in refining the nuclear structure to the corrected and merged data set of step 2 (without the *on-the-fly* option), which should give similar results as in the first step, but with better agreement factors due to a reduced number of observations (due to the merging of equivalent reflections).

4.3 Correction for the spin-filter efficiency

Usually the efficiency of the ^3He spin-filter cell is monitored by measuring e.g. the polarization P_{zz} on a purely nuclear Bragg peak - which is known to be 1 - several times a day during the experiment. The reduction from the expected value is due to the initial polarization of the neutron beam (which can be set in the *Settings* menu) and the spin-filter efficiency. In the case of a loaded *.fli file the program analyzes the lines which signal a cell change and the time of the respective observations to show the decrease of efficiency as a function of hours. On D3 depending on the used cell the decay is usually between 10 and 20% per day. The reflection on which the calibration has been performed throughout the experiment and the polarization canal has to be selected followed by clicking *Apply*. The polarization data will now be corrected with respect to the decaying spin-filter efficiency according to

$$P_{corr} = P_{mes} \cdot \frac{P_0}{P_{cell}} \quad (4.5)$$

where P_0 is the polarization of the incident neutron beam, note that setting this value to 1 in the settings of the program or in the input dialog after clicking *Apply* will correct the data also for the initial polarization. Repeated measurements of the same polarization matrix element for the same (hkl) reflection can optionally be merged by activating the

corresponding checkbox. A further checkbox can be activated, if a certain temperature-binning should be applied to the merging. A weighted average will then be calculated from the standard deviations given in the *.fli file. In order to interpolate the spin-filter efficiency for any given time an exponential decay function of the form

$$P(t) = P_{0,n} \cdot \tanh[O \cdot P_{0,He} \cdot \exp(-t/T_{1/2})] \quad (4.6)$$

is used, where $O = \lambda \cdot l \cdot p \cdot 7.282 \cdot 10^{-2}$ is the cell opacity at room temperature. The wavelength, the length of the cell l , the cell pressure p and initial cell polarization $P_{0,He}$ are fixed, while the half-life $T_{1/2}$ and the initial neutron polarization $P_{0,n}$ are refined. The results can be seen by clicking on *View cell efficiency*, which opens a window similar to the one shown in Fig. 4.5. The different cells recognized from the entries in the *.fli file

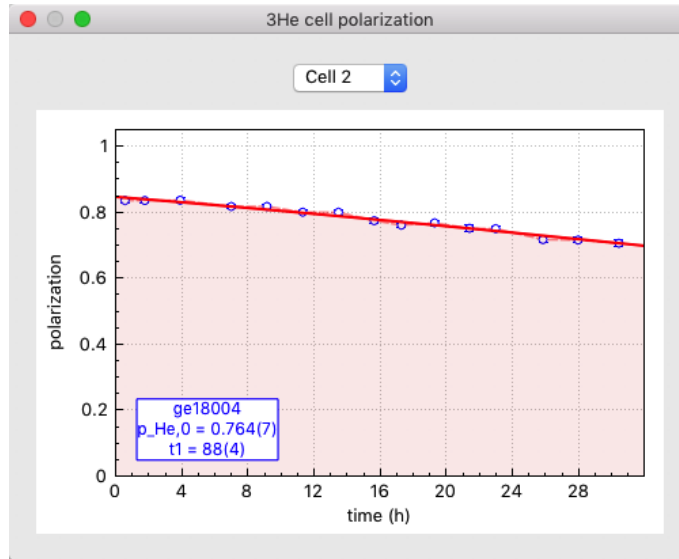


Figure 4.5: Visualization of the spin-filter efficiency decay as a function of time.

can be chosen from the combo box. The legend shows the name, the pressure and initial polarization of the cell as well as the refined values including standard deviations for the initial neutron polarization and the half-life. The refined neutron polarization should be similar to the nominal neutron beam polarization of the instrument.

The corrected data can be saved from the fit window in order not to repeat this procedure.

Note that when chiral or nuclear-magnetic interference scattering is present, the polarization data should only be corrected to the spin-filter efficiency and not to the initial polarization (i.e. the P_0 value of the incident beam needs to be entered in the MAG2POL settings) as the respective entries contain terms which are dependent on the initial neutron polarization and terms which are not. Two options are possible:

- In order to analyze the raw data the checkbox *Refine on uncorrected data using cell efficiency* should be activated before you hit the button *Apply*. The program will still take into account the cell efficiency at a given time of an observation, but it will be used in combination with the initial neutron polarization to calculate the respective entry of the polarization matrix. In this case no merging of reflections is possible.
- The raw data can be corrected for the spin-filter efficiency only. This can be done in two steps. First, click *Apply* and accept the popup input dialog with whatever value, then extract the refined incoming neutron polarization $P_{0,n}$. In a second step, delete the *.fli file and load it again. This time, when applying the correction, enter the previously refined $P_{0,n}$ value.

Loading Numors directly is intended for a special type of measurement, where the initial neutron spin is rotated within the local y - z plane. The positions and amplitudes of the minima and maxima allow important conclusions concerning the magnetic structure. In this case the polarization value (including the time of the observation) as well as the directions of the initial neutron polarization and analysis vector are extracted from the Numor files. As no information is present concerning any potential spin-filter cell changes only those data should be loaded which have been measured with the same cell. The correction with respect to the cell efficiency is done as described above (note that for a final polarization vector within the y - z plane no chiral scattering is present).

4.4 Refinement flags and constraints

All the magnetic ions defined within the magnetic structure will be listed in the same order under the *Magnetic moments* tab as M1, M2, The magnetic domains are shown under the *Domains* tab together with their corresponding symmetry, an eventual keyword signalling an inversion or chiral domain and their population. In the case of a form factor refinement, the multipole, orbital or radial integral coefficients are refinable parameters as well. By activating the checkbox next to a respective value, this parameter will be considered as a refined variable. Nuclear structure parameters can be refined, when the checkbox *Refine nuclear structure* is activated in the *Data* tab, which will insert a new tab called *Atoms* including the positions, thermal and occupational parameters, scale factor and extinction coefficients. A right-click on any table's column header or tab (except for the *Data* tab) opens a context menu for quickly (un)checking all respective parameters. Anisotropic displacement parameters can be flagged by choosing the *set betas* context menu entry after right-clicking an isotropic temperature factor. Constrained B_{ij} values and fit flags are disabled if they are constrained by symmetry.

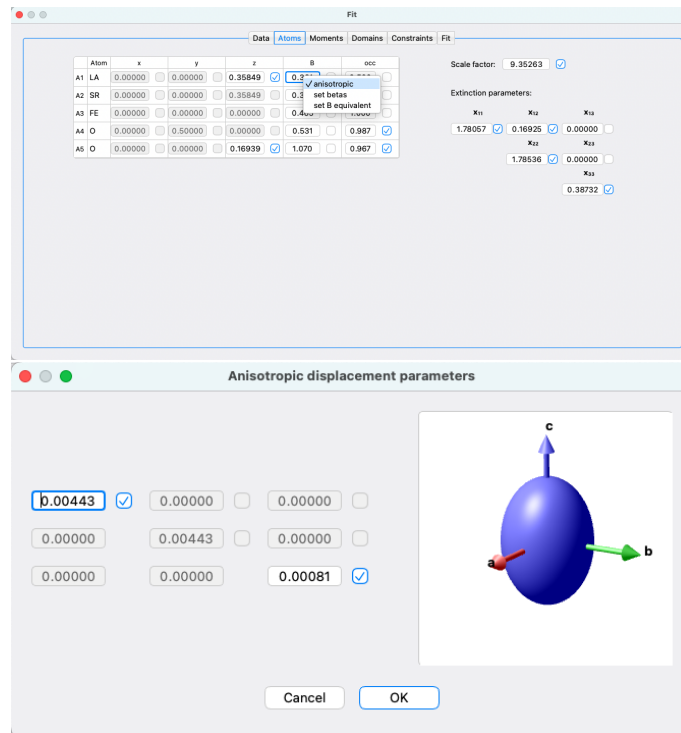


Figure 4.6: Anisotropic displacement parameters and the visualization of thermal ellipsoids.

Linear constraints can be set under the *Constraints* tab by choosing the variables and relations from the combo boxes and entering the proportionality factors and summands by hand. $M1$ refers to the whole vector of magnetic moment 1, $|M1|$ refers to the modulus of the moment, whereas $Mr1$ and $Mi1$ would denote the real and imaginary part, respectively (note that vector quantities can only be constrained to other vector quantities and that a moment modulus can only be constrained to another moment modulus). In the case of non-zero real and imaginary components, MAG2POL will constrain Mr and Mi to be perpendicular, if they are not defined as parallel. If the real components are refined, the imaginary vector will be adjusted and vice versa. If both real and imaginary components are refined, the imaginary vector will be adjusted after each iteration.

The constraints take the form of

$$p_1 = a \cdot p_2 + b \quad (4.7)$$

where p_1 depends on p_2 . If you choose the equal sign, the parameter p_1 is regarded as a constant (in relation to parameter p_2) and should therefore not be refined. For relations 'greater than' or 'smaller than' the constrained parameter p_1 should be marked as a refined parameter. If the multiplication factor a is 0, then p_2 is a dummy parameter which is not

necessarily refined and p_1 is directly related to the scalar b . If $|a| > 0$, then p_2 needs to be set as a refined parameter as well (note that errors will be shown as pop-up warnings). The keyword *various* for parameter p_1 can be used to define multiple constraints. By choosing *various* a button will appear to the right which permits to select various parameters from a list which will be constrained to p_2 (see Fig. 4.7).

In the present version of MAG2POL up to 20 constraints can be set. In case of multiple magnetic domains or structural twins, the population of the first domain/twin is automatically set to 1 minus the rest in each iteration. Constraints can be deleted by right-clicking the parameter to be constrained and then clicking *Delete*.

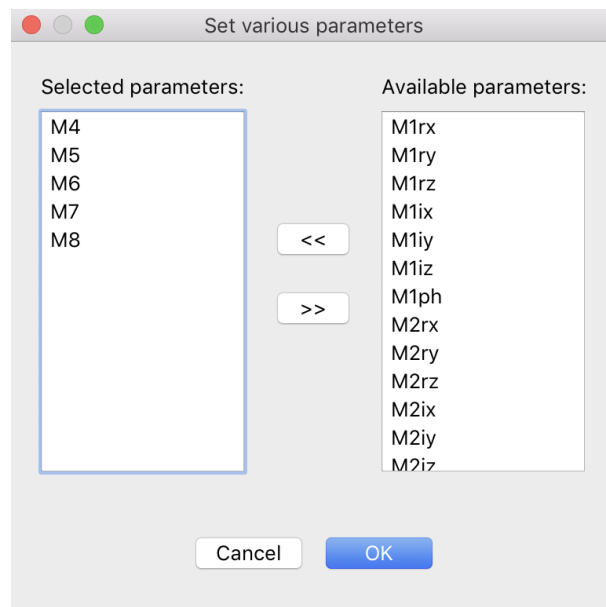


Figure 4.7: Multiple parameters can be selected after choosing *various*.

Note that constraints on atomic positions due to special Wyckoff sites, e.g. $(x \ x + \frac{1}{2} \ z)$ or $(x \ 2x \ \frac{1}{2})$, do not need to be set by the user, because MAG2POL will consider them automatically. The same applies to anisotropic temperature factors of atoms on special sites.

Freeform constraints can be constructed in a similar way as the linear constraints, but they offer additional flexibility and complexity. They can be entered freely by following a certain syntax. Parameter names need to be enclosed in quotes and mathematical expressions, e.g. \exp , \sin , need to follow C++ syntax (i.e. x^2 is written as `pow(x,2)`). On the left-hand side of the (in)equality sign either only one parameter should be entered or several parameters separated by commas. On the right-hand side, any equation can be entered. The correct syntax is visualized by green text, while the opposite is shown as

red text. It is recommended to separate the parameters from the operators by a space as eventual double minus signs can be wrongly interpreted. Parameters can also be inserted by right-clicking the line edit and by choosing from the context menu. For example, 2 site occupations constrained simultaneously to be one minus the site occupation of 3 other sites is written as `'A1occ', 'A2occ' = 1 - 'A3occ' - 'A4occ' - 'A5occ'`. Both linear and freeform constraints will show a warning in the fit output, when a boundary was hit in the case of an inequality constraint.

Simple constraints, i.e. of the form $p_1 = p_2$, can directly be set in the *Atoms*, *Moments* and *Domains* tabs by right-clicking the respective label and evoking context menus as shown in Fig. 4.8. Note that the parameter to which one wishes to constrain needs to be placed higher in the atom/moment/domain/twin list or it needs to be in a phase with lower index. E.g. the position of atom 3 in phase 2 can be constrained to atom 2 of the same phase or to atom 4 of phase 1. Parameters being lower in the list are automatically grayed out in the context menu.

In the case of atoms the parameters which can be constrained are

- position: x , y and z fractional coordinates
- B: isotropic temperature factor
- anisotropic B: all anisotropic displacement parameters
- occupation: the occupation factor
- split occupation: 1 minus the occupation factor for two atoms occupying the same site
- all atomic parameters: all of the above (except for the split occupation)

If the parameter in questions is a magnetic atom, the options are

- moment: all real and imaginary components
- moment modulus: the modulus of the moment
- real part: the parameters belonging to the real part of the complex magnetic moment
- real part modulus: the modulus of the real part of the complex magnetic moment
- imaginary part: the parameters belonging to the imaginary part of the complex magnetic moment
- imaginary part modulus: the modulus of the imaginary part of the complex magnetic moment

4 Fitting

- phase: the magnetic phase
- all magnetic parameters: all real and imaginary components as well as the magnetic phase

In the case of domains and twins the population can be constrained to any other domain/twin population with a lower index similarly to what was explained above concerning atomic sites. Note that constraining a domain (twin) population to the first domain (twin) population equally distributes the remainder of the other domain (twin) populations to 1 (i.e. 1 minus the rest) on the constrained domains (twins), which is not supported when using constraints under the *Constraints* tab. Setting a constraint in this way will disable the manual editing of the corresponding parameters and fit flags. In order to quickly find to which parameter a constraint is set, the corresponding menu fonts are set in italic. A constraint can be removed by unchecking it. Some constraint combinations will be automatically summarized as a different one, e.g. if the imaginary part of a magnetic moment is constrained after the real part was already constrained, then the constraint will be found under *Constrain moment*.

Changing a parameter will automatically update the parameter(s) which is/are constrained to it (both for constraints under the corresponding tab as well as for simple constrained which are set via context menus).

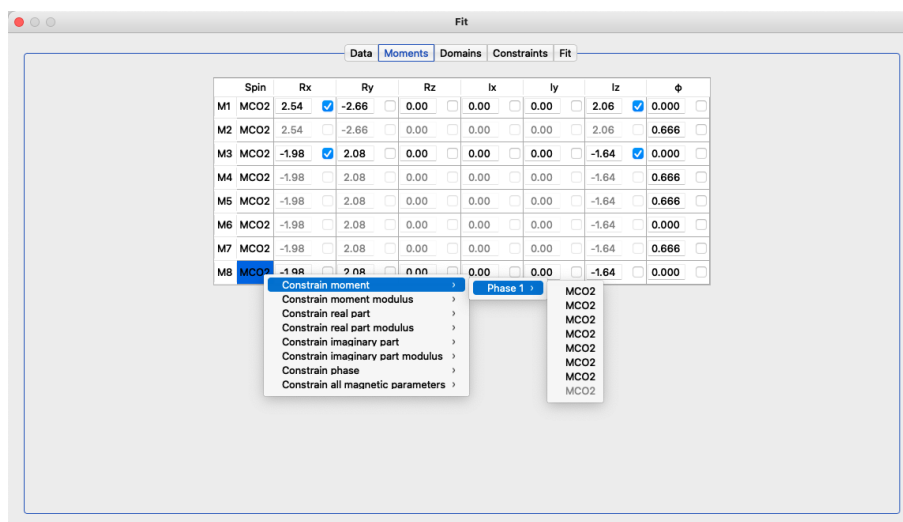


Figure 4.8: Simple constraints can conveniently be set using context menus.

4.5 Powder patterns

When at least one powder pattern has been loaded, the *Patterns* tab appears which is shown in Fig. 4.9. The left part of the tab features the pattern plot with the corresponding plot controls above it, while the scroll area on the right side contains all necessary parameters and fit flags separated into different categories. The category labels, e.g. *Geometry*, *Background*, etc., contain further options which can be evoked by right-clicking the label which opens a context menu. The context menu generally contains a list of loaded patterns and contributing phases in order to set constraints between them (see Sec. 4.5.6). Further options of certain categories are explained below. Note that the parameters depend on the type of data loaded, i.e. if it was taken on a constant-wavelength or a time-of-flight diffractometer.

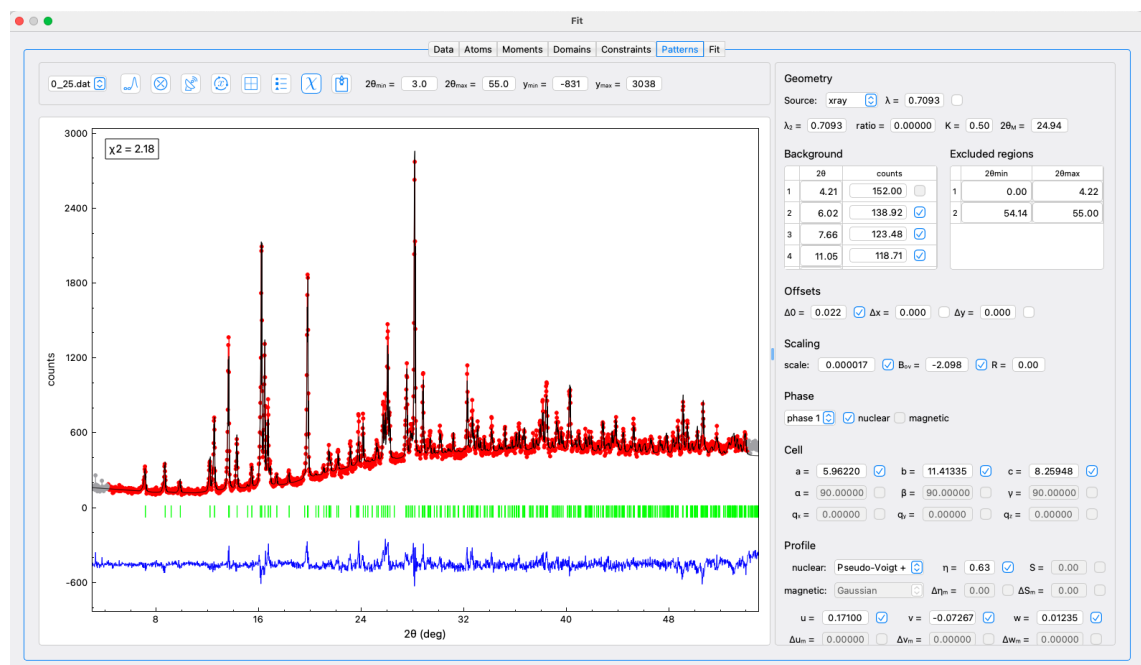


Figure 4.9: Pattern tab within the Fit window in which all parameters can be set which are necessary for the Rietveld/LeBail refinement.

4.5.1 Plot controls

The default plot options show the observed data points in red, the calculated pattern in black and the difference between the two in blue (the colors can be set in the program settings). Furthermore, the positions of nuclear and magnetic Bragg reflections calculated from the underlying model(s) are shown as green markers between the data and the

difference curve. Like in other 2D plots hovering the mouse over data points shows the respective coordinates, while hovering over the peak markers reveals the scattering angle (or time of flight, Q , d depending on the axis choice), the Miller indices and the multiplicity of the Bragg reflection. When more than one pattern file was loaded, one can switch between them by choosing from the combo box in the upper-left corner. The two buttons to the right of the combo box toggle the background and excluded regions mode which will be explained in Secs. 4.5.3 and 4.5.4. The third button activates the propagation vector finder tool, see Sec. 6.10, and the fourth button cycles the x axis unit between scattering angle / TOF, scattering vector Q or d -spacing. The next 3 buttons toggle the plot grid, the legend and the χ^2 value on the plot, whereas the last button exports the plot into either a pdf or an ASCII file taking into account the actual zoom (note that for the ASCII output the excluded angles and peak markers are labelled with an asterisk, whereas the latter are given in 2θ /TOF values after the data table). The plot boundaries for the 2θ and counts axes can be set further to the right. Those boundaries will also be used for the plot in the *Fit* tab. They can be reset to the optimal values by right-clicking on any of the 4 values and then clicking *reset boundaries*. SHIFT-clicking the plot permits to drag the pattern without changing the zoom.

4.5.2 Geometry

The *Geometry* section concerns the basic information of the used instrument like the source (neutron or x-ray) and the wavelength. Note that constant-wavelength (CW) and time-of-flight (TOF) instruments in Debye-Scherrer geometry are currently supported in MAG2POL. For CW patterns the $\lambda/2$ contamination or the $K\alpha_2$ line can be entered in the λ_2 field with the corresponding intensity ratio between λ_1 and λ_2 . When *x-ray* is selected, a right-click on the λ_1 value allows the selection between different frequently used x-ray $K\alpha_{1,2}$ lines. The values K and $2\theta_M$ are only needed in the x-ray case in order to calculate the monochromator polarisation within the Lorentz factor (see Sec. 7.7.1). For TOF patterns the detector bank angle $2\theta_B$ has to be given. From the *Geometry* context menu the instrument configuration of various instruments from different sources can be loaded, which include the wavelength, the resolution, the peak shape and asymmetry parameters for constant-wavelength diffractometers as well as time-of-flight, detector bank, rise and decay and peak shape parameters for TOF. This is a convenient way of setting up a starting point of the refinement, see Fig. 4.10.

4.5.2.1 Instrument resolution function (IRF)

The resolution function of an x-ray or neutron powder diffractometer can be loaded from and saved to an `*.irf` file (same format as for FULLPROF). Both options can be evoked

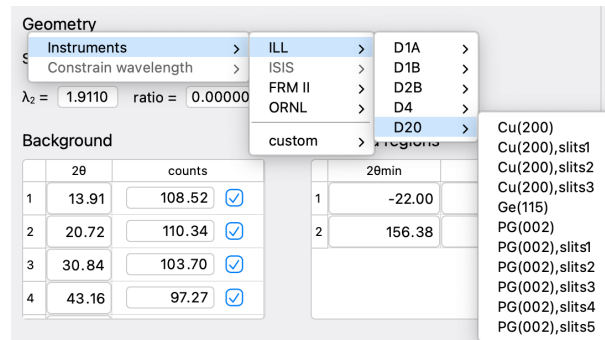


Figure 4.10: Selection of predefined instrument configurations.

from the *Geometry* context menu by choosing the *custom* submenu. After successfully loading an IRF file all read parameters will be applied to the current pattern and refinable parameters, e.g. u , v and w for CW data or σ_n , γ_n , α_n and β_n for TOF data, will be set to 0 and the respective label changes to a preceding Δ . This means that the instrumental contribution is now stored internally (the global value can be retrieved by hovering the mouse over the respective parameter label) and only the difference due to the sample contribution should be refined (see Sec. 7.7.1.8 for the respective isotropic Gaussian and Lorentzian broadening parameters). Note that the observed resolution function can be visualized (split into Gaussian and Lorentzian parts for the TCH Pseudo-Voigt profiles) by right-clicking the *Profile* label in the *Patterns* tab.

For TOF patterns the profile lookup table - containing d values vs. σ^2 , γ , α and β - supplied by FULLPROF IRF files is supported. For a particular d value in a pattern, the table values are interpolated (or extrapolated if before/after the first/last entry). This lookup table can be edited or created by clicking *edit profile table* from the *custom* submenu. When creating a lookup table from scratch, the peak finder slider can be used as well as individual peaks can be added/modified/deleted exactly as in the *Cell finder* window (see Sec. 6.9). Individual peaks can be examined by clicking on the vertical header number and the modification of the peak profile parameters leads to a live update of the plotted peak. The first fit option is fitting the table values to the polynomial d -value dependence as shown in the upper part of the window. This functionality can be useful to determine and visualize an instrument resolution function. This can be done by right-clicking any of the σ^2 , γ , α or β headers and choosing either *Plot vs. d* or *Plot vs 1/d*. Note that individual values in the table being checked are excluded from the fit. On the other hand, a global refinement to the selected sections of the diffraction pattern can be done. Each selected section is marked by a blue bar in the main window (corresponding to a d -value in the lookup table) and the fit range corresponds to the number of FWHM specified in the settings menu. Here, the checked profile values in the lookup table are

4 Fitting

independently refined from the global d dependence given by the parameters at the top of the window. The individual parameters can be constrained to vary less than a given percentage from the global value by checking the respective *shift* checkbox.

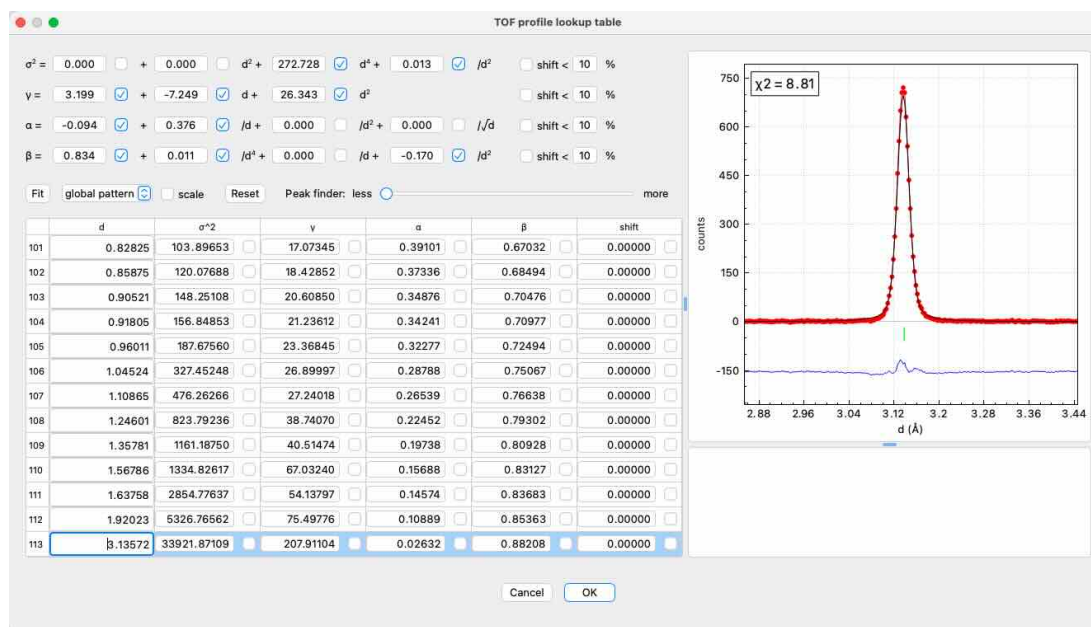


Figure 4.11: Profile lookup table for TOF powder patterns with different plot and fit functionalities.

4.5.3 Background

There are different ways to introduce the background of a powder pattern. The first is to give a list of points between which a linear interpolation is calculated. In order to do so the background mode needs to be activated by clicking on the first button next to the pattern file name. If a background is already defined it will be shown as green squares connected by green lines (see e.g. Fig. 4.9). A background point is simply added by left-clicking on the pattern. A green square will be added to the plot and the corresponding 2θ value and counts will be added to the table on the right. An already drawn point can be moved by placing the mouse over it which will turn the mouse cursor into an open hand symbol. Now simply click and drag the background point to the desired position. The coordinates of each point can also be modified by directly editing them in the table. A background point can be deleted by right-clicking it. The pattern will be calculated using the newly defined background after leaving the background mode, i.e. by clicking the corresponding button.

The background can also be modeled with a polynomial function of different degrees or

with a Debye-like model (see Sec. 7.7.1.7 for more information). In order to change the background type, simply right-click the *Background* label in the scroll area and select one of the different models, see Fig. 4.12. Note that when you select *polynomial (6 coeffs)* and you have manually introduced points before, the program will fit the coefficients (if they are all equal to 0) to the linear interpolation as a convenient starting point. From there you can eventually choose one of the two more complex models.

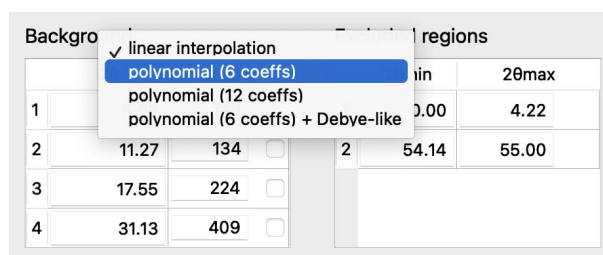


Figure 4.12: Selection of different background models.

4.5.4 Excluded regions

All regions of the powder pattern which cannot be explained by the underlying model(s), e.g. direct beam, negative intensities, zero sigmas, parasitic peaks etc., should be excluded from the refinement and from the calculation of agreement factors. In order to do so one has to activate the excluded region mode by clicking the second icon next to the pattern file name. Now, excluded regions can be drawn by left-clicking and dragging which will create a gray box (note that zooming is disabled when excluded region mode is activated). Already drawn excluded regions can be modified by placing the mouse over one of the limits which will change the mouse cursor into horizontal arrows. The lower/upper limit can now be dragged. The excluded regions can also be modified in the table on the right. An excluded region can be deleted by right-clicking it in the pattern plot. Note that depending on the chosen option in the settings menu the pattern is nevertheless calculated in these regions, but not included in the calculation of χ^2 .

4.5.5 Pattern and phase parameters

In order to allow the correlated refinement of powder patterns and single-crystal data at different temperatures, the overall temperature factor B_{ov} has a special function. If it is set to 0 and is not refined, then the temperature factors listed in the *Atoms* tab will also be used for this particular powder pattern. If a non-zero value is entered for B_{ov} or if it is flagged as a refined parameter, only the B_{ov} value will be used in the powder pattern, while the B values in the *Atoms* tab are applied to the single-crystal data. Like this it

is also possible to use anisotropic temperature displacement factors for single-crystal data sets, while using an overall isotropic temperature factor for the powder data at the same time.

The remaining parameters grouped in the *Offsets/Time of flight* and *Scaling* categories are explained in Secs. 7.7.1 and 7.7.1.6.

More than one phase can contribute to a single pattern and in that case multiple phases have to be set up in the main window (see Sec. 2.2). The parameters which are grouped in *Cell*, *Profile*, *Asymmetry/Rise and decay*, *Preferred orientation* and *Absorption and extinction* (only for TOF) concern a specific phase in a specific pattern. The pattern can be specified - as explained above - by choosing from the combo box in the upper-left part of the tab. The phase can be chosen in the *Phase* category. Furthermore, it can be defined if the phase has a nuclear contribution, a magnetic contribution or both. A right-click on the contribution labels (*nuclear* or *magnetic*) allows to toggle between Rietveld and LeBail refinement for that particular contribution. Having different sets of parameters for the same phase, which contributes to different patterns, allows for example the co-refinement of two patterns at two very different temperatures resulting in different lattice constants. The only part which is common to all patterns (and other types of data of the same phase) are the parameters listed under the *Atoms* and *Moments* tabs (except for the temperature factors if $B_{ov} > 0$ in the powder pattern). Therefore, one has to keep in mind that co-refining different data sets is only meaningful if one can assume that the fractional atomic parameters do not change too much. Note that the information given in the *Domains* tab is ignored for the calculation of powder patterns, i.e. only a single twin with a single magnetic domain is considered. If different phases with different cell metrics contribute to the powder pattern, the option *Ignore secondary phases for single crystal* needs to be checked in the settings menu, if a co-refinement with single-crystal data is intended. Otherwise, the contribution of secondary phases will be considered to the (*hkl*) reflections of the main phase, which is not correct.

Note that after accepting a fit result (click on the *Accept* button) the lattice constants and the propagation vector(s) are not automatically transferred to the model(s) in the main window as those values are in principle used in the reduction and refinement of single-crystal data (the cell and \mathbf{q} are of course saved in the powder model). One can however transfer these parameters between the main window and the models for powder patterns by right-clicking the label *Cell* or *Propagation vector q* (in the *Symmetry* and *Spins* tab of the main window) and choosing the corresponding option and pattern number.

4.5.6 Constraints

If one can safely assume that the same structural model contributes to different patterns, e.g. a neutron and an x-ray pattern taken at the same temperature or two neutron patterns taken with different wavelengths, then constraints should be set. In such a case it would be a good idea to constrain the cell parameters. Or if two phases contribute to the same pattern and one can exclude peak broadening due to strain, then the profile parameters could be constrained. Constraints can conveniently be set by right-clicking the respective category label and then choosing the pattern and phase to which the parameters should be constrained (in analogy to simple constraints described in Sec. 4.4). The example in Fig. 4.13 shows how the cell parameters of phase 1 in pattern 2 are constrained to the cell parameters of phase 1 (i.e. the same phase) in pattern 1. After setting a constraint the corresponding values are directly synchronized and the fit flags (in this case of phase 1 in pattern 2) are disabled. It is not necessary to constrain the profile and asymmetry parameters of the magnetic contribution to the nuclear contribution, since all magnetic parameters are Δ values, i.e. they are added to their nuclear counterparts. In other words, if a magnetic Δ parameter is 0, it is automatically constrained to the nuclear parameter.

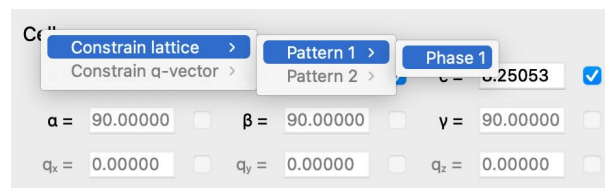


Figure 4.13: Example of how the cell parameters of one phase can be constrained to be the same in two different patterns.

4.6 Refinement and results

Once the data are loaded and the refinement flags and constraints are set, one can proceed to the *Fit* tab. Here one can control how the eventual co-refinement should be weighted. This is visualized by a weight triangle in which a draggable dot marks the different weights in trilinear coordinates (see Fig. 4.14). The weights of the respective data sets sum to 1 and are shown on the left of the triangle where they can also be set manually. If only one type of data was loaded, then the dot is fixed in one of the three corners. If two types are loaded, the user can drag the dot on one of the three lines of the triangle. And when all three data types were loaded, the dot can be dragged everywhere within the triangle. For convenience the dot snaps to the center of the triangle and to the bisections.

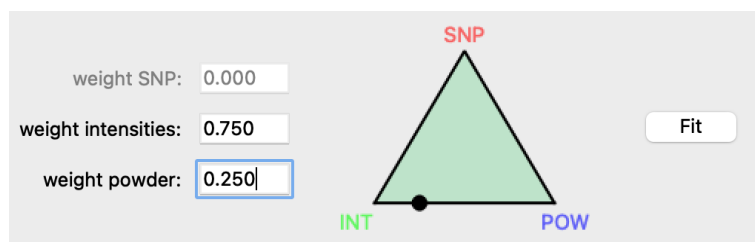


Figure 4.14: The weight triangle is a graphical way to set the respective weights of the data sets. When 2 (3) different types of data were loaded the dot can be dragged within a line (within the whole triangle). When only a single data type is present, the dot stays in the respective corner. The weights can also be set in the respective boxes, which are synchronized with the triangle.

The least-squares refinement will therefore minimize

$$\chi^2 = w_{SNP} \cdot \chi_{SNP}^2 + w_{INT} \cdot \chi_{INT}^2 + w_{POW} \cdot \chi_{POW}^2 \quad (4.8)$$

where χ_{SNP}^2 , χ_{INT}^2 and χ_{POW}^2 are the respective χ^2 values of the polarimetry, integrated intensities and powder data, respectively. Note that the weight given for intensity and powder data is further split if multiple data sets exist for which the individual weights can be set in the *Data* tab. The convergence criterium ϵ can be set in the *Settings* of the program and it refers to the maximum relative shift of a parameter in an iteration divided by its standard deviation. The refinement stops when

$$\Delta(p)/\sigma(p) < \epsilon \quad (4.9)$$

where $\Delta(p)/\sigma(p)$ represents the maximum value in an iteration for parameter p . Also the maximum number of iterations can be set.

The refinement can be started by clicking the *Fit* button and the progress as well as the results are shown in the text field to the left. For every iteration the χ^2 value will be printed together with the maximum relative parameter shift. Either when the maximum number of iterations has been reached, the convergence criterium is fulfilled or the *Stop* button is clicked (the *Fit* button changes label automatically), the refinement will stop and list the χ^2 , reduced χ^2 and R_F value (the last only applies for the integrated intensities and powder patterns). The refined parameters with their respective standard deviation are shown below. It is also possible to run a previously defined fit macro (see Sec. 4.8) by choosing it from the combo box below the *Fit* button and by pressing the play button. The macro can be stopped by pressing the stop button. Each step will be visualized and results printed as if it were a single refinement.

The refinement is visualized on the right-hand side of the window (see Fig. 4.15), where the integrated intensities are shown in an I_{obs} -vs- I_{cal} plot (flipping ratios are shown in an R_{obs} -vs- R_{cal} plot), powder patterns are represented as usual with the observed, calculated and difference lines and the polarization matrices are shown for each magnetic Bragg reflection. The latter is achieved by showing the observed polarization matrix entries as circles and the calculated ones as squares. The color code is red for x , green for y and blue for z , while those colors refer to initial polarization P_i for the marker face color and to the final polarization P_f for the marker edge color. E.g. a red square with a blue edge refers to an initial neutron polarization along the local x axis and a analysis direction along the local z axis, i.e. to the term P_{xz} of the polarization matrix. In case of multiple data sets of a single type (intensities or powder patterns) the one to plot can be selected from the combo box in the upper-right corner of the window (appears only when multiple data sets are loaded). If you have loaded Numors corresponding to a rotation of the incident

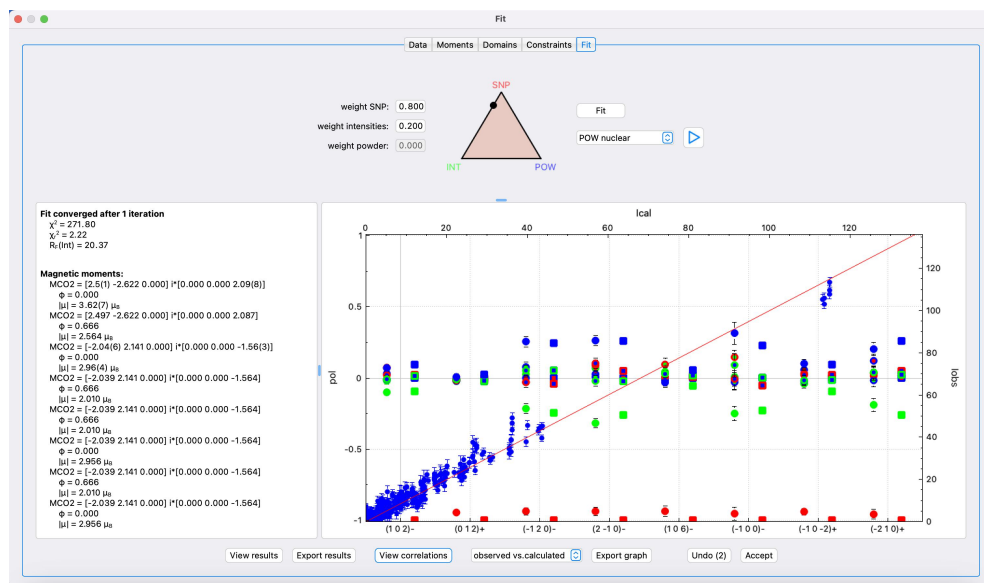


Figure 4.15: Output and visualization of the fit results.

neutron polarization within the y - z plane, the resulting plot contains the curves for each magnetic Bragg reflection on which this measurement was done (Fig. 4.16). The usual zoom controls work on this plot and the mouse can be hovered over a data point to obtain the exact values. A table of the observed and calculated intensities (also derived from powder patterns), flipping ratios as well as polarization matrices can be seen by clicking on *View results*, the same table can also be exported into an ASCII file by clicking on *Export results*. The values in the results table can be plotted against different scattering variables by right-clicking the respective column header and by choosing from the context

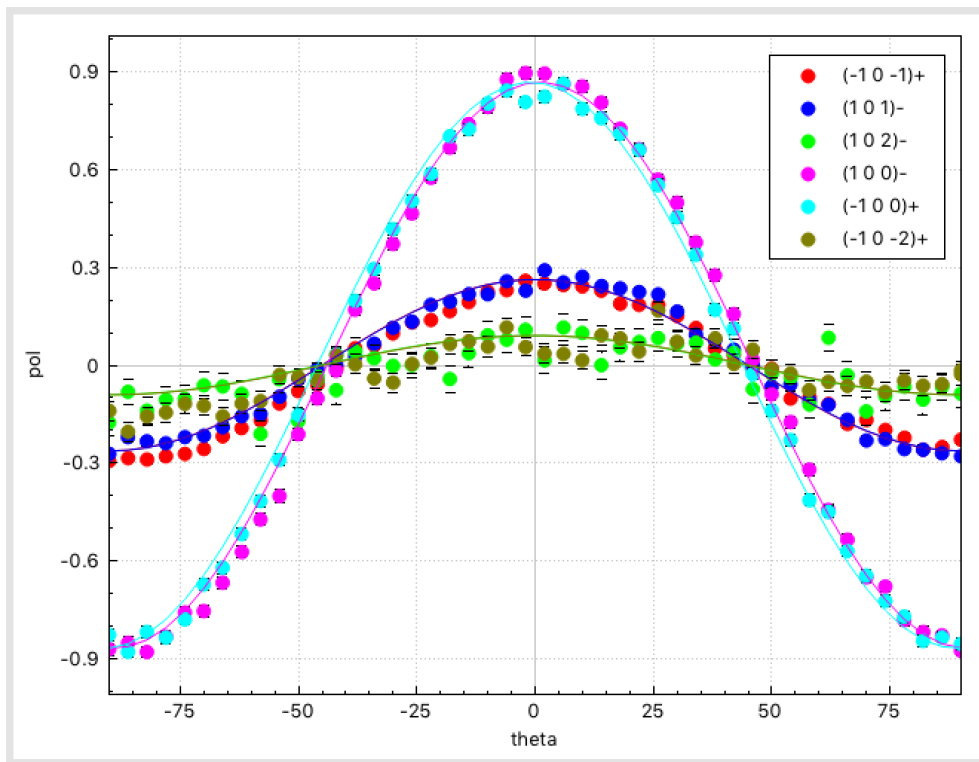


Figure 4.16: Visualization of the fit results when the data correspond to a rotation of the initial neutron polarization within the y - z plane.

menu. Note that polarization matrices can be visualized in matrix form, both using numbers or colored dots (see Sec. 6.16), by clicking on *Color plot*.

When more than one parameter is refined, the *View correlations* button is enabled which, when pressed, opens a window in which the correlation and the covariance matrix is shown. Note that if correlations exceeding 70% are present the *View correlations* button will be given the focus in order to notify the user. Within the correlations window, the (anti)correlations with more than 70% will be marked. This threshold value can be modified in order to focus on weaker or stronger correlations. Note that this window can be kept open for subsequent refinement steps, which will automatically update the values of the correlation matrix. The button focus will be set according to the actual threshold value in the correlation matrix window.

If you are satisfied with the refinement (step) you can click the button *Accept*. This will pass on the refined parameters to the main window, replot the magnetic structure and you can afterwards save it to your input file. If the fit diverged or did not improve you can close the window without clicking *Accept*, like this the initial parameters before the respective refinement step are kept in the main window. It is also possible to (repeatedly) click the *Undo* button (or CTRL/CMD + Z) which reloads the parameters and flags which were present before clicking the *Fit* button.

4.7 Batch fitting

4.7.1 Single-pattern

Batch fitting is presently only possible for powder patterns. It first requires to refine a single powder pattern (for multiple powder patterns, see Sec. 4.7.2) as described in Sec. 4.5 and accept the fit in order to transfer the refined parameters to the main window. Note that eventual constraints need to be set in this single refinement and will be used in the batch fit afterwards. The parameters to be refined will be loaded from the single refinement, but can also be modified in the batch fit window afterwards. It is also possible to open an xml file to which fit results have been saved previously. However, when the fit model is changed in the fit window, the previously stored batch fit results will be erased (a warning will be displayed before).

If an initial model is present the action *Batch fit* will be enabled in the *Fit* menu of the main window. When entering the *Batch fit* window the initial model and its corresponding pattern will be shown in the upper-right part of the window. An eventual previously saved batch fit will be shown. The same functionalities are enabled as for the pattern plot in

the *Fit* window.

A sequence of powder patterns can be loaded in the upper-left part of the window by clicking on the *Load* button. The sequence can consist e.g. of powder patterns of a sample recorded at different temperatures or of different samples with varying composition. For a meaningful use of the batch fit option the powder patterns should not vary too much from step to step. The loaded samples will be shown in the item list below the *Load* button and clicking the different items will show the different patterns in the pattern plot together with the initial model. If the loaded patterns contain metadata like temperatures (set point, regulation, sample) or composition it can be sorted according to that parameter by clicking on the *Sort* button. A dialog box will open which contains the possible variables, note that sorting according to the file name is always possible. A right-click on one of the items opens a context menu which offers several options concerning the refinement flags of that particular chosen pattern. First, in the *Fit parameters* menu, all possible fit parameters are listed which can be checked or unchecked for the refinement of that particular data set. A click on *Clear fit flags* removes all fit flags and from the *Restore fit flags* menu it is possible to either restore the refined parameters to those in the single-fit model (in the standard fit window) or to the last state which was run as a batch fit. By selecting multiple data sets and choosing *Apply fit flags to all selected* the fit flags of the item which was right-clicked will be applied to all selected items.

The loaded patterns can be cleared by clicking on the *Clear* button.

When a sequence of powder patterns is loaded, the refinement can be started by clicking on *Fit batch* or by selecting a previously prepared fit macro from the combo box and clicking the play icon. By using the option *refined values = next start values* it is more probable to have a converging fit from pattern to pattern. Otherwise, the same start parameters of the initial model will be used for every single pattern in the list. A certain range of patterns or even a single pattern can be chosen for the batch refinement by marking the respective patterns in the loaded pattern list and by activating the *fit only selected patterns* checkbox. The fit progress is shown for every pattern by outputting the iterations and χ^2 values like for standard refinements. After each fit the corresponding pattern is shown in the pattern plot. When the last pattern has been processed the refined parameters are shown in the parameter table in the center of the window. The current pattern or all patterns at one time (the pattern number will be added as an extension to the chosen file name) can be exported into pdf format. After the refinement process it is possible to export the refined parameters into a new xml file by right-clicking the file name in the list and choosing *save fit result as xml*.

Variables can easily be plotted by ticking either the check box *Plot 1* or *Plot 2* which refer to the left or right y-axis of the parameter plot on the lower-right part of the window. The plot style can be customized by changing the color, the line style and width as well as

marker type and size. Legend entries and axes labels can be entered in the corresponding text fields which are synchronized with the parameter plot. The plot can be exported either as pdf or ASCII.

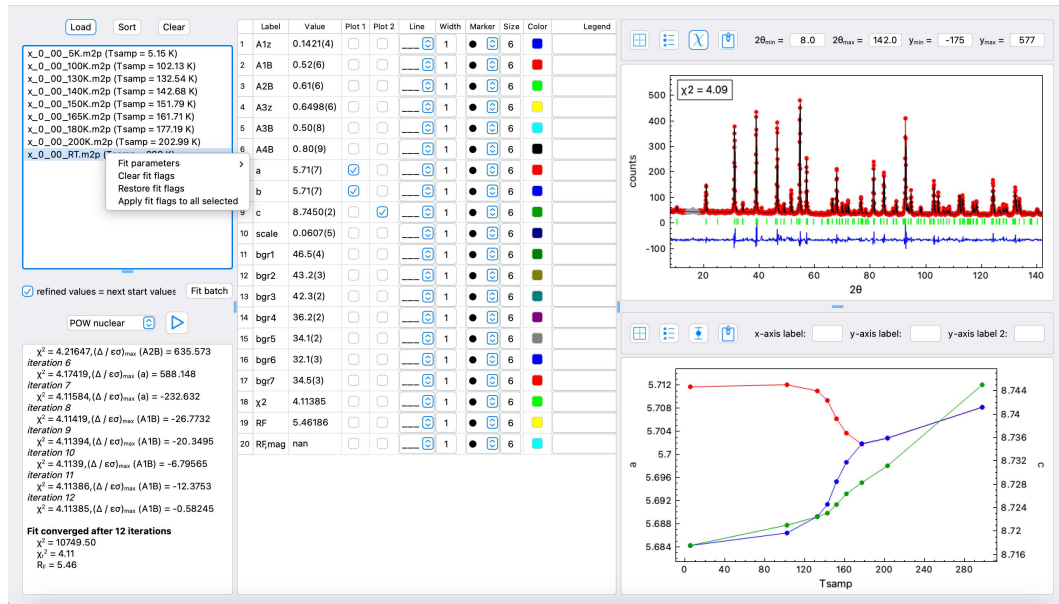


Figure 4.17: Batch fit window allowing to sequentially refine powder patterns. The refined parameters can easily be plotted against temperature, composition or pattern number.

4.7.2 Multipattern batch fitting

Multipattern batch fitting is possible as long as the number of patterns is the same for all items in the batch, e.g. for all temperature or doping steps. This feature may be used, e.g. when a neutron and an X-ray pattern have been recorded or when multiple banks are included in the refinement of TOF data at various temperatures. Everything in the previous section is also valid for the multipattern batch fitting option, there only a few additional details to consider. When the single-fit model contains two or more powder patterns and the batch-fit window is entered, a combo box will become visible situated left to the *Load* button. This allows to specify the different batches corresponding to the patterns of the single-fit model to be loaded. For example, in a single-fit a neutron powder diffraction pattern was used as the first pattern and a X-ray diffraction pattern was used as the second pattern. Then, all neutron data (e.g. as a function of temperature) have to be loaded with *Pattern 1* showing in the combo box, and all X-ray data will be attributed to *Pattern 2*. Note that *Pattern 1* data have to be loaded first and that all subsequent batches (*Pattern 2*, *Pattern 3*, ...) are added afterwards. Data files can be added step-wise, but the *Fit* button is only enabled when all patterns have the same number of elements in

the batch. When it is intended to load more data files than those that are present under *Pattern 1*, then all the excessive files will be discarded. It is also important to note that each batch has to be sorted individually, i.e. even after sorting the files under *Pattern 1* with respect to temperature, the subsequently loaded files under *Pattern 2* are not sorted although they may show the respective sample temperature. Data files in batches other than *Pattern 1* can only be sorted after the number of loaded files matches that in the *Pattern 1* batch.

4.8 Fit macros

MAG2POL offers the possibility to create up to 20 custom fit macros for a convenient automation of refinement strategies of powder and/or single-crystal data analysis. The macros can be constructed in a user-friendly and interactive way by entering the *Fit macro* window and they can be run from either the fit window or from within the batch fit window (see previous two sections).

When entering the *Fit macro* window for the very first time, three built-in macros can be chosen as an example from the combo box in the upper-left part of the window (see Fig. 4.18). The first is a sequence of refinement steps to refine the nuclear structure against a powder pattern. The second concerns the analysis of single-crystal data and the third cycles through all available irreducible representations in order to return the magnetic structure which best describes the observed data.

To construct a macro the user needs to drag icon objects from the left part of the window to the right part of the window and place them on the path indicated by gray connected squares. Once placed on the macro path a right-click on the icon allows to check the refinable parameters or choose other options which will be explained below. The available items and the related fit options are the following

- Scale
Fit options are to refine the powder or single-crystal scale factor, $\lambda/2$ contribution for single-crystal data, overall temperature factor for powder patterns as well as the option to simply adjust the powder scale factor without refining it. This can be useful when the scale factor cannot be refined due to insufficient overlap between calculated and observed peaks.
- Extinction
Set refinement flags for extinction parameters belonging to the three different implemented extinction models (isotropic ShelX, anisotropic ShelX, Becker-Coppens). The flags to be set depend on the extinction model which is actually used within the structure model.

- Atoms

Fit flags can be set for the x , y and z fractional parameters of an atomic position, the isotropic temperature as well as the anisotropic tensor (for the latter all tensor elements allowed by the site symmetry will be checked) and the occupation factor for the case that it is inferior to 1 (i.e. for a split site or a non-fully occupied site). Furthermore, the *refine atom by atom* option can be clicked in order to run a refinement process after adding atomic sites one by one, otherwise fit flags will be set for all atomic sites followed by a refinement process. It can also be decided to *refine weak scatterers* or not which depends on the scattering lengths (neutrons) or atomic number (X-rays) chosen (top of the window) to define a weak scatterer.

- Magnetic moments

Similarly to the extinction case, model-dependent parameters can be checked, i.e. depending on how the magnetic moments are described (spherical/Cartesian coordinates, basis vectors). In the case that a magnetic structure is described by basis vectors of an irreducible representation, it is possible to use the *cycle irreps* function which will go through all available irreducible representations, automatically check the available basis functions (set the multiplying coefficient to $1 \mu_B$ as a starting value) and choose the one with the smallest χ^2 . It is also possible to cycle mixed representations—either in phase or in phase quadrature—, where all combinations will be tested and a summary listed by increasing χ^2 values will be shown at the end of the refinements.

A fit flag for the phase of the magnetic moment is also possible as well as to *refine moment by moment* (in analogy to *refine atom by atom*).

- Domains, twins and phases

Fit options are to equally distribute the population of domains, twins and phases and to set the respective refinement flags. In the case of phases, the *switch phase* option allows to activate the next phase in the user-defined model to which the remaining macro steps will be applied. If all phases should be affected by each macro step, then the *apply to all phases* check box can be activated at the top of the window.

- Background

The first option is to *initialize* background points within the linear interpolation model. This is automatically done by detecting peaks with $I > 5\sigma$ between the first and last excluded region. A background point is then placed between two identified peaks, if the distance to either peak is at least 3-FWHM. Further options are convert linear interpolations into other models and the last option is to refine all background parameters.

- Offsets
For constant-wavelength powder patterns the refinable offsets are $\Delta 0$, Δx , Δy and the wavelength, whereas for time-of-flight data they are Z_0 , D_1 and D_2 (see Sec. 7.7.1.6). For multi-pattern refinements - in analogy to structure models with more than one phase - the *switch pattern* option can be activated, if the *apply to all patterns* option is deactivated, in order to apply the remaining macro steps to the next pattern in line.
- Lattice
The first option is to run the indexation algorithm with the last used values in the cell finder window (including the peak finder slider position defining the peak intensity criterion). The indexation returns the best option, if any, and overwrites the current lattice parameters. The space group and eventual transformation operator will not be overwritten. Note that if a cell axes permutation is present, the resulting lattice parameters will be attributed to the closest ones of the used structure model in the case that the nuclear contribution is set to *Rietveld* (in the case of a *LeBail* contribution the lattice parameters will be overwritten as obtained from the indexation process, since the order is insignificant due to the fact that the atomic positions do not contribute to the calculated pattern). The remaining options are fit flags for the lattice parameters a , b , c , α , β and γ as well as for the propagation vector components q_x , q_y and q_z .
- Profile Here again, the fit options can be set for constant-wavelength or for time-of-flight data. For the first, u , v , w , η , S , I_g , X and Y (as well as their magnetic counterparts) can be checked and will be refined, if the respective parameter is available in the chosen profile function (see Sec. 7.7.1.5). For the latter, the refinable parameters are σ_2 , σ_1 , σ_0 , γ_2 , γ_1 , γ_0 and I_g .
- Asymmetry / Rise and decay Asymmetry refers to the constant-wavelength parameters A_1 , A_2 , A_3 , A_4 as well as S_L and D_L (and their magnetic counterparts), whereas the latter will only be refined, if available in the chosen profile function. For TOF data, the rise-and-decay parameters α_0 , α_1 , β_0 and β_1 (or κ depending on the profile function) can be refined.

If in the course of the refinement strategy, it is intended to remove the refinement flag of a parameter, the same icon has to be placed on the path a second time, but without checking the respective parameters.

Whole blocks can be moved up and down the path by choosing *move block up* or *move block down* from the context menu. A block consists of the icons between the one selected and all connected icons down the path. A macro step can be removed by choosing *remove*

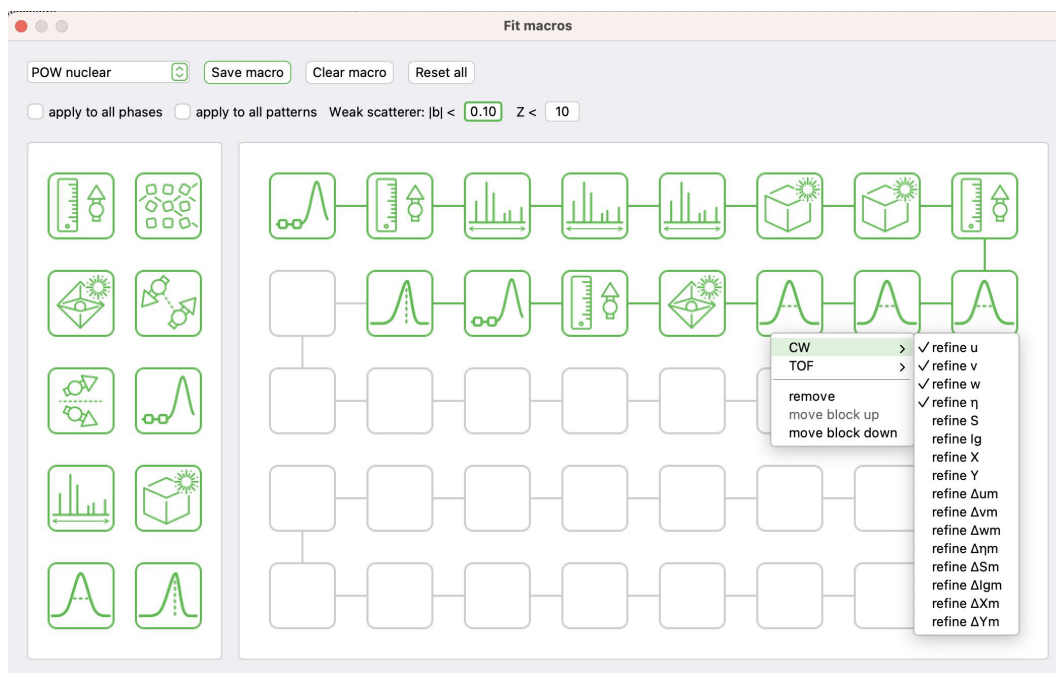


Figure 4.18: Fit macros showing a 15-step macro to refine the nuclear structure against a powder pattern.

from the context menu or by dragging the icon to the left part of the window.

In order to save a fit macro, click on the *Save macro* button, then select a slot between 1 and 20 and eventually rename the fit macro. The fit macros are saved in the system registry and will be loaded when entering the *Fit macro* window. A macro can be cleared, i.e. all steps will be removed, by clicking on *Clear macro* and a click on *Reset all* restores the 3 default macros from the very first start.

5 Reflection lists, powder patterns and maps

5.1 Reflection lists

Once a crystal and magnetic structure has been set up reflection lists can be generated via the menu entry *Generate*→*Reflection list* or using its toolbar icon or shortcut (CTRL/CMD + L). A window will pop up in which the criteria like the (hkl) or Q range, nuclear and magnetic structure factors, polarization values can be set. If an orientation matrix has been entered, then the diffractometer angles (calculated according to the instrument definition, see Sec. 3.10) and the angle α between the scattering vector and the vertical diffractometer axis can be used as a criterium as well. In that case it can be chosen, if only accessible reflections should be listed. By clicking *Create list* a table will be created which can be ordered according to a specific value by right-clicking on the horizontal header entry and choosing ascending or descending. The table can be exported in a format directly readable by MAD or NOMAD (running on ILL diffractometers) by clicking *Save*. A demo video can be seen [here](#).

5.2 Intensity maps

Intensity maps can be generated by triggering *Generate*→*Intensity map*, using its toolbar icon or shortcut (CTRL/CMD+ M). All nuclear and magnetic structure factors for integer and satellite reflections will be calculated (for the current phase in the main window) in the range from -10 to 10 for h , k and l (this is the initial setting which can be changed by right-clicking the label *Boundaries*). The initial view is the $(hk0)$ plane, which can be changed by defining two reciprocal vectors or the layer in the spin box (see Fig. 5.1). Note that the vertical direction is shown when hovering the mouse over the label z . The boundaries can be set for the horizontal and vertical axes in the second line. The resolution corresponding to the full width at half maximum of a 2D Gaussian function can be set individually for the h , k and l directions. The intensity maps' intensity color scale will automatically be rescaled to the minimum and maximum intensity of the actual map. In order to compare intensities between different maps or layers, the check box *Rescale* can

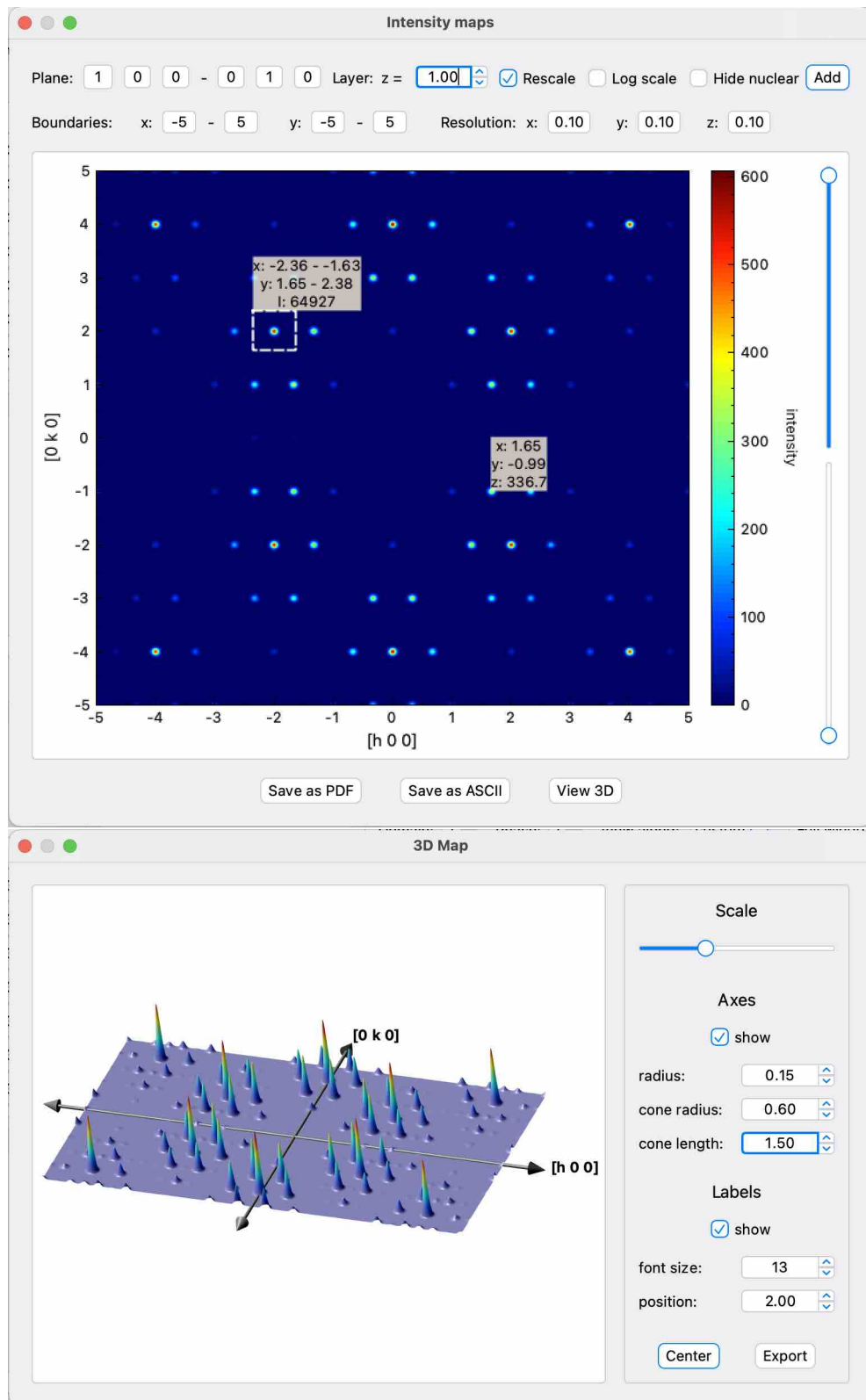
be unchecked, which will therefore conserve the scale. Furthermore, a logarithmic scale can be chosen or nuclear scattering can be hidden. Note that all the previous parameters are saved after closing the map window and will be applied upon the next map calculation. The maximum and minimum values of the intensity scale can be modified by the vertical sliders to the right of the map. This can be useful to emphasize weak reflections.

In case of multi-q magnetic structures scattering from differently modulated components of the magnetic structures can be added. For that the magnetic structure in the main window should be modified (especially the propagation vector) and regenerated. Alternatively, a second phase can be added in the main window and set as the current one. Afterwards, the scattering from that new magnetic structure can be added to the intensity map by clicking *Add*. The x , y and intensity values are visualized by hovering the mouse over the map. Zooming in and out is achieved with the usual mouse controls. Intensity maps can be saved as pdf or ASCII files by clicking the corresponding button at the bottom. By holding down the CTRL/CMD key while drawing a rectangle a projection will automatically be calculated and plotted in a new window (see Fig. 5.2). The projection is always along the shorter side of the rectangle. Zooming and point labels are enabled and the projection can be saved as pdf and ASCII as well. By holding down the ALT/OPT key an integration mask can be drawn on the 2D map (note that there is no limit as to the number of masks on the map). The mask can be moved by dragging it from its upper-left corner and resized by moving its lower-right corner. The integrated intensity is updated in the label, where also the x and y range is shown. Integration masks can be deleted by right-clicking either the upper-left or the lower-left corner (after the mouse cursor changes into an open-hand or resize cursor).

It is also possible to view maps in 3D (see lower panel of Fig. 5.1). This feature is particularly interesting for non-orthogonal systems in order to appreciate the real crystal symmetry. By clicking on the button *VIEW 3D* a new window will open, showing the map with the same boundaries and color code in three dimensions. The intensity scale (peak amplitude) and appearance of axis and labels can be adjusted before creating a high-quality picture.

5.3 Powder pattern

MAG2POL features the quick simulation of powder patterns which can be done via the menu entry *Generate*→*Powder pattern* or the toolbar icon (see also [this](#) demo video). A new window will open showing the global pattern, i.e. the sum of all phases (see Fig. 5.3). In the lower left corner of the window the geometry of the instrument can be changed, i.e. the source (neutron or X-ray), the wavelength and the resolution function via the *uvw*

Figure 5.1: Intensity map in the $(hk1)$ plane.

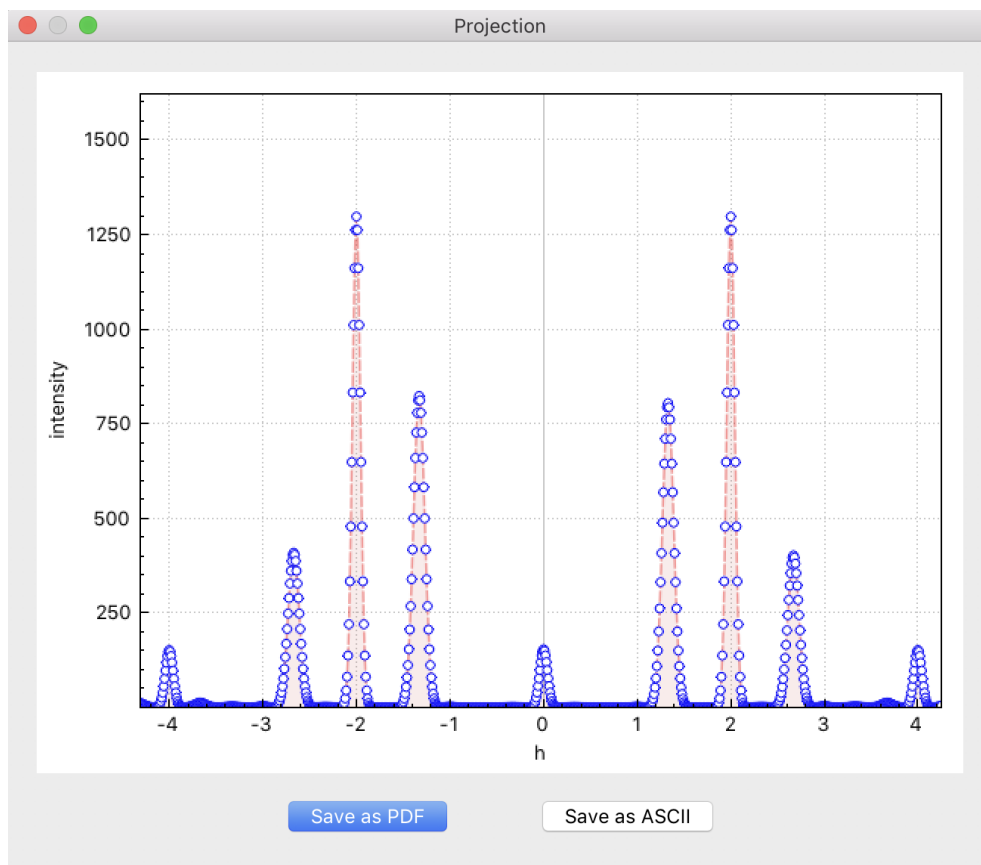


Figure 5.2: Projection along k of the scattered intensity along the $(h20)$ line of the map shown in Fig. 5.1.

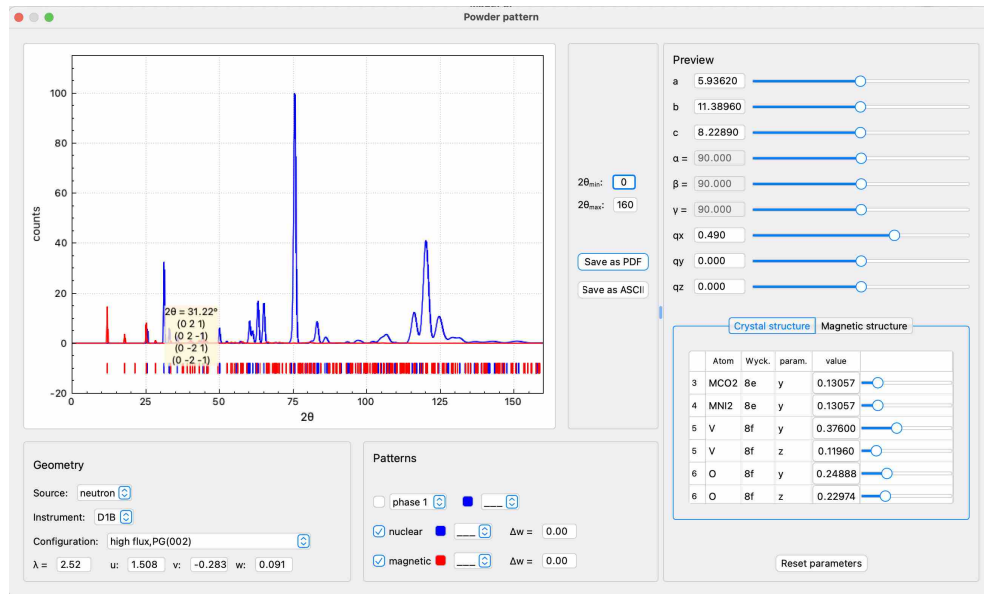


Figure 5.3: Powder pattern showing the nuclear and magnetic contribution separately.

parameters of the Caglioti formula:

$$FWHM^2 = u \tan^2 \theta + v \tan \theta + w$$

The powder diffractometers of the ILL (D1B, D2B, D20) can be chosen with different configurations from the combo boxes which will set the respective parameters automatically. When *xray* is chosen as source, then a right-click context menu is enabled for the wavelength value from which different standard x-ray wavelengths can be chosen, which will automatically use the α_1 and the α_2 line.

The plot of the powder pattern can be zoomed in with the usual rectangle zoom and zoomed out with a right click. Hovering over the peak markers below the pattern will show a tool tip containing the scattering angle and the corresponding (hkl) reflections.

In the *Patterns* frame the user can change the appearance of the powder pattern (colours and line styles) and choose whether nuclear and/or magnetic patterns should be shown individually. An additional broadening of the peaks can be introduced through the Δw value for the nuclear and magnetic patterns separately. The individual patterns can be exported into a text file or the visualized pattern(s) can be exported as a PDF file.

On the right-hand side a preview option allows to follow the changes in the diffraction pattern as a function of the lattice parameters, propagation vector components or atomic positions. The nuclear and magnetic structures are modified simultaneously in the main window (note that the presence of bonds and polyhedra can lead to a notable lag).

5.4 Magnetization density maps

Magnetization density maps (see an example in Fig. 5.4) can be created by calculating a Fourier inversion according to:

$$\rho(\mathbf{r}) = \frac{1}{V} \sum_{hkl} M \exp[2\pi i(hx + ky + lz)]$$

where the Fourier coefficients are the magnetic structure factors M . Projections, like e.g. onto the x - y plane are obtained by

$$\rho(\mathbf{r}) = \frac{1}{ab} \sum_{hkl} M \exp[2\pi i(hx + ky)]$$

Note that the theoretical magnetic structure factor of the experimentally inaccessible (000) reflection is added for scaling purposes in both calculated and observed maps. Different Fourier maps can be chosen from the combo box, e.g. calculated maps with different cut-off angles corresponding to a critical Q_c , observed maps from `*.int` or `*.fli` flipping ratio input files or difference maps. Furthermore, the user can choose from projections, cuts or slices within custom planes defined by two vectors of the real lattice. The different layers, or the vertical parameter, can be changed using the arrow buttons (note that hovering the mouse over the label z will show the vertical direction as a tool tip). A right-click on the layer value will pop up a context menu from which either the single step value can be set to the actual shown value or the whole range of layers from 0 to 1 can be calculated at once. For all calculations the program will make use of the nuclear symmetry in order to speed up the process, if the *apply symmetry* checkbox is activated. Note that each map is only calculated once, i.e. repeated scrolling through already calculated maps will not cost calculation time. However, when the bin value is changed (or the slice thickness), all previously calculated maps will be deleted. It has to be noted that the maps will sometimes show unusual details coming from binning artifacts. Therefore, the default bin has been set to 0.1 Å and the lattice constants are rounded, which usually gives good results for the Fourier maps. The zoom controls, projections and integration masks are the same as for intensity maps in reciprocal space (Sec. 5.2). The magnetization density maps can also be viewed in 3D (see Fig. 5.4). This feature is particularly interesting for non-orthogonal systems in order to visualize the correct symmetry (see also [this demo video](#)). The volumetric data can be exported by clicking on the corresponding button and visualized in other programs, e.g. VESTA [28].

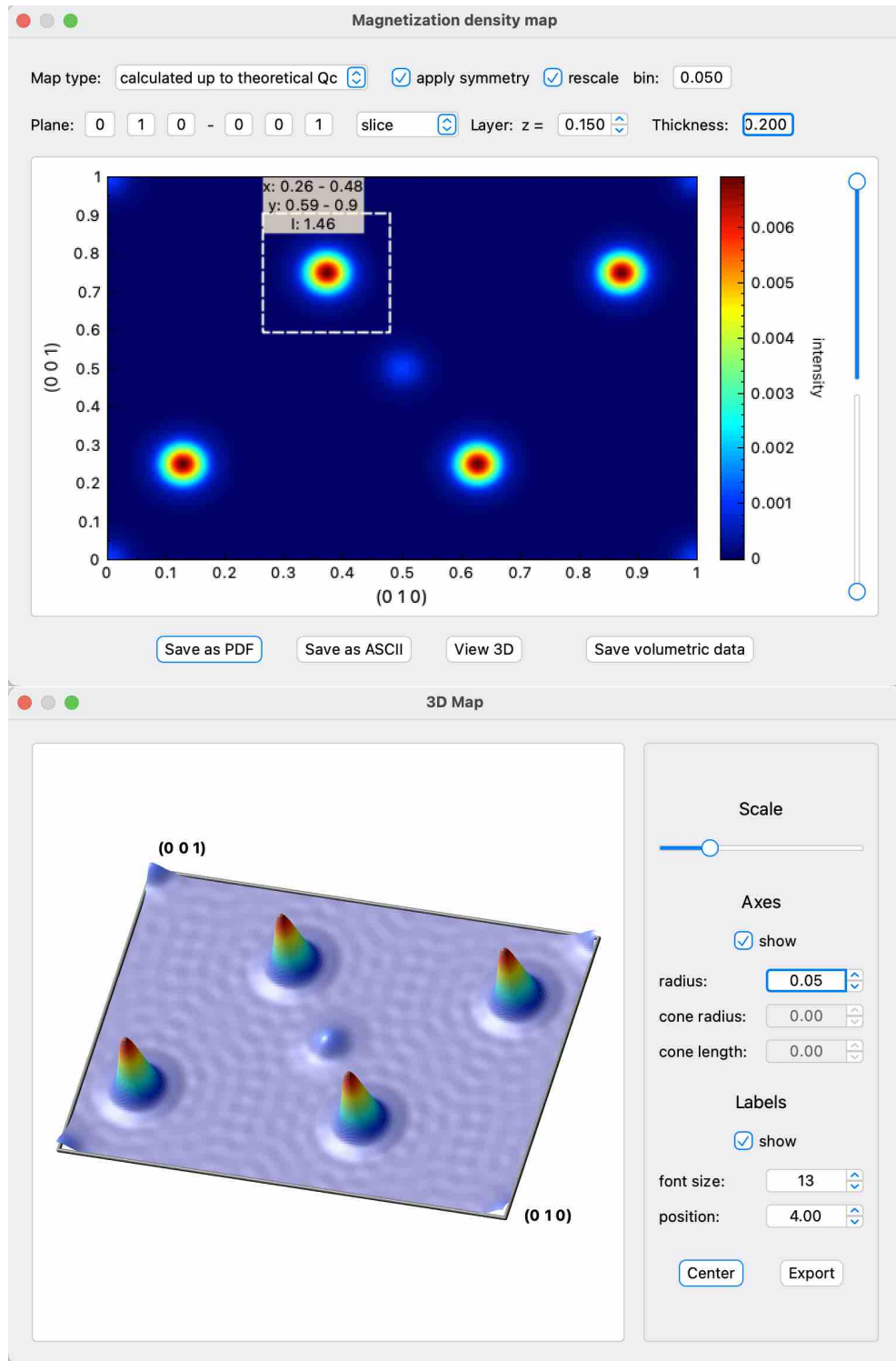
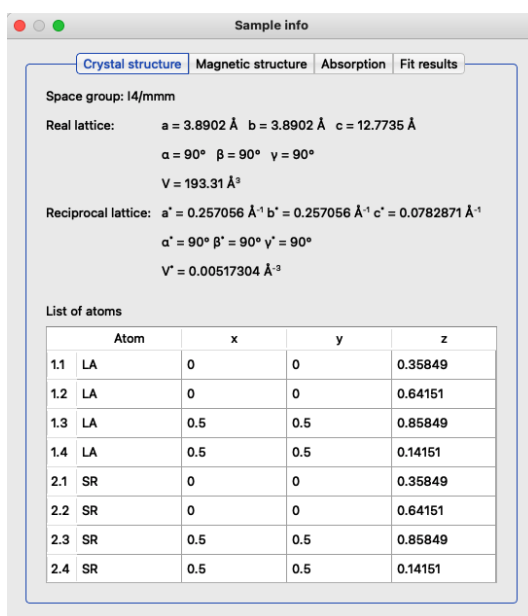


Figure 5.4: Slice of 0.2 Å thickness around $x = 0.15$ in the y - z plane in 2D (upper panel) and 3D (lower panel). The Fourier inversion is taken up to the highest measurable Q_c with the given wavelength.

6 Tools

6.1 Sample information

Once a nuclear and/or magnetic structure model has been entered it is possible to see a summary of the main parameters via the menu entry *Tools*→*Sample info* or the toolbar icon. Under the *Crystal structure* tab (see Fig. 6.1) the real and reciprocal lattice parameters and volumes are shown together with a list of all the atoms in the unit cell. A list with magnetic moments and Fourier coefficients can be found under the *Magnetic structure* tab together with the magnetic symmetry used. All information related to the absorption correction are shown under *Absorption*. Note that the interactive tool to create the sample model (Sec. 4.2.2) can directly be accessed from here. The last refinement results can be viewed under the *Fit* tab.



The screenshot shows a window titled "Sample info" with four tabs: "Crystal structure" (selected), "Magnetic structure", "Absorption", and "Fit results". The "Crystal structure" tab displays the following information:

Space group: I4/mmm

Real lattice: $a = 3.8902 \text{ \AA}$ $b = 3.8902 \text{ \AA}$ $c = 12.7735 \text{ \AA}$
 $\alpha = 90^\circ$ $\beta = 90^\circ$ $\gamma = 90^\circ$
 $V = 193.31 \text{ \AA}^3$

Reciprocal lattice: $a^* = 0.257056 \text{ \AA}^{-1}$ $b^* = 0.257056 \text{ \AA}^{-1}$ $c^* = 0.0782871 \text{ \AA}^{-1}$
 $\alpha^* = 90^\circ$ $\beta^* = 90^\circ$ $\gamma^* = 90^\circ$
 $V^* = 0.00517304 \text{ \AA}^{-3}$

List of atoms

	Atom	x	y	z
1.1	LA	0	0	0.35849
1.2	LA	0	0	0.64151
1.3	LA	0.5	0.5	0.85849
1.4	LA	0.5	0.5	0.14151
2.1	SR	0	0	0.35849
2.2	SR	0	0	0.64151
2.3	SR	0.5	0.5	0.85849
2.4	SR	0.5	0.5	0.14151

Figure 6.1: Summary of basic parameters entered by the user.

6.2 Space group tables

The space group tables and conversion tools for crystallographic (CSG), magnetic (MSG) and magnetic superspace groups (MSSG) can be consulted under *Tools*→*Space group tables* or via its corresponding toolbar icon. When entering the window without a previously defined structure model, the symmetry operators and Wyckoff positions as well as basis vectors for MSGs can be viewed for any space group with or without basis transformation. Selecting a space group to set up a structure model including the transformation of the unit cell and atomic positions is only possible with a previously defined structure model.

The *Space group tables* window is organized in four tabs, from which the first three are: CSGs, MSGs and MSSGs (see Fig. 6.2). Space groups can be entered via their (numerical) labels, e.g. $I4/mmm$ or 139, $Pm'n'a$ or 53.326, $P2.1'(0,0,g)0s$ or 3.1.5.3.m2.2, or they can be chosen from the combo boxes where they can also be sorted by system for easier navigation. As stated in Sec. 2.2, all information concerning MSGs and MSSGs is based on the computer-readable tables available on the ISOTROPY SOFTWARE SUITE website [1–3] and the work published in [4–6]. For further information, the reader may refer to the excellent reviews [29, 30]. If a space group has been correctly entered its label will be shown in green (red if not) and the crystallographic information will be shown in the text window below. This information consists of the operators of the space group (including time inversion operator for MSGs and the internal variable for MSSGs) followed by the Wyckoff positions in case the space group has been entered in its standard setting (a few non-standard CSGs are implemented in MAG2POL). The basis of any space group can be transformed to another setting which can be useful to compare a structure with another one published in a different setting, and is necessary for a reasonable use of MSGs and MSSGs. The transformation operator can be entered either by writing a string in standard notation which will display the rotational part R and translational part t of the operator, or vice versa, by entering R and t which will display the transformation string. The correct syntax will be shown in green and requires the transformation string to be enclosed in parantheses, the rotational and translational part to be separated by a semicolon and the individual axes to be separated by a comma. The identity would be expressed as (**a**, **b**, **c**; 0, 0, 0), where the spaces are optional. A swapping of the a and b axes with an origin shift along c would correspond to (**b**, **-a**, **c**; 0, 0, 1/2). Note the minus sign to conserve a right-handed set of axes and the possibility of entering fractions. The correct application of basis transformations, especially when entering information obtained from other tools (e.g. BILBAO CRYSTALLOGRAPHIC SERVER or ISOTROPY), will be shown in the next sections. When basis-transformed symmetry operators are printed as nAo (not an operator), the transformation was probably wrong.

The fourth tab *Preview* serves to visualize the crystal and magnetic structure in the main window and allows to modify the degrees of freedom, i.e. atomic positions and basis vectors of magnetic moments respecting the underlying symmetry. If bonds and polyhedra were drawn beforehand, the program will show their deformation in real time. Note that this tool works optimally, when all atomic positions are defined as the first position of the Wyckoff site (see Sec. 2.2 for a straightforward conversion) and if only positive xyz parameters are used.

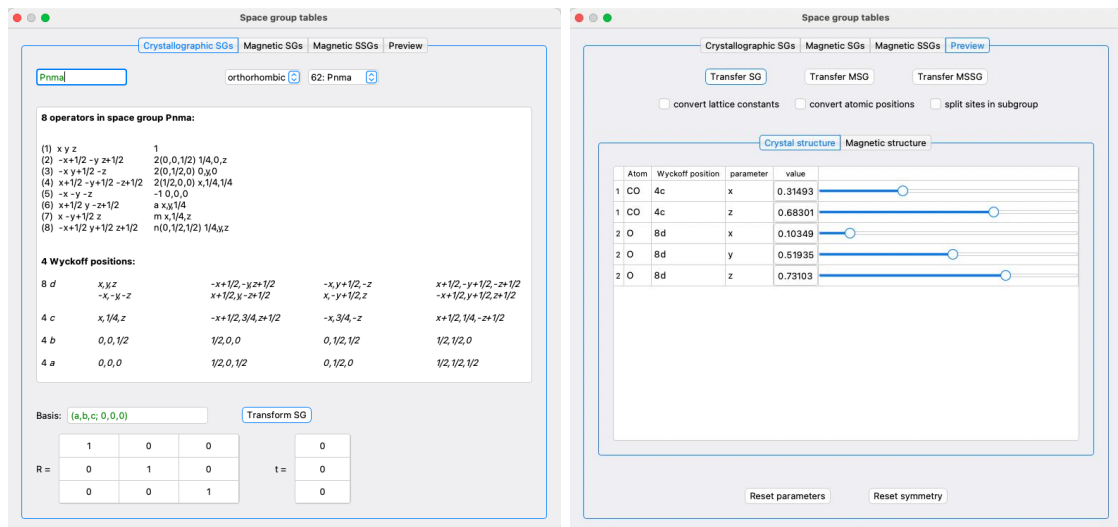


Figure 6.2: Left: Space group tables for crystallographic, magnetic and magnetic super-space groups containing information about symmetry operators, Wyckoff positions and basis vectors. Furthermore, any transformation can be applied to any of the space groups. Right: Preview window allowing to transfer a space group to the main window, to modify the degrees of freedom and to visualize the crystal and magnetic structure.

6.2.1 Space group transformations

After choosing a space group from the combo boxes or by entering its (numerical) label, MAG2POL will always load the untransformed operators and Wyckoff sites regardless of the given transformation operator. The basis transformation is only applied when clicking on *Transform SG*, which will update the crystallographic information in the text box above, which is also shown by the basis transformation string next to the space group label.

If the user wishes to transfer the space group to the structure model initiated in the main window, this can be achieved by clicking *Transfer SG* in the *Preview* tab. Several options

exist which depend on what the user wishes to achieve. If the checkbox *convert lattice constants* is activated, the rotational part of the transformation operator is applied to the lattice which will be updated in the main window. The same applies to *convert atomic positions* which - if activated - will convert the position vectors by taking into account the rotational and translational part. The last checkbox *split sites in subgroup* should be activated, when a group was chosen in the *Space group tables* which is a subgroup of that in the main window. In this case, the program will identify the symmetry operators missing in the subgroup and create new atoms in the structure model, if sites split into different orbits. Two examples will clarify the use of these checkboxes:

- Convert a structure expressed in *Pnma* to *Pnam*

Enter the *Space group tables* with a *Pnma* structure model in the main window. The transformation to *Pnam* is expressed by $(a, c, -b; 0, 0, 0)$ or equivalently by $(a, -c, b; 0, 0, 0)$ which should be entered in the corresponding field under the *Crystallographic SGs* tab. Alternatively, the rotation matrix can be entered, which will create the transformation string as a confirmation. Click *Transform SG* to apply the transformation and check the results in the text box above.

Now switch to the *Preview* tab. Due to the swap of *b* and *c* axes the lattice parameters and the atomic positions previously defined in the main window should be updated in order to conserve the structure. Therefore, *convert lattice parameters* and *convert atomic positions* should be activated. On the other hand, all symmetry operators of *Pnam* will be different from the ones in *Pnma*, but the site multiplicity remains unchanged. Therefore, the *split sites in subgroup* checkbox should not be activated. Now click *Transfer SG* and inspect the structure in the main window. You can move the sliders or enter values for free positional parameters to verify the structural degrees of freedom and you can go back to the initial values by clicking *Reset parameters*. If the transformation does not show the expected results, it can be reverted by clicking *Reset symmetry* which will take the structure back to its state before entering the *Space group tables* window. If the *Space group tables* window was closed after transferring the space group and converting the structural data, it is still possible to recover the original structure by right-clicking the *Space group* label in the main window and choosing the appropriate action from the *reset transformation* menu. Any of the options will set the transformation operator to identity, i.e. the symmetry operators of the original space group will be used to generate the cell. The optional conversion of the lattice parameters and the atomic positions will be done with the inverse of the former transformation operator. In this example, the correct option would therefore be *convert both*.

- Convert a structure expressed in *Pnma* to its non-isomorphic subgroup *P2₁ma*

From the International Tables Vol. A [8] one can obtain the following information concerning the non-isomorphic subgroup: $P2_1ma$ ($Pmc2_1$, 26) 1; 4; 6 ;7. The subgroup $P2_1ma$ is a non-standard setting of space group 26, $Pmc2_1$, and the symmetry operators 1, 4, 6 and 7 of $Pnma$ are conserved. Since MAG2POL lists the operators in the exact same order, it is straightforward to compare the respective space groups. First, set up the structure in $Pnma$ symmetry in the main window and then enter the *Space group tables* window (copy the symmetry operators for a more comfortable comparison afterwards). Choose space group $Pmc2_1$ under the *Crystallographic SGs* tab, which now has to be converted to $P2_1ma$. The rotational part of the transformation is easy to extract by comparing the two space group labels. Therefore, in a first step the transformation (c, a, b; 0, 0, 0) can be entered followed by a click on *Transform SG*. Now, paste the $Pnma$ symmetry operators below the converted ones and compare operators 1, 4, 6 and 7. It is apparent that a rotation of the basis is not sufficient and that a shift of origin is necessary. It can be verified that the correct transformation is (c, a, b; 1/4, 1/4, 0). Enter the string and click *Transform SG* (note that for each transformation the original space group is reloaded before applying the transformation, i.e. one cannot do a chain of transformations), which should produce the four symmetry operators of $Pnma$ numbered 1, 4, 6 and 7. The transfer of the new symmetry to the main window is effectuated in the *Preview* tab. In this case, the axes and atomic positions have been transformed to match those of the original structure in $Pnma$, so the first two checkboxes should not be activated. On the other hand, since the general multiplicity of $P2_1ma$ is 4, while it is 8 in $Pnma$ not all atomic positions will be generated in the subgroup, for which the *split sites in subgroup* option needs to be activated. Finally, click on *Transfer SG* and verify the result.

The conversion from the non-standard setting $P2_1ma$ to $Pmc2_1$, if intended, can be done by closing the *Space group tables* window and by resetting the transformation via the *Space group* label context menu as explained in the previous point.

6.2.2 Magnetic space group transformations

The basic use of magnetic space groups and their transformations is very similar to the explanations in the previous section with a few exceptions. The first is related to the fact that the transformation operators are always applied to the parent space group which is the definition used by the programs of the BILBAO CRYSTALLOGRAPHIC SERVER for example. Therefore, the chosen magnetic space group is transformed with the inverse of the shown transformation, since the direct transformation is applied to the parent space group which is (related to) the paramagnetic space group. The second difference concerns

the transformation of lattice constants and atomic positions which are always calculated according to the transformation operator under the *Crystallographic SGs* tab. This makes it possible to effectuate complex transformations of both the CSG and the MSG to obtain the desired result. A good starting point for finding appropriate MSGs is the use of the MAXMAGN program [30] on the BILBAO CRYSTALLOGRAPHIC SERVER. After entering the crystallographic space group and the commensurate propagation vector one obtains a list of maximal magnetic space groups. By clicking the *Show* button in the *General positions* column one can obtain both the augmented transformation matrix for the CSG and for the MSG. How to correctly enter this information will be shown in the following example from [30].

- Magnetic space group $P_a ca 2_1$ as a child of the parent space group $Pbam$
The use of MAXMAGN with space group $Pbam$ and propagation vector $\mathbf{q} = (1/2 \ 0 \ 0)$ reveals four maximal magnetic space groups, one of them being $P_a ca 2_1$ (#29.104), but in a special setting. First of all, set up the paramagnetic $Pbam$ structure in the main window and enter the *Space group tables* window. Here, enter the basis transformation of the parent space group which is given as $(2\mathbf{a}, \mathbf{b}, \mathbf{c}; 0, 0, 0)$ on the *General positions* page of the MAXMAGN output (or simply copy and paste it). Click *Transform SG* which will result in doubling the symmetry operators of space group $Pbam$ due to the additional translation $t(1/2 \ 0 \ 0)$. Now switch to the *Magnetic SGs* tab and enter either `P_a ca 2_1` or `29.104` which will show the symmetry operators, Wyckoff positions and basis vectors for that magnetic space group. Enter the transformation of the MSG, this time given in matrix form in the MAXMAGN output, which becomes $(\mathbf{a}, -\mathbf{c}, \mathbf{b}; 1/8, 0, 0)$, and click *Transform MSG*. Alternatively, you can also copy the 12 numerical values from the website and paste them into the table by right-clicking any of the cells and choosing *paste (R|t)*. At this point it is important to compare the symmetry operators in both tabs. If the transformations were applied correctly, the MSG should be a subgroup of the SG and reveal a subset of the symmetry operations (primed or unprimed) of the latter. In this example the 8 MSG operators can be found in the CSG (operators 1, 3, 6, 8, 9, 11, 14 and 16). Now the MSG can be transferred from within the *Preview* tab. Since the CSG was adapted to the doubling along the a axis, the lattice parameters and the atomic positions need to be changed accordingly, i.e. the *convert lattice constants* and *convert atomic positions* checkboxes need to be activated. Furthermore, since the MSG only reveals a subset of the symmetry operators in the CSG, not all the atomic positions can be generated, for which the *split sites in subgroup* checkbox needs to be activated as well. Now, click *Transfer MSG*, inspect the resulting structure in the main window by adjusting the degrees of freedom under the *Crystal*

structure and *Magnetic structure* tabs and accept the result by closing the *Space group tables* window. As described above, the transformation of the MSG can be converted back to the original $P_a ca 2_1$ setting by evoking the context menu on the *Space group* label in the main window.

6.2.3 Magnetic superspace group transformations

The use of MSSGs is almost the same as for MSGs with the exception that no transformation of the parent paramagnetic space group is necessary. When selecting a MSSG symmetry (either by typing its label or by choosing it from the list) and transferring it to the main window in the same way as described for MSGs, MAG2POL automatically calculates the basis vectors for all the magnetic ions in the structure model. Depending on their point symmetry certain components may be extinct or relations between real and imaginary components might exist. Note that the order of basis vectors is not necessarily the same as shown in the ISOVIZ plotting tool and that split sites are treated as independent sites in MAG2POL. The interested reader may consult [29] for a complete overview on MSSGs.

A good starting point to identify possible MSSGs for the underlying crystal structure and incommensurate propagation vector is the use of the ISOTROPY SOFTWARE SUITE website [1–3]. A *.cif file can be exported from MAG2POL and loaded on the website to start a new distortion (choose only magnetic). Enter the propagation vector using *Method 2: General method - search over specific k points*, enter the necessary propagation vector coefficients, set the number of incommensurate modulations to 1 [note that only (3+1)d modulations can be treated with the present version of MAG2POL] and click *OK*. On the next page all necessary input parameters can be found for the different possible modes. Either extract the information from this page or select a mode and click *OK*. On the next page it is possible to download an *.isoviz or *.cif file, from which the latter can be directly loaded in MAG2POL after changing its extension to *.mcif. The *.mcif files downloaded from the ISOTROPY SOFTWARE SUITE contain the original setting and the one adapted to a standard paramagnetic space group. On loading the file, it can be chosen which setting to employ. By selecting *Employ parent-like basis vectors* on the first page the *.mcif file will be adapted to the conventional cell of the original structure (recommended). Note that for MSSGs with origin translations \mathbf{t} such that the dot product with the propagation vector \mathbf{q} is non-zero, the visualization in the conventional cell might look different than that of the untransformed MSSG. The correct use of the MSSG transformation is shown in the following example.

- Magnetic superspace group $P2_1/b.1'(0, 0, g)00s$ as a child of the parent space group $P2_1/c$ with propagation vector $\mathbf{q} = (0 \ 0.32 \ 0)$

First, set up a structure in $P2_1/c$ symmetry and export it to a *.cif file which can be uploaded on the ISOTROPY SOFTWARE SUITE website. Enter the propagation vector under *Method 2* by choosing $LD, k3 (0, b, 0)$ and enter $b = 0.32$, set the number of incommensurate modulations to 1 and click *OK*. On the next page, select the first mode corresponding to the MSSG $P2_1/b.1'(0,0,g)00s$. From here the necessary input can already be transferred to MAG2POL by entering the given basis transformation. In this example the output $\text{basis}=\{(1,0,0,0), (0,0,1,0), (0,-1,0,0), (0,0,0,1)\}$, $\text{origin}=(0,0,0,0)$ needs to be entered as

$$R = \begin{pmatrix} 1 & 0 & 0 & 0 \\ 0 & 0 & -1 & 0 \\ 0 & 1 & 0 & 0 \\ 0 & 0 & 0 & 1 \end{pmatrix} \quad t = \begin{pmatrix} 0 \\ 0 \\ 0 \\ 0 \end{pmatrix} \quad (6.1)$$

followed by a click on *Transform MSSG*. Alternatively, the whole string can be copied to the clipboard, i.e. including e.g. **basis** or **origin**, as long as the 20 numerical values are included. Then, by right-clicking any cell in the rotational or translational part of the basis transformation, the transformation string can be pasted by selecting *paste (R|t)*. At this point, it should be verified that the transformed operators constitute a subset of the ones in the parent space group $P2_1/c$. As this is the case one can transfer the MSSG from the *Preview* tab. The parent space group is left unchanged for which no conversion of lattice constants and atomic positions is necessary. Furthermore, the general site multiplicity is the same in both MSSG and CSG. Therefore, all the options should be unchecked before clicking *Transfer MSSG*.

6.3 Data converter

Data from ILL Triple Axes Spectrometers (TAS) and from PSI muPAD can be opened with MAG2POL and converted to a *.fli file under certain conditions:

- each Numor contains a 1-point (peak) or 3-point scan (left background - peak - right background)
- the scan was done using a PAL file which defines the polarization channels to measure
- the information concerning \mathbf{P}_i and \mathbf{P}_f are listed as output parameters for each point of the scan

If these criteria are not met, the program will show an error message for each corresponding Numor which could not be (fully) loaded (see Fig. 6.3). The loaded polarization matrix elements can optionally be merged in the final *.fli file by activating the corresponding

ILL TAS

Numor	h	k	l	Date	Time	T	Pi	Pf	pol	dpol	R	dR	
1	21095	0.5433	0	0.3584	06-Sep-19	15:30:20	0	+x	+x	-0.8958	0.0014	0.0549	0.0008
2	21095	0.5433	0	0.3584	06-Sep-19	15:30:20	0	+x	+y	0.0639	0.0026	1.1365	0.0059
3	21095	0.5433	0	0.3584	06-Sep-19	15:30:20	0	+x	+z	0.0026	0.0026	0.9954	0.0052
4	21095	0.5433	0	0.3584	06-Sep-19	15:30:20	0	+y	+x	0.0025	0.0025	0.8417	0.0043
5	21095	0.5433	0	0.3584	06-Sep-19	15:30:20	0	+y	+y	0.0014	0.0014	0.0645	0.0008
6	21095	0.5433	0	0.3584	06-Sep-19	15:30:20	0	+y	+z	0.0026	0.0026	0.9655	0.005
7	21095	0.5433	0	0.3584	06-Sep-19	15:30:20	0	+z	+x	0.0026	0.0026	0.9074	0.0048
8	21095	0.5433	0	0.3584	06-Sep-19	15:30:20	0	+z	+y	0.0026	0.0026	0.9388	0.0048
9	21095	0.5433	0	0.3584	06-Sep-19	15:30:20	0	+z	+z	0.0014	0.0014	15.8872	0.2037
10	21096	1.6277	0	1.0891	07-Sep-19	00:50:29	0	+x	+x	0.0007	0.0007	0.0585	0.0039
11	21096	1.6277	0	1.0891	07-Sep-19	00:50:29	0	+x	+y	0.0485	0.0087	1.1019	0.0193
12	21096	1.6277	0	1.0891	07-Sep-19	00:50:29	0	+x	+z	-0.0251	0.0088	0.951	0.0168
13	21096	1.6277	0	1.0891	07-Sep-19	00:50:29	0	+y	+x	-0.0679	0.0086	0.8728	0.0152

merge repeated matrix elements $\Delta T <$ $\Delta Q <$

No PALs for 21094!
Scan 21097 xx incomplete!
Scan 21097 xy incomplete!
Scan 21097 xz incomplete!
Scan 21097 yx incomplete!
Scan 21097 yy incomplete!

Figure 6.3: List of loaded polarization data. Incomplete information will be output with a warning message.

checkbox at the bottom of the window. The binning values for temperature and Miller indices can also be given.

6.4 Irreducible representations

MAG2POL offers the possibility to calculate the irreducible representations (irreps) which yield magnetic structure models with different symmetries that are allowed by the underlying crystal structure and the propagation vector (see [this](#) demo video). The method of obtaining the so-called little group irreps is based on the induction method which is very well explained in [31]. In fact, in order to obtain the irreps of space group $G(\mathbf{q})$ one has to find the irreps of its invariant subgroup $G'(\mathbf{q})$ of index 2 or 3. This co-set decomposition is done iteratively until the translation group or a cyclic group is reached, whose irreducible representations can readily be written down. The case of cubic space groups is dealt with separately in the original paper and has been adopted as well in MAG2POL. The irreps of the full group (or paramagnetic group) are induced from the little group irreps according to the symmetry operators (coset representatives) that transform \mathbf{q} to $-\mathbf{q}$ or \mathbf{q}_1 to \mathbf{q}_2 following the procedure detailed in [32]. In fact, MAG2POL offers to use both the induced irreps (as calculated within the program) and the tabulated irreps following [32], which—in particular—differ for type-1 irreps that have been brought into real form in the latter case. Note that both results are equivalent, i.e. the irreps only differ by an equivalence transformation and therefore the projection operator produces different sets of basis vectors, which, nevertheless, are linear combinations of one another. The user can choose between the little group irreps, complex irreducible representations (CIR) and physically irreducible representations (PIR). The latter are those that are used on the ISODISTORT website.

The menu item *Generate→Irreducible representations* and the toolbar icon will be enabled after generating a structure with at least one magnetic site. Note that depending on the magnetic symmetry operators remaining in the little group certain magnetic sites split into several orbits. This will automatically be updated by the program in the main window, when a little-group irrep is activated (note that split sites should be grouped together in the atom list, when a structure model is entered manually, i.e. without using the irrep tool). Similarly, if the given structure already contains split sites (either because the user entered them or because the irreps calculation has already been run at least once), they will not be split again. I.e. the irreps calculation can be performed several times without the need of modifying the sites in the main window.

Triggering *Generate→Irreducible representations* will open a new window in which a summary of the symmetry information will be shown in the *Symmetry* tab (see Fig. 6.4).

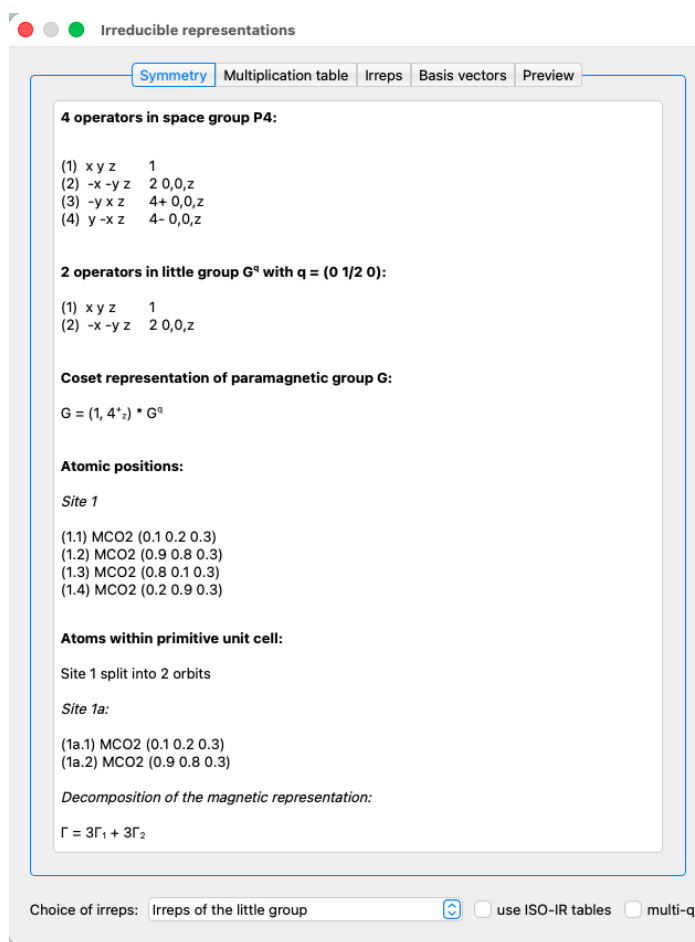


Figure 6.4: Irreducible representations window showing the symmetry operators, the coset representation of the paramagnetic group, the atomic positions and a summary of the calculation.

The symmetry operators are shown exactly as in the International Tables for Crystallography Vol.A including the same order. Further below, the symmetry operators of the little group are shown, i.e. those symmetry operators which are compatible with the magnetic translation symmetry. If the little group G^q is a subgroup of the paramagnetic group, the coset representation will be printed, i.e. which coset representatives induce the group $G^{q\bar{q}}$ and G starting from G^q . Then a list containing the magnetic atom positions is shown including the information if a split orbit is present and which symmetry operator (lost in the transition) relates the orbits. Under the tab *Multiplication table* (see the left panel of Fig. 6.5) one can see how the symmetry operators act under the group multiplication. The note below the table changes depending on the active cell and adds the information if a phase shift needs to be applied, when a non-zero propagation vector is present.

The tab *Irreps* contains the table of the irreducible representations (see central panel of Fig. 6.5). The combobox at the bottom of the window offers the choice between *Irreps of the little group*, *Irreps of the paramagnetic group* (CIR) and *Physically irreps of the paramagnetic group* (PIR). The checkbox to the right, *use ISO-IR tables* selects between the irreps induced by MAG2POL and those tabulated by ISO-IR [1, 32] (for PIRs only the ISO-IR result is available for the moment). When $G^{q\bar{q}}$ is a subgroup of G , i.e. \mathbf{q}_2 exists which is not equivalent to \mathbf{q}_1 or $-\mathbf{q}_1$, an additional checkbox *multi-q* appears. When selected, additional basis vectors for the different \mathbf{q}_n will be calculated. This output corresponds to the basis vector calculation of ISODISTORT for a commensurate propagation vector.

By hovering the mouse over the labels Γ_1 , Γ_2 etc., the Cracknell-Davies-Miller-Love (CDML) label [33] will be shown as a tooltip, e.g. mGM_1^+ , mGM_2^+ , etc. This information is extracted from the file `CIR_data.txt` based on the work published in [32]. Note that the CDML labels are shown with respect to the standard setting of the space group, i.e. the Brillouin zone label might be different for a non-zero propagation vector and depending on the type of basis transformation.

Within the table, eventual exponential factors are abbreviated and explained in the legend below the table. There are two ways to activate one or more irreps and to use them as a magnetic structure model. The first is done via a right-click on the vertical header item, e.g. Γ_1 , popping up a menu in which this particular irrep can be transferred to the current phase in the main window (note that the transfer of irreps can even be done while refining a magnetic structure in the fit window, which allows for a quick testing of different models). By highlighting two irreps and right-clicking either one a mixed irrep can be set. If no particular basis vectors are selected in the tab *Basis vectors* all basis vectors are transferred to the current magnetic structure in the main window. Note that a maximum of 6 basis vectors can be used per site, for which an error message will pop up, if this number is exceeded. In that case, or also if certain basis vectors can be excluded, the basis vectors

to export can be highlighted in the *Basis vectors* tab (see third panel of Fig. 6.5) for the corresponding irrep(s). The basis vectors can be visualized in different ways: basis vector of the first atom of each site normalized to 1, normalized with abbreviated exponential factors or with the smallest component normalized to 1. Note that the basis vector will always be exported normalized to 1 so that the multiplying coefficients can be interpreted as Bohr magnetons. Each basis vector can (repeatedly) be multiplied by i , e.g. to combine two irreps in phase quadrature. By default the basis along the principal crystallographic axes is chosen in order to calculate the basis vectors. An orthogonal basis can be chosen instead by activating the corresponding checkbox. A right-click on the checkbox opens a menu that allows the user to introduce a custom basis by entering 9 numerical values that are interpreted as 3 vectors (click *set basis*). If the checkbox is activated, MAG2POL will check if the vectors are orthogonal. The basis can be reset to its default value by clicking *reset basis* in the popup menu.

The second way of activating one or multiple irreps is via the *Preview* tab (see right

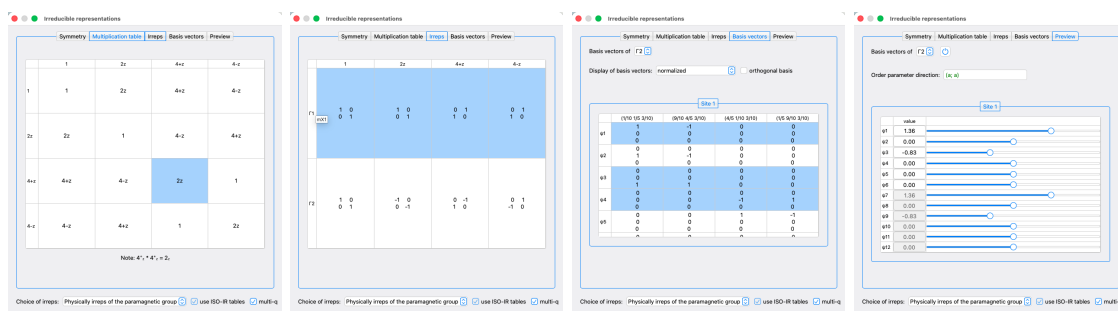


Figure 6.5: Irreducible representations window showing the multiplication table, the irreducible representations, the basis vectors and the preview sliders with an order parameter constraint.

panel of Fig. 6.5). Here, the corresponding irrep can be chosen from the combobox and then activated by clicking the on/off button next to the combobox. Sliders permit the direct visualization of the magnetic structure in the main window. Note that only the first six non-zero basis vectors will be considered per site. The shortcut *Shift+Z* sets all basis vectors of the selected irrep to 0. An additional irrep can be activated by selecting it in the combobox and clicking on the on/off button again.

When a CIR or a PIR is chosen, the order parameter direction (OPD) can be specified. Special OPDs result in constrained basis vectors and a higher magnetic symmetry, and can directly be transferred from the ISODISTORT output for the case of a PIR (or a type-1 CIR, since type-2 and type-3 PIR have double the dimension compared to the corresponding CIRs). The correct OPD syntax is fed back by green text, red otherwise. A right-click on the OPD field allows to reset the order parameter direction to the general one. For

example, the irrep mX1 of space group $P4$ with an OPD of $(\mathbf{a}; \mathbf{a})$ reveals a magnetic structure with $P4$ symmetry, instead of $P2$ for an OPD of $(\mathbf{a}; 0)$ which corresponds to the little-group symmetry. Note that with CIRs and PIRs it is not necessary to multiply basis vectors by the imaginary factor as for little group irreps, since the imaginary counterparts are automatically calculated if $-\mathbf{q}$ is not equivalent to $+\mathbf{q}$.

The coefficients, which are multiplied to the basis vector can also be set in the main window (under the *Magnetic structure* tab). The irreps information will be saved in the input file, so that the calculation does not need to be repeated. Hovering over the coefficients in the main window will show tool tips explaining to which irrep and basis vector the coefficients belong. Note that when the magnetic structure results from an irrep calculation it is not necessary to explicitly enter the magnetic symmetry operators by hand. They are internally stored together with the corresponding magnetic phases. One can also look up the basis vectors in *Structure*→*Basis vectors* and change the way of setting up the magnetic structure, i.e. use symmetry-adapted basis vectors from the irreps calculation, use user-defined basis vectors or use no basis vectors at all (i.e. use uvw coefficients).

6.5 Spin correlations

MAG2POL offers a spin-correlation tool which calculates the spin-correlation function $\langle S(\mathbf{R}) \rangle$, the intensity as a function of Q and the magnetic pair distribution function (mPDF). To calculate those distributions it is only necessary to enter a magnetic structure in the main window and click on *Tools*→*Spin correlations* or the corresponding toolbar icon. A new window will open and the 3 distribution functions will be calculated based on the R_{min} and R_{max} values which can be set to the right of the $\langle S(\mathbf{R}) \rangle$ plot. For the $I(Q)$ and mPDF plots start and end values as well as a step width can be chosen. For the latter the resolution can be taken into account via a $FWHM$ value. The underlying formalism is explained in Sec. 7.6.

The structure plot offers the same functionalities as the main window, i.e. one can click on the atoms and spins to retrieve information concerning the position, spin components, distances and angles. In the spin-correlations window the 3D plot is interactively linked with the 2D plots of the respective distribution functions. Shift-clicking two atoms to evoke their distance will automatically show the corresponding distance in the $\langle S(\mathbf{R}) \rangle$ and mPDF plots. It also works the other way round: clicking on a bar in the $\langle S(\mathbf{R}) \rangle$ bar plot will draw the bond between all spins separated by this particular distance. This offers an intuitive way to understand the correlation functions. All distribution functions can be exported either as PDF or ASCII via the *File*→*Export* menu.

The spin-correlation tool furthermore offers the possibility to visualize the results of reverse Monte-Carlo simulations performed with the SPINVERT program [34]. This can be done

by opening a `*_spins_xx.txt` file containing the spin configuration within the supercell. Note that the atomic positions in SPINVERT and MAG2POL should roughly agree (precision of 0.01) in order to identify the correct positions for plotting the structure. The R_{max} value will be set automatically depending on the used supercell. Eventually there is a huge number of spins in the supercell, therefore, in order to increase rendering speed and fluidity the object resolution can be reduced. The visualized supercell can also be adapted using the box boundary values.

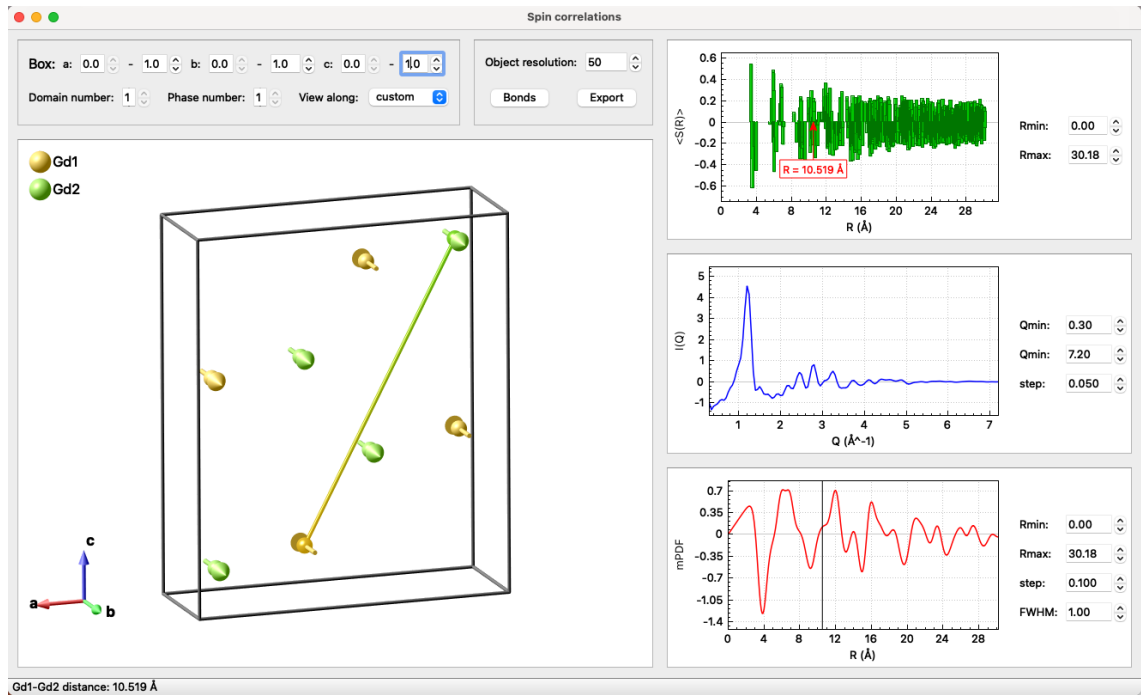


Figure 6.6: Spin-correlation window showing the magnetic structure and the different distribution functions. The 2D and 3D plots are interactively linked to each other so as to identify correlations at a particular distance.

6.6 Multi- \mathbf{q} magnetic structures

Multi- \mathbf{q} magnetic structures, e.g. conical or fan-like structures, are not only beautiful but also tricky to visualize. With MAG2POL this is very easy to do. One only needs to set up two phases in the main window (see Sec. 2.2) which have exactly the same crystal structure (note that different space groups may be used as long as the atomic positions coincide), but different magnetic parameters. In the example shown in Fig. 6.7 a ferromagnetic ($\mathbf{q}=0$) component along the c axis has been used together with a helical component in the a - b plane modulated by the propagation vector $\mathbf{q}=(0\ 0\ 1/7)$. In order to

visualize the resulting multi- \mathbf{q} structure one has to click on *Tools*→*Multi-q structure* or the corresponding toolbar icon, which will open a new window. The case might occur where the different components have been set up with a different number of magnetic domains. If the domain number to plot is superior than the number of domains in that phase, then the first domain is chosen by default. In order to combine more than two \mathbf{q} vectors, e.g. for skyrmion lattices, a single phase with different q -domains can be set up.

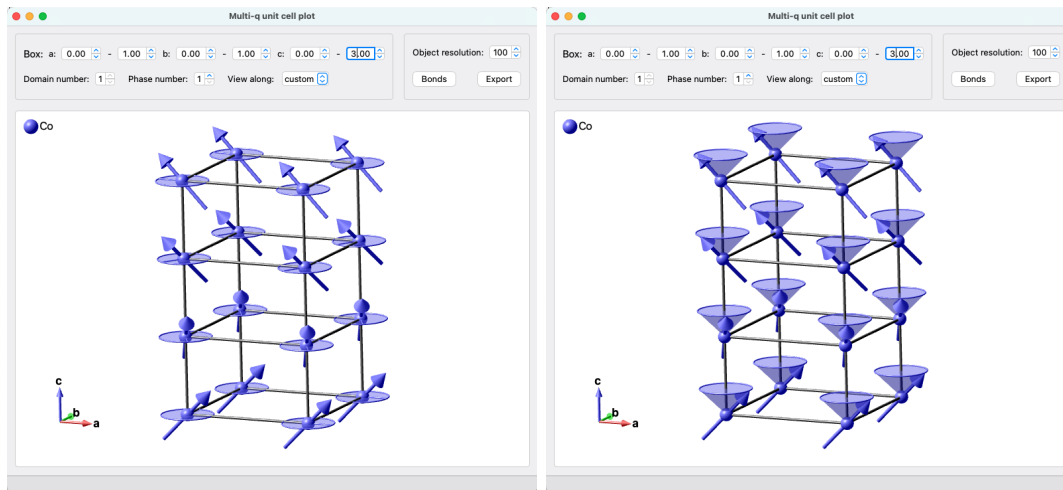


Figure 6.7: Multi- \mathbf{q} window showing the superposition of two magnetic structure components, one being ferromagnetic along the c axis and the other one being a helically modulated component in the a - b plane. The resulting superposition is a conical magnetic structure. The modulated in-plane component can be emphasized by an ellipse, where the spin direction is marked by a thin cylinder (left panel) or by a cone tracing the spin rotation (right panel).

6.7 \LaTeX export \TeX

The presentation of nuclear and magnetic structure parameters as well as information about the magnetic symmetry are the central part of a scientific report or publication. With MAG2POL it is possible to create tables in \LaTeX format containing

- nuclear structure parameters (including standard deviations from the last accepted and saved refinement)
- magnetic structure parameters (including standard deviations from the last accepted and saved refinement)
- the multiplication table of the given space group or little group

- the table of irreducible representations
- the table of basis vectors for a given irreducible representation and atomic site

These tables can be copied to the clipboard by clicking on *Tools*→*LaTeX export* and pasted into an open `*.tex` document.

6.8 Pattern editor

The pattern editor is a tool which offers the following features

- plot patterns in 1D, 2D and 3D and export as `*.pdf`
- add offsets on the 2θ /TOF/ Q/d and counts axes of loaded patterns
- create new patterns by building sums and differences
- export patterns in the MAG2POL format
- index patterns (see Sec. 6.9)

Patterns can be loaded by clicking the *Load* button and then selecting the corresponding format from the input dialog window. If the wrong format was chosen, an error message will be shown, otherwise the patterns will be shown as a 1D-plot in the panel on the left part of the window. The loaded files and the corresponding properties are shown in the table on the right. It contains the file name, wavelength (or D_1 values for TOF data), temperature, offsets and plot styles. The table can be sorted according to file name, wavelength/ D_1 or temperature by right-clicking the respective column header and choosing either ascending or descending from the *Sort* menu. The listed temperature can be switched between sample, regulation and setpoint by right-clicking the temperature header and selecting from the list within the *Temperature* menu.

As in all other plots zooming is done by clicking and dragging, while a right-click re-establishes the boundaries which are specified above the plot. If these are changed by the user they can be reset to the optimal values by right-clicking any of these values and then clicking *reset boundaries*. The first button to the right of the plot boundaries switches between 2θ /TOF, Q and d -spacing for the x axis. The remaining three buttons toggle the legend, error bars and plot grid, respectively. Hovering the mouse over the data points shows the 2θ values and counts when no more than 5 patterns are plotted.

The appearance of each data set can be modified with the respective line and marker options and the checkbox *Show* allows to show or hide a particular pattern. A right-click on the *Show* header allows to select between *Show all*, *Show every nth* and *Hide all*. Choosing the second option will open an input dialog in which the value n can be entered. In 1D-plotting mode or in order to manipulate and export patterns, offset values can be added to the 2θ or counts axes. There is a convenient way to apply a gradual offset and even a gradual color change to all visible patterns: Select the offset/color of the first and last visible pattern in the table and then right-click on the respective column header and select *Set gradient*. Choosing *Set as first* obviously sets the respective property to the one for the first pattern in the list. The legend entries can be either typed in manually or set to the temperature (the one selected in the table) or to the file name by right-clicking the *Legend* header and selecting the corresponding option.

When at least 2 patterns are visible the *View 2D* button is enabled which - after activating it - shows all visible 1D patterns in a 2D plot where the vertical axes corresponds to the temperature and the intensity is represented in a color code. Zoom and plot boundaries work as in 1D mode, additionally, the minimum and maximum values of the color bar can be adjusted by the vertical sliders on the right side of the plot. Note that any offset values in 2θ and counts are only considered in 1D plots. The *reset boundaries* context menu further allows to set the map's bin size on the temperature axis and to set the interpolation mode (on or off).

Clicking the button *Export plot* will save the shown plot (1D or 2D) in *.pdf format. As for other 2D maps holding down the CTRL/CMD button and zooming will calculate the projection of the data along the shorter side of the rectangle and the result will be shown in a new window. After a 2D map has been plotted it can also be shown in 3D by clicking on the enabled button *View 3D* which opens a OpenGL plot. Like for intensity and magnetization density maps the plot appearance can be adjusted and the plot can be exported in high resolution.

The loaded list can be cleared or exported in MAG2POL format with *.m2p extension by clicking on the *Clear* or *Save all* button, respectively. Individual patterns can be exported or removed by right-clicking the vertical header number. The file name shown in the table will be used to save the file, however, the program will remove any other extension and replace it with *.m2p, therefore, no original data can be overwritten. Note that patterns are always exported in 2θ or TOF, even if the pattern is plotted against Q or d -value. New patterns can be created from the loaded ones, e.g. sums or differences, by typing an equation in the field below the table. Each pattern is represented by the letter p and by its corresponding number in the table. Each pattern, e.g. p3, needs to be preceded

by a multiplying factor, e.g. $2*p3$ and the different patterns are combined by either the + or - sign, e.g. $2*p3-1*p4$. The correct syntax is visualized by a green font, while a red font means that there is an error in the equation. When the font is green, the *Create* button becomes active and clicking it creates a new pattern which is added to the table and plotted. At the same time the standard deviations are calculated according to the error propagation rule.

6.9 Indexation of powder patterns

The indexation tool, which helps to determine the unknown cell from the instrument geometry and the observed peak positions in a powder pattern, is based on the successive dichotomy method [35–37]. It can be opened from within the pattern editor by clicking on the cell-finder button (on the far right above the pattern plot) after loading at least one powder pattern file. When multiple patterns are loaded, an input dialog will pop up to determine which pattern should be indexed. All remaining patterns will be removed from the plot in order to improve visibility.

The *cell finder* window contains all necessary input parameters and options for running the successive dichotomy method and in principle it is not necessary to change a lot of them. First of all, the user needs to identify the positions of observed peaks. This can be done by clicking and dragging individual peaks in the pattern plot, but an automatic peak search provides a quicker result. The latter is triggered by simply moving the slider below the *Peak finder* label, where the far-right position corresponds to including peaks as weak as 1/100 of the maximum peak intensity. The detected peaks will be marked by dark blue rectangles in the pattern editor. It is possible to add (left-click), remove (right-click on a blue rectangle) or move (by dragging the blue rectangle) peaks. The information is automatically updated in the cell finder window. Peak positions can also be updated in the *obs* column of the table, which will in turn modify the position of the peak marker.

The lattice systems which are checked will be tested individually starting from the cubic case working its way down to the less symmetric ones. The indexation algorithm is very fast down to the orthorhombic case for which it is reasonable to make a preliminary search including cubic, hexagonal, tetragonal and orthorhombic systems. Note that trigonal and rhombohedral systems are included in the hexagonal case, the latter via the hexagonal setting of rhombohedral space groups. When this preliminary search does not yield any result or at least no convincing result, then the monoclinic and triclinic cases can be tested separately.

6 Tools

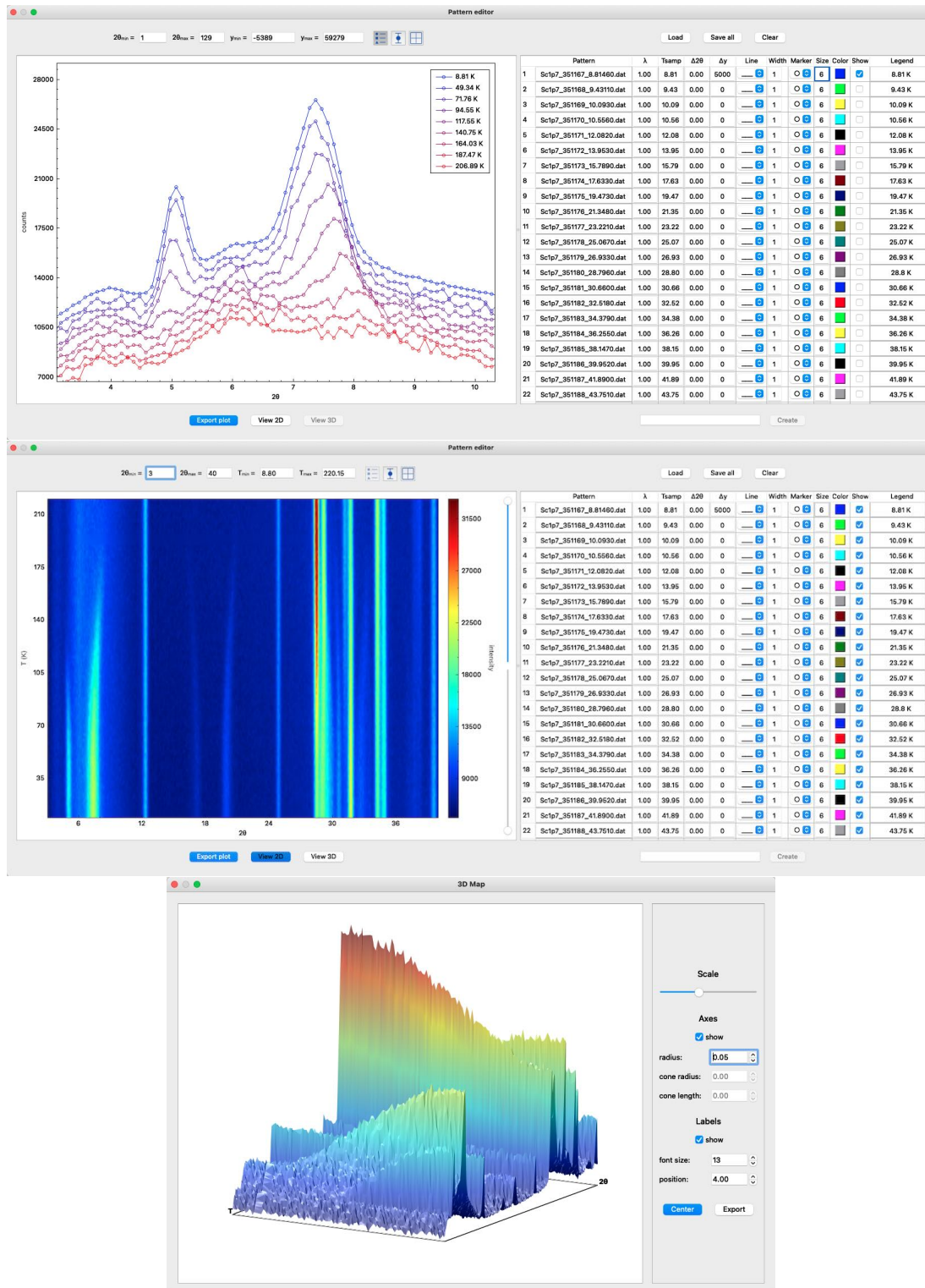


Figure 6.8: Upper panel: Pattern editor showing diffraction patterns in 1D mode. Center panel: When at least 2 diffraction patterns are set to be shown, a 2D thermodiffractogram can be shown by clicking on the *View 2D* button. Bottom panel: After viewing the plot in 2D the *View 3D* button can be clicked which opens a 3-dimensional OpenGL plot of the thermodiffractogram.

The *Precision* section contains several options which will influence the number of solutions which will be found, e.g. to use the first m peaks and allow a maximum of n impurity peaks within those m peaks. Δ_{obs} defines the absolute error which is tolerated when comparing a calculated with an observed peak position. The $V_{\text{S}}/V_{\text{min}}$ value is a criterion for new solutions with volume V_{S} to be kept after another solution with V_{min} has been found. With the default value $V_{\text{S}}/V_{\text{min}}$ only solutions with the same or smaller volumes will be kept, while increasing this parameter will keep more solutions and can be useful when a non-zero number of impurity peaks is expected. V_{max} is the maximal volume a solution can have and the search is carried out in shells of 400 Å. All found solutions will be refined including at least the lattice constants as refinable parameters (other parameters, like offsets, will be explained later) and it can be chosen in which σ interval solutions are considered to be equivalent. Furthermore, the *use reduced (Niggli) cell* option can be checked in order to avoid equivalent solutions in monoclinic and triclinic symmetries (the Niggli cell is calculated using the algorithm described in [38]).

In the *Ranges* section the minimum and maximum as well as the step values of linear and angular cell parameters can be entered. Note that the maximum angle of triclinic angles is internally limited to 115°.

The *Refinement* section contains a reduced but sufficient amount of parameters to be refined. The refinement can be done either only on the peak positions of those peaks included in the algorithm or by doing a full-pattern LeBail fit. The latter is activated by checking the corresponding checkbox. The three offset parameters can be refined to both refinement options, whereas the remaining parameters only apply to the LeBail fit. A profile function can be chosen from a combo box and the points of a linearly interpolated background can be refined. Note that an approximate description of the peak width (through the uvw parameters for constant-wavelength patterns or through the σ_n and γ_n values for TOF data) is necessary for a correct initialization of the background. The peak width and asymmetry parameters can in turn be refined depending on the chosen profile function. A right-click on the *Le Bail* label evokes a context menu from which the configuration of different diffractometers can be set conveniently. Once a set of solutions is found, it can be refined using different fit flags by clicking on *Refine solutions*.

The search algorithm is started by clicking the *Find solutions and refine* button. The progress of the search and the number of solutions found in every step for each symmetry is printed in the output box in the lower-right part of the window. If one or more solutions have been found, a space-group analysis will be performed by checking the compatibility of the m observed and used peaks with all space groups of the respective lattice system.

Finally, the list of solutions will be shown in the lower part of the window sorted by increasing χ^2 value of the refinement process. The table lists the lattice system, the refined lattice parameters, the refined volume, the most symmetric compatible space group, the number of unindexed observed peaks as well as the figures of merit M_{20} , F_N and χ^2 . M_{20} is given by

$$M_{20} = \frac{Q_{20}}{2\langle\epsilon\rangle N_{20}} \quad (6.2)$$

with Q_{20} being the Q ($\sim 1/d^2$) value of the 20th observed peak, N_{20} the number of different calculated Q values up to Q_{20} and $\langle\epsilon\rangle$ the average absolute discrepancy between the observed and calculated peak positions. F_N is given by

$$F_N = \frac{1}{\langle\epsilon\rangle} \frac{N}{N_{\text{poss}}}, \quad (6.3)$$

where N_{poss} is the number of possible peaks up to the N^{th} observed line. More information can be found in [39].

The different solutions can be shown by clicking on the vertical header number of the solutions table, which will update the calculated angles and (hkl) indices in the peak table as well as the predicted peak positions in the pattern editor. If the LeBail fit option was activated, the refined pattern is shown in addition to the predicted peak positions. In that case, it is also possible to visualize the expected peak positions within the different compatible space groups. This can be done by right-clicking the space group label and choosing a different space group from the context menu, which automatically refits and displays the LeBail fit in the pattern editor. In order to improve clarity the peak markers originating from the peak finder tool together with the indexed peak markers can be removed by toggling the respective checkboxes in the *Peak finder* section. The influence of the lattice parameters on the calculated peak positions can be studied by clicking a parameter value in the lower-right corner of the window and by dragging the slider, which will in turn modify the light blue markers.

6.10 Propagation vector finder

The first step in analyzing a magnetic structure from powder neutron diffraction data is indexing the magnetic Bragg peaks for which it is necessary to know the propagation vector, i.e. the magnetic translation symmetry in comparison to the nuclear cell. When the propagation vector is unknown, but a number of additional magnetic intensities are observable in the diffraction pattern, then the satellite tool in MAG2POL can be used. It can be found in the fit window under the *Patterns* tab and is ideally launched after the nuclear scattering has been correctly described. A click on the *Satellites* icon opens a new window which will list the selected satellite peaks and provides control for the subsequent

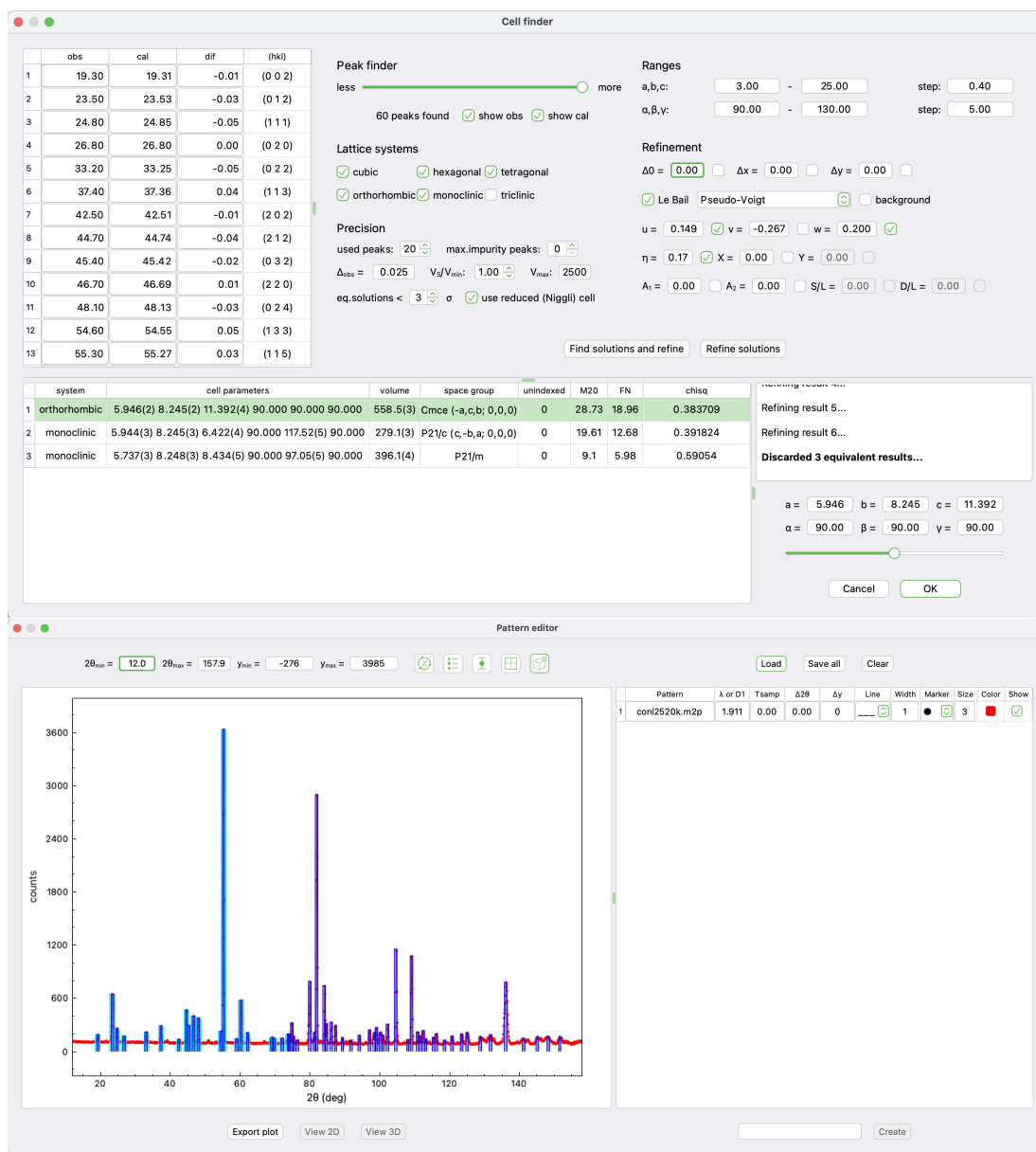


Figure 6.9: Upper panel: Cell finder window showing the results of an indexation run. Lower panel: Visualization of one of the results in the pattern editor.

search for a possible propagation vector (note that the corresponding phase needs to be activated in the fit window before entering the *Satellites* tool). In order to add a satellite to the list, simply left-click on a magnetic Bragg peak in the pattern (note that the zoom controls are still active). A vertical dark blue bar will be drawn at that position and the corresponding 2θ /TOF value will be shown in the *obs* column of the table in the *Satellites* window. The selection can be modified by hovering the mouse over the vertical bar - which changes the mouse cursor to an open-hand symbol - and dragging it to another position. In order to assist the user in finding the best possible position, the height of the bar will be modified in order to reflect the amplitude of the satellite peak at that position. The position can also be modified in the table which is synchronized with the plot. A selected peak can be deleted by right-clicking on the vertical bar.

After selecting a few satellites, the search for a possible propagation vector can be started. Different propagation vector symmetries can be included in the search algorithm, whereas the high-symmetry lines of the Brillouin zone are selected by default. The checkboxes in the second row denote planes in the Brillouin zone and activating the box in the third row would include the search of a propagation vector with triclinic symmetry. Initial guesses for possible propagation vectors are generated with a user-definable step size along the a^* , b^* and c^* directions and the best n guesses (in terms of χ^2 , $n = 20$ by default) will be used as starting parameters in a least-squares refinement with the corresponding refinable parameters. Note that the explored parameter range depends on the centering label of the space group. The results of the refinement are shown in the table in the lower part of the *Satellites* window sorted by decreasing χ^2 values. The best result is automatically highlighted and the calculated positions are shown as larger light-blue bars in the diffraction pattern as well as in the *cal* column of the upper table. The difference between the observed and calculated positions is shown together with the corresponding $(hkl)\pm$ indices. By clicking on the vertical header labels one can cycle through the different results, which will update the plot in the fit window. It is also possible to manually modify the refinable propagation vector components. This can be done by clicking on one of the three \mathbf{q} components in the lower-right part of the *Satellites* window and then by dragging the horizontal slider below the values, which will move the calculated peak positions in the pattern plot. This is particularly useful to check, if a resulting \mathbf{q} component is incommensurate or not.

By clicking the *OK* button, the propagation vector is transferred to the active phase of the active pattern in the fit window.

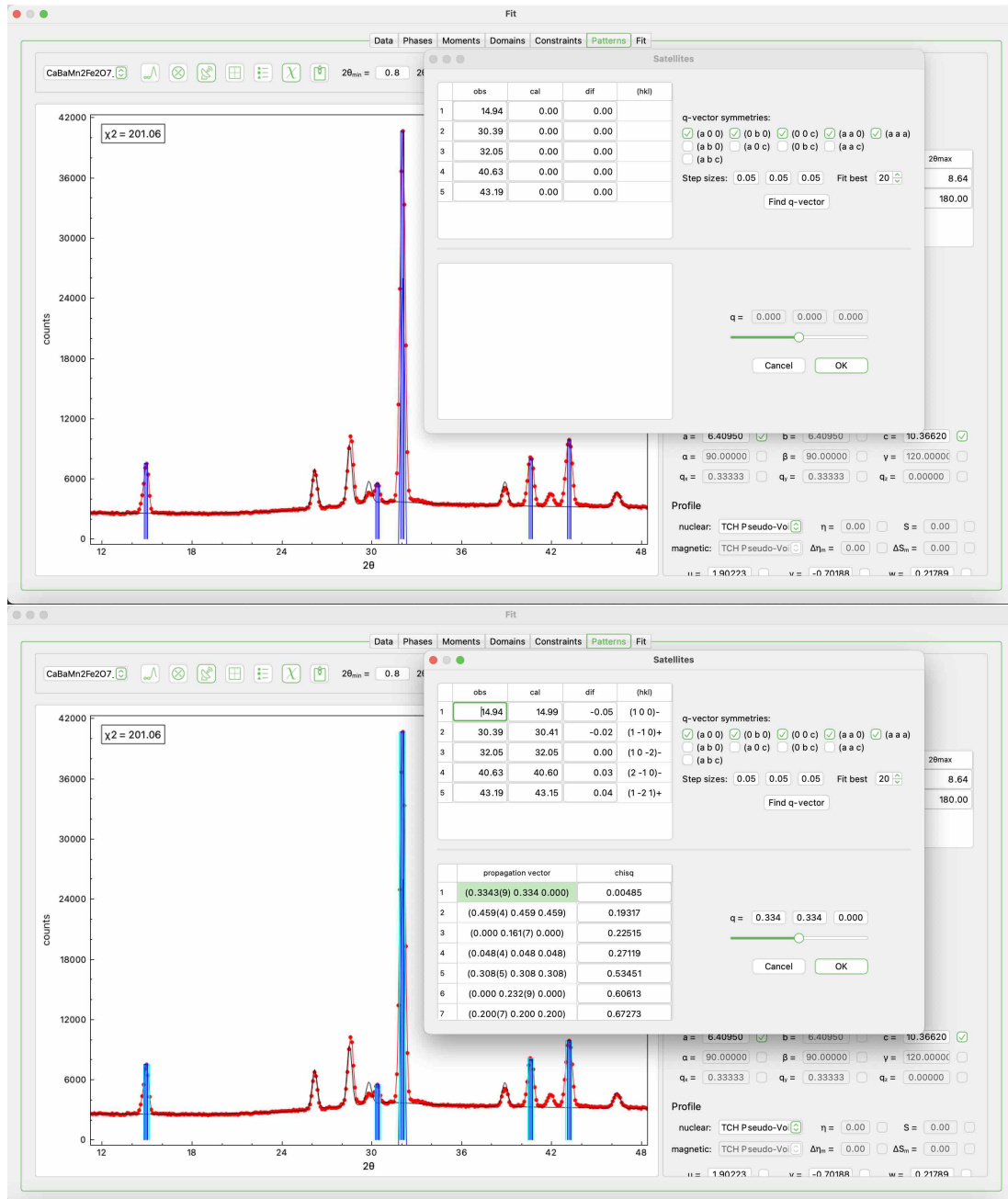


Figure 6.10: Upper panel: Selected magnetic satellites shown by dark blue vertical bars. Lower panel: A list of possible propagation vectors is shown with decreasing χ^2 values.

6.11 Guides to the eye

Certain nuclear and magnetic structures benefit from guides to the eye which highlight their peculiarities. With MAG2POL such hints can be added to the OpenGL unit cell plot in 3D through the following objects (with their corresponding customizable properties):

- Arrow (position, direction, shaft radius, cone radius, cone length, color)
- Cylinder (start position, end position, radius, start color, end color, transparency, gradient)
- Sphere (position, radius, color)
- Ellipse (position, first axis, second axis, color, transparency)
- Torus (position, first axis, second axis, radius, color)
- Spiral (position, first axis, second axis, radius, height, windings, phase, start color, end color)
- Sine (position, propagation direction, amplitude, radius, cycles, phase, start color, end color)
- Plane (at least 3 points, color, transparency)
- hkl plane (hkl indices, color, transparency, family)
- Box (position, length, width, height, color, transparency)
- Text (position, text, font size, color)

All positions are given in fractional coordinates with respect to the unit cell (just like atomic positions), while all vector quantities are defined in units along the crystallographic axes, i.e. in the same way as magnetic moments (the length corresponds to the that of magnetic moments with a plot scale of 1.0). Note that the vectors are not normalized, i.e. the size of an ellipse or the wavelength of a sine (through the propagation direction) depend on the length of the vectors. The best way to invert the handedness of a spiral is to define negative number of windings (it is also possible to define a negative height, but the spiral will propagate in the opposite direction). Depending on the object it is possible to define the transparency or a color gradient.

The *Guides to the eye* window can be accessed via the *Tools* menu or directly via its toolbar icon. It shows a list of all guides to the eye presently defined in the unit cell plot. From here it is possible to create a new guide to the eye (*New* button), modify a present

one (*Edit* button), duplicate (*Duplicate* button) or delete it (*Delete* button). A click on the *New* button opens a dialog from which one of the listed objects can be chosen. This opens another window in which the respective properties can be entered (see Fig. 6.11). Atomic positions and spin vectors can be pasted into the respective fields by selecting an atom/spin in the unit cell plot and then by right-clicking on the respective label in the object dialog (e.g. *Position*, *Start*, *End*, *Direction*, etc.). By selecting two atoms (as for calculating the distance) the right-click menu allows to copy the midpoint between those two atoms.

The visibility of guides to the eye can be triggered in the settings window under the

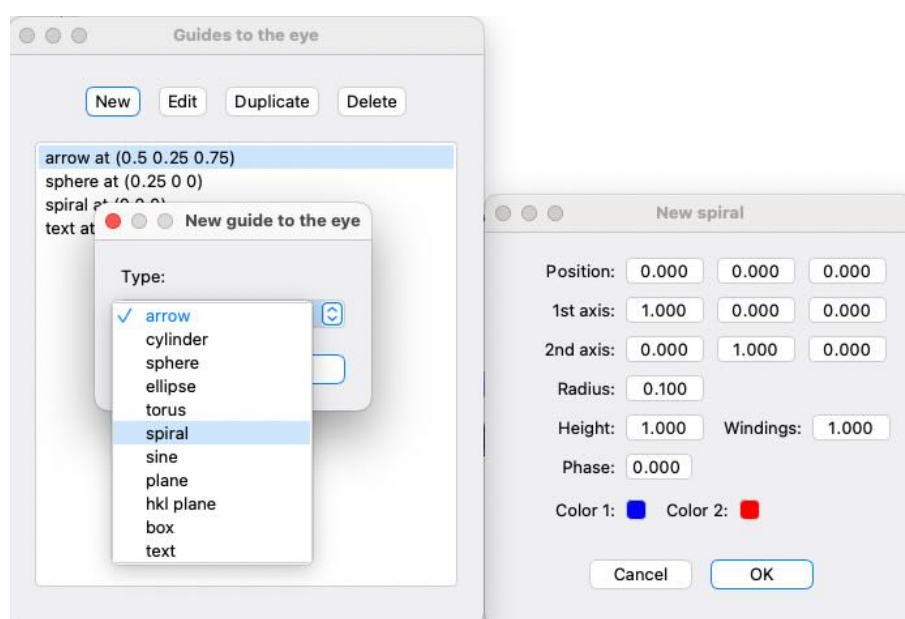


Figure 6.11: *Guides to the eye* window (left) showing a list of objects which are depicted in the unit cell plot. New guides to the eye can be created, edited or deleted. A click on the *New* button opens a dialog from which one of the implemented objects can be chosen. Afterwards, the object can be customized in the object property window (right).

Plot tab. The figures below show some examples in which 3-dimensional guides to the eyes may be useful (and one example where they are absolutely useless).

6.12 Phase transitions

In single-crystal diffraction experiments, nuclear and/or magnetic phase transitions are best identified and illustrated by following e.g. the integrated intensity of selected Bragg reflections as a function of temperature, magnetic field or pressure. MAG2POL offers a

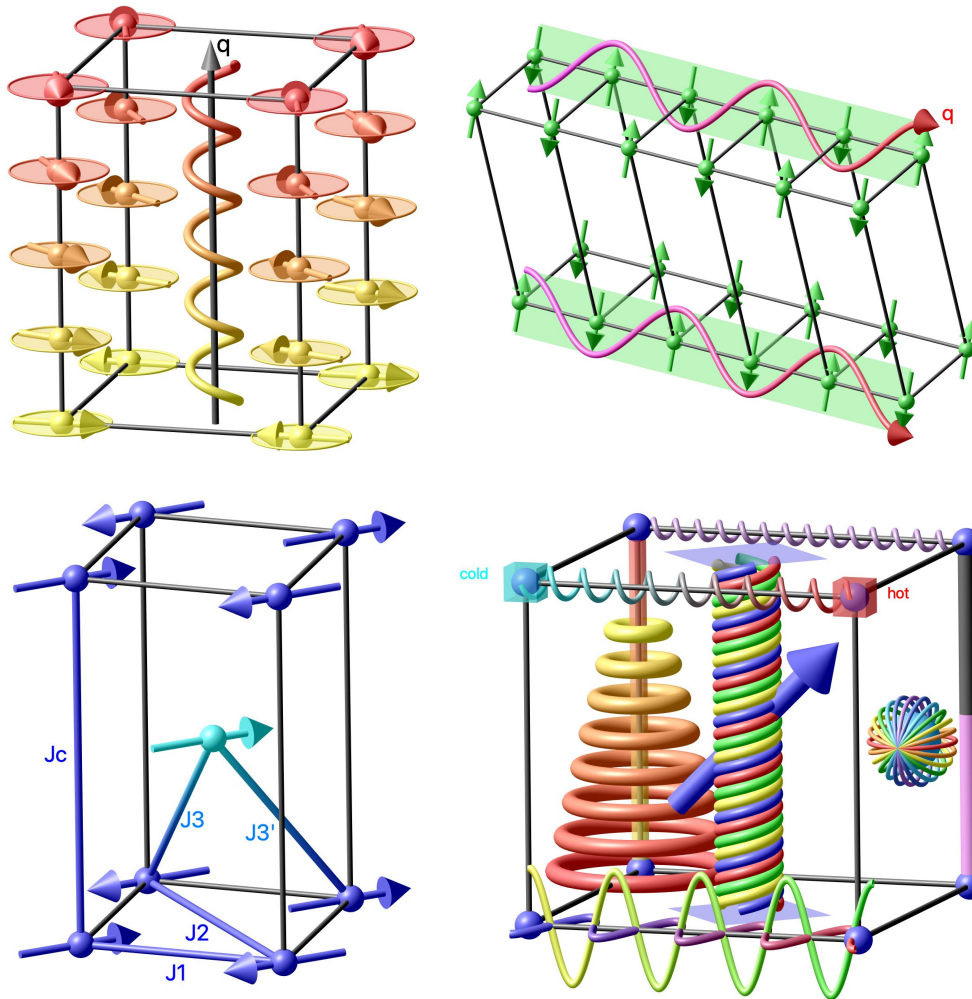


Figure 6.12: Examples of 3-dimensional guide-to-the-eye objects.

Phase transition tool which helps to find appropriate (hkl) reflections showing a significant difference between the involved structures, or - the other way round - to check if certain structures explain an observed transition. In order to use this tool it is necessary to define at least 2 phases in the main window, which are listed in the upper left part of the *Phase transitions* window. Each phase is given an x value according to its number, which can be changed in order to be taken into account in the plot on the right part of the window. In the lower left part, a list of Bragg reflections reflections can be created by entering the h , k , l and $\pm\mathbf{q}$ values and clicking the *Add* button. The quantities according to the combo boxes *y axis1* and *y axis 2* will be calculated and plotted against the different phases. The plot can be modified with respect to the marker and line styles (note that a different style is automatically applied for the right y axis, if enabled). User-defined axes, tick and legend labels can be entered to customize the plot, which can be exported as a pdf or ASCII file. Reflections can be removed by right-clicking the vertical header labels and then clicking *Remove reflection*.

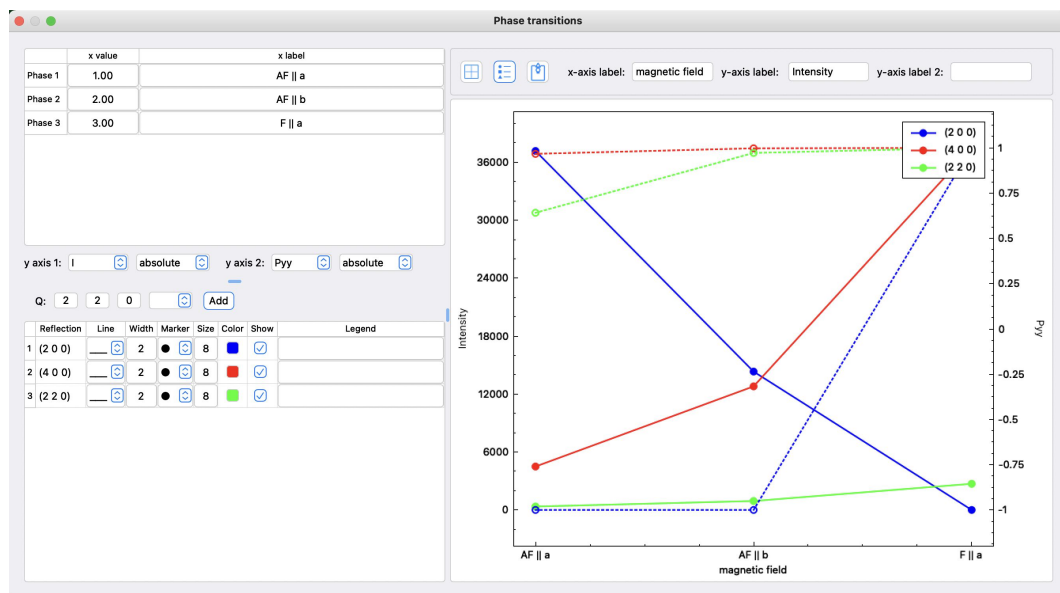


Figure 6.13: Phase transitions window.

6.13 Crystal calculator

After a crystal structure has been generated in the main window, the crystal calculator can be used to compute distances, angles, vector cross products as well as matrix products and inversions. Distances and vectors will be shown in the unit cell for a visual confirmation.

- Distances

Two positions need to be entered in fractional coordinates of the direct lattice. The result is given in Å and the points and distance are shown in the unit cell plot. Similarly to the guides to the eye window, a right-click on the *Position 1* or *Position 2* label allows to copy the position of a previously selected atom (or the midpoint of two previously selected atoms) in the main window unit cell plot.

- **Angles**

Here, two options are possible: the angle can be calculated by defining either two vectors or three points. The angle which is plotted in the unit cell depends on the *Show* checkbox. The vector coefficients can be entered in different bases and can even be mixed which allows all the flexibility for the user. The *direct* and *reciprocal* bases have the direct and reciprocal lattice vectors as basis vectors. The *spin* basis uses the normalized direct lattice vectors as a basis. The *diffractometer* and *Busing-Levy* bases refer to the orthonormal coordinate axis of the instrument (as defined in the *Instrument* window) and of the Busing-Levy reference frame, respectively. Again, a right-click on the vector and position labels allows to copy the atomic position or spin direction of previously selected objects.

- **Vectors**

Two vectors can be entered using different bases and the cross product can be expressed in another basis. This allows for example to calculate the spin direction which would maximize the intensities of two magnetic Bragg reflections which are expressed by reciprocal lattice vectors as shown in Fig. 6.14. Another useful application is to deduce the angle between a crystal axis or a magnetic moment and the vertical diffractometer axis (UB matrix necessary). The labels *Vector 1* and *Vector 2* can be right-clicked in order to copy the spin values of a selected spin in the main window unit cell plot and a right-click on *Cross product* copies the result to the *Angles* tab for eventual further calculations.

- **Matrices**

The product of two matrices or the inverse of a matrix can be calculated. Right-click context menus can be used to set the rotation matrix of a symmetry operator or to copy the resulting matrix to one of the first slots in order to make another calculation. If the matrix that has been set or calculated corresponds to the rotational part of a symmetry operator the label of the latter will be shown as a tooltip when hovering over the matrix elements.

- **Magnetization**

The magnetization along a given axis can be calculated, if the magnetic structure model in the main window is ferro- or ferrimagnetic. The result is given in SI and

CGS units and can be conveniently converted by directly modifying the respective values and units.

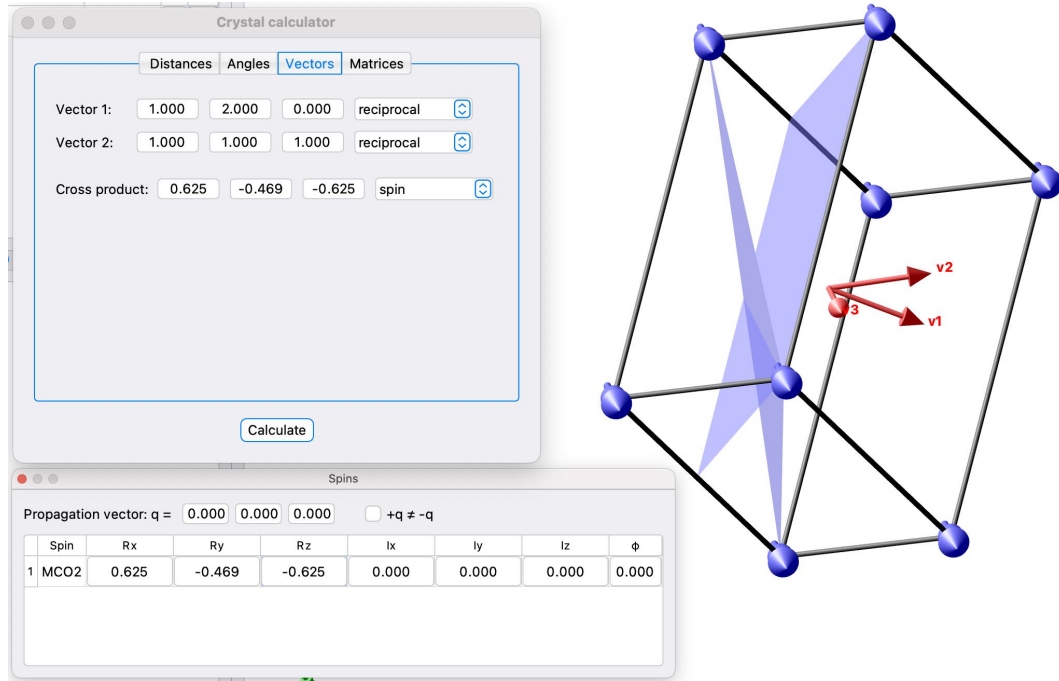


Figure 6.14: Crystal calculator window with the different options under the 4 tabs *Distances*, *Angles*, *Vectors* and *Matrices*. The example shows the cross product of two vectors given in reciprocal lattice units, where the result is converted to spin coefficients which can directly be used to generate a magnetic structure which would maximize the intensities of these two reflections, whose (hkl) planes are visualized as guides to the eye.

6.14 Cell animation

The unit cell plot of a crystal or magnetic structure can be animated in order to provide a better understanding of the structural characteristics in different perspectives. Such an animation can be useful to create vivid clips which can be used in presentations. The *Cell animation* tool allows to do this in a very intuitive way.

After opening the tool via *Tools* \rightarrow *Cell animation* or the corresponding toolbar icon, one can choose from three built-in animations. Up to ten user-defined animations can be saved and played from any *.xml file. The section *Initial position* defines the start of the animation which is expressed in spherical coordinates, where θ is the rotation angle around the viewport y axis (pointing upwards), ϕ is the rotation angle around the viewport z axis (pointing out of the viewport, towards the observer) and χ is a rotation around the c^*

axis of the unit cell. The horizontal and vertical translations of the structure within the viewport can be set with dx and dy . The zoom and depth values are the same as in the unit cell plot in the main window (the latter is only used, if the perspective projection is activated via the corresponding button). The easiest way to set a cell orientation is to manipulate the structure in the OpenGL plot and to click the *Get* button afterwards. The opposite can also be done, by adjusting the angle, offset and zoom values and then by clicking the *Set* button, which will position the cell in the OpenGL plot.

The next part is the *Animation sequence*, where the number of steps and the frames per second (fps) can be set. For each step, the difference in the orientation, position and zoom values of the cell are adjustable in the same way as for the initial position, i.e. using the *Get* and *Set* buttons. In addition, the duration (in seconds) of each step can be set. A click on the *Play* button shows the animation in the main window, which can be recorded using a separate screenshot tool. Alternatively, the graphics can be exported at each step by activating the checkbox under the *Export setting* section. The zoom factor has the same function as for exporting graphics from the main window. The output folder has to be set and an optional file prefix can be set to which the extension `_stepnumber_imagenumber` will be added.

6.15 Bond distances

This tool generates a list of bond distances between user-definable atoms and ranges and offers the visualization of individual bonds from the list. After correctly generating a crystal structure, this tool becomes available under *Tools* → *Bond distances*. Upon entering the *Bond distances* window, atom pairs can be chosen from the combo boxes under *Atom 1* and *Atom 2* which are ordered by elements and—after the separator—by sites. For each chosen atom pair the minimum and maximum bond lengths can be constrained. A click on the *Add* button adds the bond distance parameters to a numbered table. The bonds corresponding to that input are shown in the bottom table. Note that the information in the upper table can be modified as the bottom table is synchronized. By clicking on the value of a particular bond length, the corresponding bonds are plotted in the main window. Two options are available for increased visibility: (1) by activating *hide present bonds and polyhedra*, the user-defined structural characteristics are temporarily removed in order to clearly display the selected bonds. (2) The option *show all connected atoms* extends the plot boundaries to include connected atoms outside of the user-defined box. The bond distance table can be exported to an ASCII file by clicking on the button on the lower-right of the window.

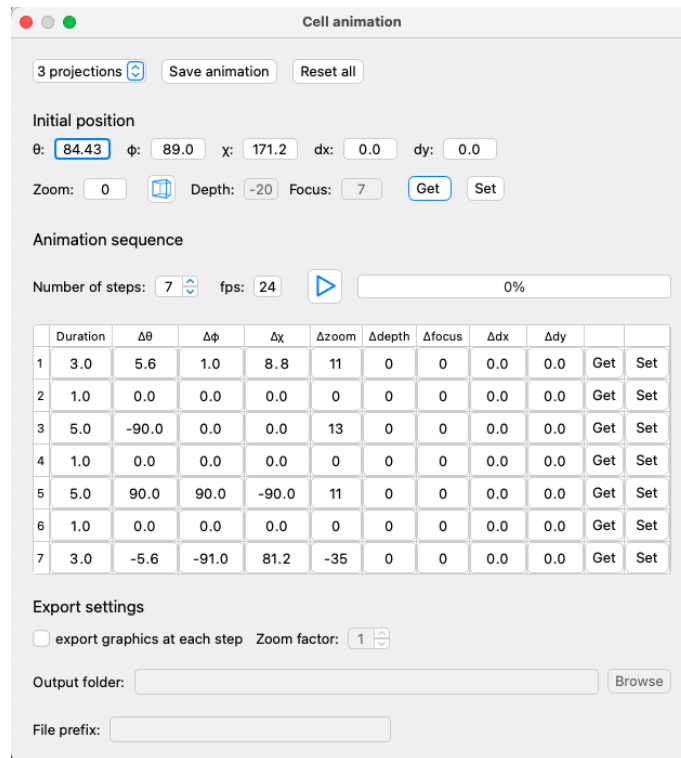


Figure 6.15: *Cell animation* window showing the built-in sequence which focuses on the three high-symmetry projections of an orthogonal system.

6.16 Polarization matrix plot

Instead of listing all individual elements in the *View data* or *View results* windows, polarization matrices can be visualized in matrix form using a polar color gradient going from red (+1) over white (0) to blue (-1). Hereby, the table will be read from top to bottom and different matrices (corresponding to (hkl) values and the cross section, e.g. ++, -- etc) will be filled. This feature produces meaningful plots, when a certain structure of the table exists, i.e. the matrix elements should be grouped by Miller indices and cross sections and repeated measurements should be averaged first. Such a case is shown in Fig. 6.16 where eight complete polarization matrices were recorded, which are conveniently shown in an automatically created grid. The table to the left lists the different reflections and the measured cross section (i.e. the sign of the polarization and analysis axes) and some plot controls. The *plot* checkbox toggles the visibility of the respective matrix, the index is the placement in the grid (and allows to modify the plot order) and the label is based on the (hkl) , which can be modified by the user. The matrices are by default plotted with elements $P_{i,f}$ (according to the way of working on the D3 instrument), where i and f stand for the direction of the polarization and analysis axes, respectively. The plots can be transposed by selecting $P_{f,i}$ from the combo box in order to plot matrices according to the correct definition relating the incoming and final neutron polarization by $\mathbf{P}_f = \mathcal{P}\mathbf{P}_i$ (for the rotational part), see also Sec. 7.2. Different plot types can be chosen from the next combo box, which is rather self-explaining. Nevertheless, note that the graphical representation of the error bars is encoded in the gray scale of the marker edge which ranges from 0 (black) to the maximal error among all observations (white). For plots comparing calculated and observed values each marker is horizontally divided into left = observed and right = calculated. Hovering above the matrix elements will show the exact values as a tool tip. The checkbox *numbers* also allows to plot the numerical data/results in matrix form. A right-click on any matrix evokes a menu from which one can choose to copy the \LaTeX code to the clipboard (note that this option is disabled for observed vs. calculated comparisons).

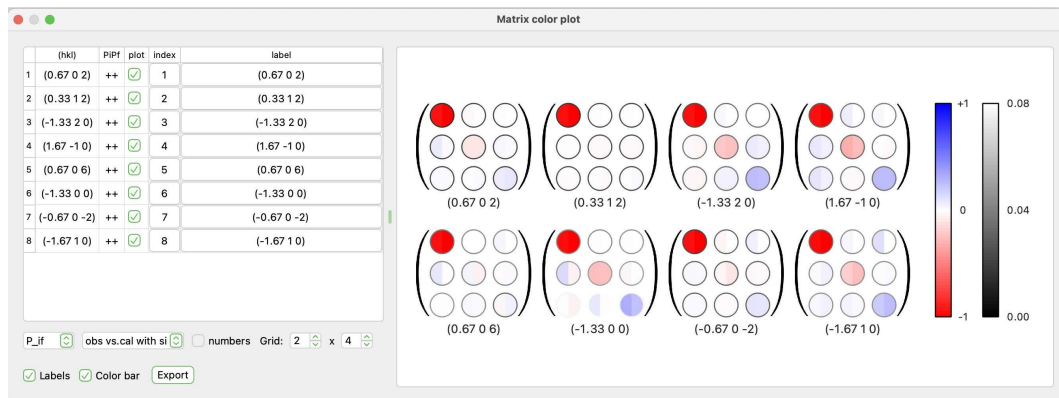


Figure 6.16: Matrix color plot of a fit result with data containing 8 complete polarization matrices.

7 Mathematical information

7.1 Basic equations

MAG2POL uses the plane wave function following conventions of quantum mechanics, which is generally used for neutron scattering and which is the complex conjugate of that used in x-ray scattering:

$$\psi_{QM} = \psi_{XR}^* = e^{i(\mathbf{k}\mathbf{r} - \omega t)}$$

which requires

$$b = b' - ib'' \quad \text{with} \quad b'' > 0$$

for the scattering length and yields the scattered wave as a superposition of the plane wave and the spherical wave in the form of

$$\psi(\mathbf{r}) = e^{i\mathbf{k}\mathbf{r}} + f(\theta, \phi) \frac{e^{ikr}}{r}.$$

The scattering amplitude is the Fourier transform of the scattering potential and is given by

$$f(\theta, \phi) \propto - \int V(\mathbf{r}) e^{-i\mathbf{Q}\mathbf{r}} d\mathbf{r}$$

with the scattering vector $\mathbf{Q} = \mathbf{k}_f - \mathbf{k}_i$. Note that using the conventions for X-ray scattering or $\mathbf{Q} = \mathbf{k}_i - \mathbf{k}_f$ leads to the complex conjugate of the scattering amplitude. The nuclear structure factor can therefore be written as

$$N(\mathbf{Q}) = \sum_j o_j b_j e^{-2\pi i(hx_j + ky_j + lz_j)} e^{-B_j \sin^2 \theta / \lambda^2}$$

with the second exponential term being the Debye Waller factor. The sum is done over all the atoms in the unit cell and o_j denotes the multiplicity and occupation of atom j . Note that the leading minus sign has been dropped as the square of the structure factor is used in all calculations.

The magnetic structure factor writes as

$$\mathbf{M}(\mathbf{Q}) = \sum_j p_n o_j \mathbf{S}_j f_j(\mathbf{Q}) e^{-2\pi i(hx_j + ky_j + lz_j)} e^{-B_j \sin^2 \theta / \lambda^2}$$

where $p_n = 0.2695420113693928312$ is the conversion factor between Bohr magnetons and scattering lengths. A factor 0.5 is applied, when the non-zero propagation vector $+\mathbf{q}$ is

inequivalent to $-\mathbf{q}$. \mathbf{S}_j are the Fourier coefficients of the magnetic moment expansion according to

$$\boldsymbol{\mu} = \frac{1}{2} \sum_{\mathbf{q}} S_{\mathbf{q}} e^{i\mathbf{q}\mathbf{R}} + S_{\mathbf{q}}^* e^{-i\mathbf{q}\mathbf{R}}$$

The Fourier coefficients of a given magnetic moment contain a phase factor determined by symmetry and a refinable one. For the calculation of $(hkl) - \mathbf{q}$ satellites the complex conjugate of \mathbf{S}_j .

The calculated intensities, which are to be compared to the observed ones, are given by

$$I_N(\mathbf{Q}) = scale \cdot y \cdot NN^*$$

and

$$I_M(\mathbf{Q}) = scale \cdot y \cdot \mathbf{M}_{\perp}(\mathbf{Q})\mathbf{M}_{\perp}^*(\mathbf{Q})$$

with the magnetic interaction vector

$$\mathbf{M}_{\perp} = \hat{\mathbf{Q}} \times (\mathbf{M}(\mathbf{Q}) \times \hat{\mathbf{Q}})$$

scale is a simple scaling factor and *y* is the extinction correction mentioned in Sec. 3.3.

7.2 Polarization matrices

The polarization values are calculated using the density matrix formalism [40] according to

$$P_f = \frac{\text{Tr}(\boldsymbol{\sigma} \cdot \mathcal{M} \cdot \boldsymbol{\rho} \cdot \mathcal{M}^{\dagger})}{\text{Tr}(\mathcal{M} \cdot \boldsymbol{\rho} \cdot \mathcal{M}^{\dagger})}$$

with

$$\boldsymbol{\sigma} = \begin{pmatrix} P_{f,z} & P_{f,x} - iP_{f,y} \\ P_{f,x} + iP_{f,y} & -P_{f,z} \end{pmatrix},$$

$$\boldsymbol{\rho} = \frac{1}{2} \begin{pmatrix} 1 + P_{i,z} & P_{i,x} - iP_{i,y} \\ P_{i,x} + iP_{i,y} & 1 - P_{i,z} \end{pmatrix},$$

and

$$\mathcal{M} = \begin{pmatrix} N + M_{\perp,z} & -iM_{\perp,y} \\ iM_{\perp,y} & N - M_{\perp,z} \end{pmatrix}.$$

\mathcal{M}^{\dagger} denotes the conjugate transpose of \mathcal{M} . The coordinates x , y and z refer to the local coordination system, where x is always parallel to the scattering vector \mathbf{Q} , z is vertical and y completes the right-handed coordination system. The initial neutron polarization is considered by multiplying it to the matrix of the incident beam $\boldsymbol{\rho}$. The finite ^3He cell

efficiency is considered in the same way in the matrix of the analyzed beam σ .

The final neutron spin \mathbf{P}_f is related to the initial one by

$$\mathbf{P}_f = \mathcal{P}\mathbf{P}_i + \mathbf{P}'$$

where \mathcal{P} is a rotation matrix acting on the initial neutron spin \mathbf{P}_i and \mathbf{P}' is the created/annihilated polarization. By aligning the initial neutron polarization along the directions x , y or z and by analyzing the component of the final neutron spin along these directions, one can summarize nine measurements in the so-called polarization matrix, which is better defined as a pseudomatrix, since it combines the rotation and the created/annihilated polarization. For the general case, i.e. including nuclear, magnetic and interference terms as well as different degrees of polarization and analyzer efficiency for the different directions, the polarization matrix is

$$\mathbf{P}_{f,i} = \begin{pmatrix} p_{fx} \frac{p_{ix}(N^2 - M^2) - J_{yz}}{I_x} & p_{fx} \frac{-p_{iy}J_{nz} - J_{yz}}{I_y} & p_{fx} \frac{p_{iz}J_{ny} - J_{yz}}{I_z} \\ p_{fy} \frac{p_{ix}J_{nz} + R_{ny}}{I_x} & p_{fy} \frac{p_{iy}(N^2 + M_{\perp y}^2 - M_{\perp z}^2) + R_{ny}}{I_y} & p_{fy} \frac{p_{iz}R_{yz} + R_{ny}}{I_z} \\ p_{fz} \frac{-p_{ix}J_{ny} + R_{nz}}{I_x} & p_{fz} \frac{p_{iy}R_{yz} + R_{nz}}{I_y} & p_{fz} \frac{p_{iz}(N^2 - M_{\perp y}^2 + M_{\perp z}^2) + R_{nz}}{I_z} \end{pmatrix}$$

with $N^2 = NN^*$, $M^2 = \mathbf{M}_{\perp}\mathbf{M}_{\perp}^*$, $M_{\perp y}^2 = M_{\perp y}M_{\perp y}^*$ and $M_{\perp z}^2 = M_{\perp z}M_{\perp z}^*$. The mixed magnetic terms are $R_{yz} = 2\Re(M_{\perp y}M_{\perp z}^*)$ and $J_{yz} = 2\Im(M_{\perp y}M_{\perp z}^*)$, while the nuclear-magnetic interference terms are $R_{ny} = 2\Re(NM_{\perp y}^*)$, $R_{nz} = 2\Re(NM_{\perp z}^*)$, $J_{ny} = 2\Im(NM_{\perp y}^*)$ and $J_{nz} = 2\Im(NM_{\perp z}^*)$. The respective matrix elements are normalized to the scattered intensity depending on the initial neutron polarization:

$$\begin{aligned} I_x &= N^2 + M_{\perp y}^2 + M_{\perp z}^2 + p_{ix}J_{yz} \\ I_y &= N^2 + M_{\perp y}^2 + M_{\perp z}^2 + p_{iy}R_{ny} \\ I_z &= N^2 + M_{\perp y}^2 + M_{\perp z}^2 + p_{iz}R_{nz} \end{aligned}$$

In the absence of nuclear scattering, i.e. for a purely magnetic peak, $N = R_{ny} = R_{nz} = J_{ny} = J_{nz} = 0$. One can in general assume the same degree of incident neutron polarization as well as analyzer efficiency for the different directions: $p_{ix} = p_{iy} = p_{iz} = p_0$ and $p_{fx} = p_{fy} = p_{fz} = p_f$. The latter is equal to 1 for data which have been already corrected for the analyzer efficiency. The above polarization matrix is obtained by applying the density matrix formalism for each individual element.

7.3 Flipping ratios

The flipping ratio R of a Bragg reflection is defined as the intensity ratio between spin-up and spin-down neutrons and is given by

$$R = \frac{I^+}{I^-} = \frac{NN^* + (N\mathbf{P}_0\mathbf{M}_\perp^* + N^*\mathbf{P}_0\mathbf{M}_\perp) + M_\perp M_\perp^*}{NN^* - (N\mathbf{P}_0\mathbf{M}_\perp^* + N^*\mathbf{P}_0\mathbf{M}_\perp) + M_\perp M_\perp^*}$$

where \mathbf{P}_0 is the vector of the initial neutron polarization to be taken along the vertical axis of the diffractometer and the dot product $\mathbf{P}_0\mathbf{M}_\perp$ gives the projection of the magnetic interaction vector onto the vertical polarization axis.

The extinction correction for flipping ratios corresponds to the one which is applied in FULLPROF [15], see the *Flipping Ratios in FullProf* manual. The flipping ratio is then written as

$$R = \frac{(NN^* + M_{\perp,z}M_{\perp,z}^*)p_p^+ + (N^*\mathbf{p}_m^+\mathbf{M}_\perp + N\mathbf{p}_m^+\mathbf{M}_\perp^*) + (1 - q^2)M_\perp M_\perp^* y_{pm}}{(NN^* + M_{\perp,z}M_{\perp,z}^*)p_p^- + (N^*\mathbf{p}_m^-\mathbf{M}_\perp + N\mathbf{p}_m^-\mathbf{M}_\perp^*) + (1 - q^2)M_\perp M_\perp^* y_{pm}}$$

with the correction factors

$$p_p^\pm = \frac{1}{2} \left[(1 \pm P_0) \left(1 + \frac{0.001 I^+ \lambda^3 x_{aniso}}{4 \sin^2(\theta/\lambda) \sin(2\theta)} \right)^{-1/2} + (1 \mp P_0) \left(1 + \frac{0.001 I^- \lambda^3 x_{aniso}}{4 \sin^2(\theta/\lambda) \sin(2\theta)} \right)^{-1/2} \right]$$

$$\mathbf{p}_m^\pm = \frac{1}{2} \left[(1 \pm P_0) \left(1 + \frac{0.001 I^+ \lambda^3 x_{aniso}}{4 \sin^2(\theta/\lambda) \sin(2\theta)} \right)^{-1/2} - (1 \mp P_0) \left(1 + \frac{0.001 I^- \lambda^3 x_{aniso}}{4 \sin^2(\theta/\lambda) \sin(2\theta)} \right)^{-1/2} \right] \hat{\mathbf{P}}_0$$

$$y_{pm} = \left(1 + \frac{0.001 x_{aniso} (1 - q^2) M_\perp M_\perp^* \lambda^3 r}{4 \sin^2(\theta/\lambda) \sin(2\theta)} \right)^{-1/2},$$

where P_0 is the beam polarization and I^\pm are the uncorrected intensities for a spin-up and spin-down beam, respectively. $q = \sin \alpha$ with α being the angle between the scattering vector and the vertical axis.

MAG2POL version 3.0 introduced the feature of calculating magnetization density maps. For the observed maps and difference maps, the magnetic structure factors (the coefficients of the Fourier inversion) are obtained by isolating M from the flipping ratio expression:

$$M^2 + aM + b = 0$$

with

$$a = \frac{2Nq^2(Rp_m^- - p_m^+)}{q^4(Rp_p^- - p_p^+) + (1 - q^2)q^2 y_{pm}(R - 1)}$$

and

$$b = \frac{N^2(Rp_p^- - p_p^+)}{q^4(Rp_p^- - p_p^+) + (1 - q^2)q^2 y_{pm}(R - 1)}$$

Note that the present version of MAG2POL uses the calculated M to derive the extinction correction factors analytically although this is an approximation. A numeric method will be implemented in a future release.

7.4 Multipoles

The magnetization density $m(\mathbf{r})$ is described by

$$m(\mathbf{r}) = R'_0 C'_0 d'_0(\hat{\mathbf{r}}) + \sum_{l=0}^4 R_l(r) \sum_{m=-l}^l C_l^m d_l^m(\hat{\mathbf{r}})$$

where the d_l^m are the density-normalized real spherical harmonics y_l^m whose normalization constants can be found in [41]. The primed quantities denote the first monopole besides the one specified by R_0 , C_0^0 and d_0^0 . R_l is the radial dependence of a Slater-type orbital:

$$R_l(r) = \frac{Z^{n_l+3}}{(n_l + 2)!} r^{n_l} \exp(-Zr)$$

where n and Z can be chosen to be different for each l value. Z and the coefficients C_l^m are refinable parameters. The normalization is such that:

$$\int_{r=0}^{\infty} R_l r^2 dr = 1.$$

The real spherical harmonics y_l^m are obtained from the spherical harmonics Y_l^m according to

$$y_l^m = \begin{cases} \sqrt{2} \operatorname{Im}(Y_l^{|m|}), & \text{if } m < 0 \\ Y_l^0, & \text{if } m = 0 \\ \sqrt{2} \operatorname{Re}(Y_l^{|m|}), & \text{if } m > 0 \end{cases}$$

The spherical harmonics parametrized in the angles θ and φ are given by

$$Y_l^m(\theta, \varphi) = \sqrt{\frac{2l+1}{4\pi} \cdot \frac{(l-m)!}{(l+m)!}} P_l^m(\cos \theta) e^{im\varphi}$$

As indicated e.g. in [42] the Condon-Shortley phase $(-1)^m$ which can be seen in some textbooks is included in the associated Legendre polynomials P_l^m so that, e.g. $P_1^1(x) =$

$-(1-x^2)^{\frac{1}{2}}$ and $P_1^{-1}(x) = -\frac{1}{2}P_1^1(x)$. Therefore, the density-normalized real spherical harmonics are normalized so that:

$$\int_{\theta=0}^{\pi} \int_{\varphi=0}^{2\pi} |d_l^m(\theta, \varphi)| \sin(\theta) d\varphi d\theta = \begin{cases} 1, & \text{for } l = 0 \\ 2, & \text{for } l > 0 \end{cases}$$

The magnetic form factor is given by the Fourier transform of the magnetization density and results in

$$f(\mathbf{Q}) = \langle j_l'(Q) \rangle C_0'^0 d_0'^0(\hat{\mathbf{Q}}) + \sum_{l=0}^4 i^l \langle j_l(Q) \rangle \sum_{m=-l}^l C_l^m d_l^m(\hat{\mathbf{Q}})$$

where $\hat{\mathbf{Q}}$ is parametrized in terms of θ and φ and $\langle j_l(Q) \rangle$ being the Fourier-Bessel transform of the radial density:

$$\langle j_l(Q) \rangle = \int_{r=0}^{\infty} R_l(r) j_l(Qr) 4\pi r^2 dr$$

$j_l(x)$ are the spherical Bessel functions:

$$j_0(x) = \frac{\sin x}{x}$$

$$j_1(x) = \frac{\sin x}{x^2} - \frac{\cos x}{x}$$

$$j_2(x) = \frac{3}{x^2 - 1} \frac{\sin x}{x} - \frac{3 \cos x}{x^2}$$

etc. Note that in the spherical Bessel functions Q is expressed in atomic units by multiplying the Bohr atomic radius a_0 in Å and that $f(\mathbf{Q}=0)=1$ for $C_0^0 = 1$, since $\langle j_0(0) \rangle = 4\pi$ and $d_0^0(\hat{\mathbf{Q}}) = \frac{1}{4\pi}$.

7.5 Orbitals

Here, the magnetization density $m(\mathbf{r})$ is given by

$$m(\mathbf{r}) = |\phi_l(\mathbf{r})|^2 = \left| R_l(r) \sum_{m=-l}^l C_l^m d_l^m(\hat{\mathbf{r}}) \right|^2 = R_l^2(r) \sum_{l'=0,2,\dots}^{2l} \sum_{m=-l'}^{l'} \beta_{l'}^m d_{l'}^m(\hat{\mathbf{r}})$$

The product of two spherical harmonics is expressed as a sum over spherical harmonics according to the contraction rule and the relation between the coefficients C_l^m and β_l^m are obtained by equating the orbital expansion with the multipole expansion which results in the so called \mathbf{M} matrix (see [21]). Therefore, the magnetic form factor becomes

$$f(\mathbf{Q}) = \sum_{l'=0,2,\dots}^{2l} i^{l'} \langle j_{l'}(Q) \rangle \sum_{m=-l'}^{l'} \beta_{l'}^m d_{l'}^m(\hat{\mathbf{Q}})$$

with $\langle j_\nu(Q) \rangle$ expressed like in the previous section

$$\langle j_\nu(Q) \rangle = \int_{r=0}^{\infty} R_\nu^2(r) j_\nu(Qr) 4\pi r^2 dr$$

The radial part can be expressed by using the tabulated $\langle j_\nu(Q) \rangle$ as for the sum of radial integrals or by using Slater-like orbitals like in the multipole approach. A third option is the hydrogen-like radial function which writes as

$$R_{n,l} = \left[\frac{\xi}{2n} (n-l-1)!(n+l)! \right]^{\frac{1}{2}} \exp\left(-\frac{\xi r}{2}\right) (\xi r)^{l+1} \sum_{\nu=0}^{n-l-1} \frac{(-\xi r)^\nu}{\nu!(\nu+2l+1)!(n-l-1-\nu)!}$$

with $\xi = \frac{2Z}{na_0}$.

7.6 Spin correlations

Given a periodic magnetic structure or the result of a reverse Monte-Carlo simulation in a large supercell the intensities $I(Q)$ can be calculated according to

$$I(Q) = C[\mu f(Q)]^2 \cdot \frac{1}{N} \sum_{i,j} \left[A_{ij} \frac{\sin Qr_{ij}}{Qr_{ij}} + B_{ij} \left(\frac{\sin Qr_{ij}}{(Qr_{ij})^2} - \frac{\cos Qr_{ij}}{(Qr_{ij})^2} \right) \right], \quad (7.1)$$

where $C = \left(\frac{\gamma_n r_e}{2}\right)^2 = 0.07265$ barn, μ is the effective magnetic moment, $f(Q)$ is the magnetic form factor, N is the number of atoms in the super cell, Q is the scattering vector and the sum runs over the pairs of spins i and j separated by the distance r_{ij} . In order to calculate the powder-averaged magnetic neutron scattering intensity for each spin pair in the sum a local coordination system is defined where z is along the vector r_{ij} , y is parallel to $\mathbf{S}_i \times \mathbf{z}$ and x completes the right-handed system. With this definition $A_{ij} = S_i^x S_j^x$ and $B_{ij} = 2S_i^z S_j^z - S_i^x S_j^x$ as implemented in SPINVERT [34].

The analytical form of the mPDF was derived for the first time in [43] by calculating the Fourier transform of the neutron scattering cross section from a collection of magnetic moments. We have adapted the original formula by adjusting the prefactors in order to be consistent with Eq. 7.1:

$$I(r) = \frac{C[\mu f(Q)]^2}{b_M^2} \cdot \frac{1}{N} \sum_{i,j} \left[\frac{A_{ij}}{r} \delta(r - r_{ij}) + B_{ij} \frac{r}{r_{ij}^3} [1 - \Theta(r - r_{ij})] \right]. \quad (7.2)$$

b_M^2 is the square of the magnetic scattering length 3.055 barn/str/Gd and 0.635 barn/str/Nd, respectively. Furthermore, in order to allow the comparison with the Fourier transform of the corrected raw data (without dividing by the magnetic form factor) we have replaced

the delta function $\delta(r)$ and the step function $\Theta(r)$ by Gaussian and Error functions, respectively, with a full width at half maximum (FWHM) in real space corresponding to a Gaussian fit to the squared magnetic form factor in reciprocal space [$FWHM_R \approx 4 \cdot \ln(4)/(4\pi FWHM_{f^2(Q)})$] (note that the factor 4π is due to the crystallographers' definition of Q widely used in particular for the analytical approximation of magnetic form factors, which is also adapted in MAG2POL).

7.7 Powder patterns

Rietveld refinement is a method which compares an experimentally observed powder (x-ray or neutron) diffraction pattern with a calculated line profile in a least-squares algorithm until the best possible agreement is found. The intensities of the Bragg reflections are calculated based on the supplied nuclear/magnetic structure model, while for a LeBail refinement the *calculated* intensities are set to the values of the *observed* intensities after each refinement step (note that MAG2POL does not save the somewhat artificial intensities of each Bragg reflection in a LeBail refinement, but iteratively recovers them when reloading a saved refinement until the difference in χ^2 is less than 0.005 with a maximum of 1000 cycles). MAG2POL supports diffraction patterns recorded on constant-wavelength and time-of-flight instruments and the data should contain the scattering variable 2θ or TOF, the intensity and eventually the standard deviation of the intensity. If the latter is not given (depending on the input file format), the program takes the square root of the intensity.

The following features and equations are based on the FULLPROF manual. For the sake of completeness of this manual, the implemented equations are listed here as well.

7.7.1 Calculated profile

The theoretical profile is calculated from the given structure model with nuclear and/or magnetic contribution. A single point in this profile is calculated according to

$$y_{cal,i} = \sum_P S_P \sum_Q I_{P,Q} \cdot \Lambda(2\theta_i - 2\theta_{P,Q} - \Delta 2\theta) + b_i$$

where the sum runs over the number of phases P and all Bragg reflections Q which contribute to the point $y_{cal,i}$. S_P is the scale factor of phase P , Λ is the profile function with its peak at $2\theta_{P,Q}$ ($\Delta 2\theta$ contains all systematic offsets, see Secs. 7.7.1.5 and 7.7.1.6) and b_i is the background which is calculated according to the model used (see Sec. 7.7.1.7). The intensity of the Bragg reflection Q of phase P writes as

$$I_{P,Q} = (m \cdot L \cdot A \cdot P \cdot T \cdot F^2)_{P,Q}$$

F^2 is the square of the nuclear/magnetic structure factor corresponding to NN^* or $\mathbf{M}_\perp\mathbf{M}_\perp^*$ as shown in Sec. 7.1 and m is the multiplicity of the peak [e.g. $m = 4$ for a (200) reflection in tetragonal symmetry]. The remaining quantities are described in the following sections.

7.7.1.1 Lorentz and polarisation factor

The Lorentz and polarisation factor L (in Debye-Scherrer geometry) is given by

$$L = \frac{1 - K + K \cos^2(2\theta_M) \cos^2(2\theta)}{2 \sin^2(\theta) \cos(\theta)}$$

with θ_M being the monochromator take-off angle and K the polarization factor, which is 0 for neutrons, 0.5 for characteristic non-polarised x-ray radiation and around 0.1 for synchrotron radiation. Therefore, the take-off angle does not need to be given in the neutron case.

7.7.1.2 Asymmetry

A is the peak asymmetry, a function which is multiplied to the profile function

$$A(x) = 1 - \frac{A_1 F_a(x) - A_2 F_b(x)}{\tanh(\theta)} - \frac{A_3 F_a(x) + A_4 F_b(x)}{\tanh(2\theta)}$$

with

$$x = \frac{2\theta_i - 2\theta_Q - \Delta 2\theta}{FWHM}$$

$\Delta 2\theta$ combines all systematic line-shifts which are explained in more detail in Sec. 7.7.1.6. The functions $F_{a,b}(x)$ are given by

$$F_a(x) = 2z \exp(-z^2)$$

$$F_b(x) = (2z^2 - 3)F_a(x)$$

The parameters A_1 to A_4 can be refined. Note that the subtle differences in the equations in comparison to the FULLPROF manual are on purpose, they have been adapted to obtain the same asymmetries.

7.7.1.3 Preferred orientation

The two following preferred orientation functions are implemented in MAG2POL:

- Exponential function

The correction factor for the calculated intensities is given by

$$P_Q = P_2 + (1 - P_2) \exp(-P_1 \alpha_Q^2)$$

α_Q is the acute angle between the scattering vector Q and the normal of the preferred orientation (hkl) vector which has to be defined by the user. P_1 and P_2 are refinable parameters.

- Modified March's function

Here the correction is calculated by

$$P_Q = P_2 + (1 - P_2) \left\{ [P_1 \cos(\alpha_Q)]^2 + \frac{\sin^2(\alpha_Q)}{P_1} \right\}^{-\frac{3}{2}}$$

and P_1 and P_2 are again refinable parameters. $P_1 = 1$ means no preferred orientation, $P_1 < 1$ refers to a platy habit (α_Q is the acute angle between the scattering vector and the normal of the crystallites) and $P_1 > 1$ to a needle-like habit (α_Q is the acute angle between the scattering vector and the axis of the needle).

7.7.1.4 Absorption and extinction

The effects of sample absorption depend on the scattering angle and can be corrected by the following transmission factor for constant wavelength and Debye-Scherrer geometry:

$$T_Q = \exp \left\{ - [1.7133 - 0.0368 \sin^2(\theta_Q)] \mu_\lambda R + [0.0927 + 0.375 \sin^2(\theta_Q)] [\mu_\lambda R]^2 \right\}$$

The linear absorption coefficient is automatically calculated based on the given structure model (averaged over the volumes of the contributing phases) and the corresponding wavelength (λ_1 or λ_2), but the radius R of the cylindrical sample has to be given by the user.

For time-of-flight data different refinable absorption models are implemented:

- Model 1

Here the parameters μ_1 and μ_2 can be refined to mimic an effective $\mu_\lambda R$ according to

$$\mu_\lambda R = \mu_1 \cdot \lambda_Q + \mu_2$$

with λ_Q being the wavelength associated with the particular reflection Q and the transmission factor is given by

$$T_Q = \begin{cases} 1 - \mu_\lambda R (1 - \frac{2}{3} \mu_\lambda R), & \text{if } \mu_\lambda R \leq 0.001 \\ \frac{1 - \exp(-2\mu_\lambda R)}{2\mu_\lambda R}, & \text{if } \mu_\lambda R > 0.001 \end{cases}$$

- Model 2

This model corresponds to the one for the constant-wavelength case, but with a refinable parameter μ_1 which is multiplied with λ_Q representing $\mu_\lambda R$:

$$T_Q = \exp \left\{ - [1.7133 - 0.0368 \sin^2(\theta_B)] \mu_1 \lambda_Q + [0.0927 + 0.375 \sin^2(\theta_B)] [\mu_1 \lambda_Q]^2 \right\}$$

Hereby, θ_B is half the scattering angle of the corresponding detector bank.

- Model 3

Again, the parameter μ_1 is multiplied with λ_Q associated to the reflection Q , therefore describing an effective μR , and the transmission factor is

$$T_Q = \exp(-\mu_1 \lambda_Q)$$

- Model 4

This is the Loganov & alte da Veiga model [44]. For $\mu_1 \lambda_Q = \mu R < 3 \text{ cm}^{-1}$

$$T = \exp [-k_0 \mu_1 \lambda_Q - k_1 (\mu_1 \lambda_Q)^2 - k_2 (\mu_1 \lambda_Q)^3 - k_3 (\mu_1 \lambda_Q)^4]$$

with

$$k_0 = 1.697653$$

$$k_1 = \left[25.99978 - 0.01911 \sqrt{\sin(\theta_B)} \right] \exp(-0.024514 \sin^2(\theta_B)) \\ + 0.109561 \sin(\theta_B) - 26.0456$$

$$k_2 = -0.02489 - 0.39499 \sin^2(\theta_B) + 1.219077 \sin^3(\theta_B) - 1.31268 \sin^4 \theta_B \\ + 0.871081 \sin^5(\theta_B) - 0.2327 \sin^6(\theta_B)$$

$$k_3 = 0.003045 + 0.018167 \sin^2(\theta_B) - 0.03305 \sin^4(\theta_B)$$

For $\mu_1 \lambda_Q = \mu R > 3 \text{ cm}^{-1}$ the transmission factor is given by

$$T = \frac{k_4 - k_7}{[1 + k_5 (\mu_1 \lambda_Q - 3)]^{k_6}} + k_7$$

with

$$k_4 = 1.433902 + 11.07504 \sin^2(\theta_B) - 8.77629 \sin^4(\theta_B) \\ + 10.02088 \sin^6(\theta_B) - 3.36778 \sin^8(\theta_B)$$

$$k_5 = [0.013869 - 0.01249 \sin^2(\theta_B)] \exp [3.27094 \sin^2(\theta_B)] \\ + \frac{0.337894 + 13.77317 \sin^2(\theta_B)}{[1 + 11.53544 \sin^2(\theta_B)]^{1.555039}}$$

$$k_6 = \frac{1.933433}{[1 + 23.12967 \sin^2(\theta_B)]^{1.686715}} - 0.13576 \sin(\theta_B) + 1.163198$$

$$k_7 = 0.044365 - \frac{0.04259}{[1 + 0.41051 \sin^2(\theta_B)]^{148.4202}}$$

For time-of-flight data a primary extinction correction is implemented which is calculated according to [45]. The extinction correction E is a combination of Bragg and Laue components

$$E = E_B \sin^2(\theta_B) + E_L \cos^2(\theta_B),$$

where

$$E_B = \frac{1}{\sqrt{1+x}}$$

and

$$E_L = 1 - \frac{x}{2} + \frac{x^2}{4} - \frac{5x^3}{48} + \dots \text{ for } x < 1$$

or

$$E_L = \sqrt{\frac{2}{\pi x}} \left(1 - \frac{1}{8x} - \frac{3}{128x^2} - \frac{15}{1024x^3} - \dots \right) \text{ for } x > 1$$

where

$$x = r_{bl} \left(\frac{\lambda_Q F}{V} \right)^2$$

where F is the calculated structure factor and V is the unit cell volume. r_{bl} is a refinable parameter and is a measure of the mosaic block size in μm^2 . Note that a direct comparison of this value with FULLPROF is only possible, if the *.pcr file contains the occupation factor as the ratio between special site and general site multiplicity.

7.7.1.5 Profile functions

Except for the numerical and the split Pseudo-Voigt profile all constant-wavelength profile functions available in FULLPROF are implemented in MAG2POL, in the current version two time-of-flight peak profiles are implemented. If not otherwise specified, for all constant-wavelength profiles the full width at half maximum Γ is composed of the Cagliotti formula (u, v, w refinable parameters) and isotropic Gaussian broadening (I_G refinable parameter):

$$\Gamma^2 = u \cdot \tan^2(\theta) + v \cdot \tan(\theta) + w + \frac{I_G}{\cos^2(\theta)}$$

- Gaussian

$$\Lambda(x) = G(x) = \frac{2}{\Gamma} \sqrt{\frac{\ln 2}{\pi}} \exp\left(-\frac{4 \ln 2}{\Gamma^2} x^2\right)$$

- Lorentzian

$$\Lambda(x) = L(x) = \frac{a_L}{1 + b_L x^2}$$

$$a_L = \frac{2}{\pi \Gamma} \quad b_L = \frac{4}{\Gamma^2}$$

- Modified Lorentzian

$$\Lambda(x) = \frac{a_{ML}}{(1 + b_{ML}x^2)^2}$$

$$a_{ML} = \frac{4\sqrt{\sqrt{2}-1}}{\pi\Gamma} \quad b_{ML} = \frac{4(\sqrt{2}-1)}{\Gamma^2}$$

- Intermediate Lorentzian

$$\Lambda(x) = \frac{a_{IL}}{(1 + b_{IL}x^2)^{3/2}}$$

$$a_{IL} = \frac{\sqrt{2^{2/3}-1}}{\Gamma} \quad b_{IL} = \frac{4(2^{2/3}-1)}{\Gamma^2}$$

- Pearson VII

$$\Lambda(x) = \frac{a_{VII}}{(1 + b_{VII}x^2)^m}$$

$$a_{VII} = \frac{\Gamma(m)}{\Gamma(m) - 1/2} \frac{2\sqrt{2^{1/m}-1}}{\sqrt{\pi}\Gamma} \quad b_{VII} = \frac{4(2^{1/m}-1)}{\Gamma^2}$$

The refinable parameter m can optionally be set to be a function of the scattering angle (in degrees):

$$m = m_0 + \frac{100 \cdot X}{2\theta} + \frac{1000 \cdot Y}{(2\theta)^2}$$

where X and Y are further refinable parameters.

- Pseudo-Voigt

$$\Lambda(x) = pV(x) = \eta \cdot L(x) + (1 - \eta) \cdot G(x) \quad 0 \leq \eta \leq 1$$

where $L(x)$ and $G(x)$ have the same full width at half maximum Γ . The mixing parameter η can optionally be set to be a function of the scattering angle (in degrees):

$$\eta = \eta_0 + X \cdot 2\theta$$

- Tripled Pseudo-Voigt

$$\Lambda(x) = X \cdot pV(x - D) + (1 - X - Y) \cdot pV(x) + Y \cdot pV(x + D)$$

$$D = \frac{S}{d \cos(\theta)}$$

where d is the d -spacing of the (hkl) reflection for which the profile is calculated and S is a refinable parameter. The three Pseudo-Voigt profiles have the same η_0 and Γ and are mixed according to the refinable parameters X and Y .

- Pseudo-Voigt with Finger-Cox-Jephcoat asymmetry [46]

$$\Lambda(x) = \frac{\sum_{n=1}^{N_{max}} \frac{w_n W(\delta_n, 2\theta) pV(x+2\theta-\delta_n)}{h(\delta_n) \cos(\delta_n)}}{\sum_{n=1}^{N_{max}} \frac{w_n W(\delta_n, 2\theta)}{h(\delta_n) \cos(\delta_n)}}$$

The sum is a numerical integration corresponding to a Gauss-Legendre quadrature procedure with w_n and x_n being the Gauss-Legendre weights and abscissae associated with the n^{th} point and N_{max} is the number of points chosen. In the original paper it is recommended that $N_{max} \geq 30$ for values within six half-widths of the profile peak and $N_{max} = 10$ outside this region. MAG2POL uses $N_{max} = 30$ for every point which yields smooth peak profiles with sufficiently fast calculation times.

$$h(\delta) = \sqrt{\frac{\cos^2(\delta)}{\cos^2(\theta)} - 1} \quad \delta_n = \frac{1}{2}(2\theta + 2\varphi_{min}) + \frac{x_n}{2}(2\theta - 2\varphi_{min})$$

$$W(2\varphi, 2\theta) = \begin{cases} S_L + D_L - h(\delta_n), & \text{for } 2\varphi_{min} \leq 2\varphi < 2\varphi_{infl} \\ 2 \min(S_L, D_L), & \text{for } 2\varphi_{infl} \leq 2\varphi \leq 2\theta \\ 0, & \text{else} \end{cases}$$

The inequalities above apply to $2\theta < 90^\circ$ and have to be inverted for $2\theta > 90^\circ$. Bragg peaks with a scattering angle closer than 0.1° to 90° are not corrected in MAG2POL. The respective limiting 2φ angles are given by

$$2\varphi_{min} = \cos^{-1} \left[\cos(2\theta) \sqrt{(S_L + D_L)^2 + 1} \right]$$

$$2\varphi_{infl} = \cos^{-1} \left[\cos(2\theta) \sqrt{(D_L - S_L)^2 + 1} \right]$$

The parameters S_L and D_L are refinable. The first refers to half the sample height divided by the sample-to-detector distance and the second is half the detector height divided by the sample-to-detector distance. The implemented code was successfully compared to the example given in the original paper as well as with FULLPROF examples. The recast of variables for special values of S_L and D_L in the refinement procedure as proposed in [47] is implemented but needs to be tested more thoroughly as the resulting standard deviation proved to be a bit high for some examples.

- Thompson-Cox-Hastings Pseudo-Voigt with Finger-Cox-Jephcoat asymmetry
In comparison to the Pseudo-Voigt profile above the parameter η is not refinable but calculated from the Lorentzian and Gaussian linewidths:

$$\Gamma_G = \sqrt{u \cdot \tan^2(\theta) + v \cdot \tan(\theta) + w + \frac{I_G}{\cos^2(\theta)}}$$

$$\Gamma_L = X \cdot \tan(\theta) + \frac{Y}{\cos(\theta)}$$

with X and Y being refinable parameters. The numerical Pseudo-Voigt approximation of the convolution between the Lorentzian and a Gaussian function yields

$$\Gamma = (\Gamma_G^5 + 2.69269 \cdot \Gamma_G^4 \Gamma_L + 2.42843 \cdot \Gamma_G^3 \Gamma_L^2 + 4.47163 \cdot \Gamma_G^2 \Gamma_L^3 + 0.07842 \cdot \Gamma_G \Gamma_L^4 + \Gamma_L^5)^{1/5}$$

$$\eta = 1.36603 \cdot \frac{\Gamma_L}{\Gamma} - 0.47719 \cdot \left(\frac{\Gamma_L}{\Gamma}\right)^2 + 0.11116 \cdot \left(\frac{\Gamma_L}{\Gamma}\right)^3$$

These values Γ and η are then used in the Pseudo-Voigt function $pV(x)$ and the optional Finger-Cox-Jephcoat asymmetry is calculated as described in the previous point.

- Convolution of Pseudo-Voigt with a pair of back-to-back exponentials

$$\Lambda(x) = pV(x) \otimes E(x) = \int_{-\infty}^{\infty} pV(x-t)E(t)dt$$

$$= (1-\eta)N [e^u \operatorname{erfc}(y)e^v \operatorname{erfc}(z)] - \frac{2N\eta}{\pi} \{\Im[e^p E_1(p)] + \Im[e^q E_1(q)]\}$$

with erfc being the complementary error function, E_1 the exponential integral and

$$N = \frac{\alpha\beta}{2(\alpha + \beta)}.$$

The exponents u and v are given by

$$u = \frac{1}{2}\alpha(\alpha\sigma_G^2 + 2x) \quad v = \frac{1}{2}\beta(\beta\sigma_G^2 - 2x),$$

the arguments y, z by

$$y = \frac{\alpha\sigma_G^2 + x}{\sqrt{2\sigma_G^2}} \quad z = \frac{\beta\sigma_G^2 - x}{\sqrt{2\sigma_G^2}}$$

and the arguments p and q by

$$p = \alpha x + \frac{i\alpha\Gamma}{2} \quad q = -\beta x + \frac{i\beta\Gamma}{2}.$$

The Gaussian component of the Pseudo-Voigt function is expressed by

$$\sigma_G^2 = \sigma_0 + \sigma_1 \cdot d^2 + (\sigma_2 + I_G) \cdot d^4 + \sigma_Q/d^2 = \frac{\Gamma_G^2}{8 \ln 2}$$

and the Lorentzian component writes as

$$\gamma_L = \gamma_0 + \gamma_1 \cdot d + \gamma_2 \cdot d^2 = \Gamma_L.$$

Note that the Lorentzian size broadening is not yet implemented in MAG2POL. The relations between Γ_G , Γ_L and Γ as well as η are the same as for the Thompson-Cox-Hastings Pseudo-Voigt function. The rise and decay constants α and β are given by

$$\alpha = \alpha_0 + \frac{\alpha_1}{d} + \frac{\alpha_Q}{\sqrt{d}} \quad \beta = \beta_0 + \frac{\beta_1}{d^4} + \frac{\beta_Q}{d^2}$$

- Convolution of Pseudo-Voigt with the Ikeda-Carpenter function

The Ikeda-Carpenter function is the result of the convolution of two functions

$$S_k(t) = \frac{\alpha^3}{2} t^2 e^{-\alpha t} \quad R_k(t) = (1 - R)\delta(t) + R\beta e^{-\beta t},$$

which describe leakage of fast and slow neutrons from the moderator with the fast and slow decay constants α and β :

$$\begin{aligned} I_k(t) &= S_k(t) \otimes R_k(t) = (1 - R)S_k(t) \otimes \delta(t) + R\beta S_k(t) \otimes e^{-\beta t} \\ &= (1 - R)S_k(t) + R\beta \int_{-\infty}^{\infty} S_k(\tau) \left[e^{-\beta(t-\tau)} \right] d\tau \\ &= (1 - R)S_k(t) + R\beta e^{-\beta t} \int_0^t S_k(\tau) e^{\beta \tau} d\tau \\ &= \frac{\alpha^3}{2} \left\{ (1 - R)t^2 e^{-\alpha t} + \frac{2R\beta}{(\alpha - \beta)^3} \left[e^{-\beta t} - e^{-\alpha t} \left((\alpha - \beta)^2 \frac{t^2}{2} + (\alpha - \beta)t + 1 \right) \right] \right\} \end{aligned}$$

The implemented peak profile is obtained by the convolution of a Pseudo-Voigt function with the Ikeda-Carpenter function:

$$\Lambda(x) = pV(x) \otimes I_k(x) = \int_{-\infty}^{\infty} pV(x - t) I_k(t) dt = N [(1 - \eta)\Lambda_G(x) + \eta\Lambda_L(x)]$$

with

$$N = \frac{\alpha(1 - k^2)}{4k^2}$$

The Gaussian part Λ_G is given by

$$\Lambda_G(x) = N_u e^u \operatorname{erfc}(y_u) + N_v e^v \operatorname{erfc}(y_v) + N_s e^s \operatorname{erfc}(y_s) + N_r e^r \operatorname{erfc}(y_r)$$

with

$$N_u = (1 - R \frac{\alpha^-}{w}) \quad N_v = (1 - R \frac{\alpha^+}{z}) \quad N_s = -2(1 - R \frac{\alpha}{y}) \quad N_r = 2R\alpha^2 \beta \frac{k^2}{wyz}$$

and

$$y_u = \frac{\alpha^- \sigma_G^2 - x}{\sqrt{2\sigma_G^2}} \quad y_v = \frac{\alpha^+ \sigma_G^2 - x}{\sqrt{2\sigma_G^2}} \quad y_s = \frac{\alpha \sigma_G^2 - x}{\sqrt{2\sigma_G^2}} \quad y_r = \frac{\beta \sigma_G^2 - x}{\sqrt{2\sigma_G^2}}$$

where $k = 0.05$, $R = \exp\left(-\frac{81.799}{\kappa\lambda^2}\right)$, $\alpha^- = \alpha(1 - k)$, $\alpha^+ = \alpha(1 + k)$, $w = \alpha^- - \beta$, $y = \alpha - \beta$ and $z = \alpha^+ - \beta$. The parameters α and β are

$$\alpha = \frac{1}{\alpha_0 + \lambda\alpha_1} \quad \beta = \frac{1}{\beta_0}$$

The u , v , s and r arguments of the exponential functions are

$$u = \frac{1}{2}\alpha^-(\alpha^-\sigma_G^2 - 2x) \quad v = \frac{1}{2}\alpha^+(\alpha^+\sigma_G^2 - 2x) \quad s = \frac{1}{2}\alpha(\alpha\sigma_G^2 - 2x) \quad r = \frac{1}{2}\beta(\beta\sigma_G^2 - 2x)$$

The Lorentzian part is described by

$$\Lambda_L(x) = -\frac{2}{\pi} \{N_u \Im [e^{z_u} E_1(z_u)] + N_v \Im [e^{z_v} E_1(z_v)] + N_s \Im [e^{z_s} E_1(z_s)] + N_r \Im [e^{z_r} E_1(z_r)]\}$$

with the z_n being

$$z_s = -\alpha x + \frac{1}{2}i\alpha\gamma_L \quad z_u = -\alpha^- x + \frac{1}{2}i\alpha^-\gamma_L \quad z_v = -\alpha^+ x + \frac{1}{2}i\alpha^+\gamma_L \quad z_r = -\beta x + \frac{1}{2}i\beta\gamma_L$$

Note that σ_G and γ_L have the same definition as for the previous peak profile (convolution of Pseudo-Voigt and back-to-back exponentials).

7.7.1.6 Offsets / Time of flight

Systematic line-shifts in a powder pattern can occur due to an improper alignment of the sample and/or the detector. The first offset parameter, $\Delta 0$ simply adds to the calculated 2θ value of a Bragg reflection and corresponds to the zero-shift of the detector. The sample-dependent line-shifts result from the eccentricity e of a sample with radius R from the central position

- perpendicular to the incident beam direction

$$\Delta 2\theta = \frac{e}{R} \cos(2\theta) = \Delta x \cos(2\theta)$$

- parallel to the incident beam direction

$$\Delta 2\theta = \frac{e}{R} \sin(2\theta) = \Delta y \sin(2\theta)$$

The above equations apply to the Debye-Scherrer geometry and the parameters Δx and Δy are refinable. Note that the correction perpendicular to the incident beam direction is different from the $\cos(\theta)$ term in the FULLPROF manual, but both programs yield no shift for $2\theta = 90^\circ$.

For TOF data the instrumental offsets in the peak positions are given by the 4 parameters Z_0 , D_1 and D_2 and D_{-1} which yield the time of flight T for a reflection Q with d -spacing d :

$$T = Z_0 + D_1 \cdot d + D_2 \cdot d^2 + D_{-1}/d$$

7.7.1.7 Background

The different possibilities to describe the background of a powder diffraction pattern in MAG2POL are explained below

- linear interpolation

The user defines a number of discrete background points as explained in Sec. 4.5.3 and the program calculates a linear interpolation. The slope beyond the first and last point is simply continued. When 0 points are defined, the background is 0 everywhere; when 1 point is defined, the background is flat and goes through that point.

- polynomial (6 coefficients)

$$b_i = \sum_{m=0}^5 C_m \left(\frac{2\theta_i}{B_0} - 1 \right)^m$$

where the coefficients C_0 to C_5 are refinable parameters and B_0 is the adaptable origin of the polynomial.

- polynomial (12 coefficients)

$$b_i = \sum_{m=-3}^{-1} C_m (2\theta_i)^m + \sum_{m=0}^8 C_m \left(\frac{2\theta_i}{B_0} - 1 \right)^m$$

where the coefficients C_{-3} to C_8 are refinable parameters and B_0 is the adaptable origin of the polynomial.

- polynomial (6 coefficients) + Debye-like

$$b_i = \sum_{m=0}^5 C_m \left(\frac{2\theta_i}{B_0} - 1 \right)^m + \sum_{n=1}^6 C'_n \frac{\sin(Q_i r_n)}{Q_i r_n}$$

with $Q_i = 4\pi \frac{\sin(\theta_i)}{\lambda}$. The coefficients C_0 to C_5 as well as C'_1 to C'_6 and r_1 to r_6 are refinable parameters and B_0 is the adaptable origin of the polynomial.

7.7.1.8 Size/strain broadening and microstructure analysis

Isotropic Gaussian and Lorentzian size and strain broadening depend differently on the scattering variable and can therefore be refined simultaneously, when the instrument resolution is function is known and loaded (see Sec. 4.5.2.1). Within the Thompson-Cos-Hastings Pseudo-Voigt profile function the different sample contributions to the peak broadening of a CW pattern can be quantified as follows:

$$\Gamma_{G,s} = \sqrt{\Delta u \cdot \tan^2(\theta) + \frac{I_G}{\cos^2(\theta)}}$$

$$\Gamma_{L,s} = \Delta X \cdot \tan(\theta) + \frac{\Delta Y}{\cos(\theta)},$$

where I_G and ΔY are the Gaussian and Lorentzian size broadening, while Δu and ΔX are the Gaussian and Lorentzian strain broadening.

The corresponding expressions for the TOF case are:

$$\Gamma_{G,s} = \sqrt{8 \ln 2} \cdot \sigma_{G,s}$$

$$\sigma_{G,s}^2 = I_G \cdot d^4 + \Delta\sigma_1 \cdot d^2$$

$$\Gamma_{L,s} = \Delta\gamma_2 \cdot d^2 + \Delta\gamma_1 \cdot d,$$

with I_G and $\Delta\gamma_2$ being the Gaussian and Lorentzian size broadening and $\Delta\sigma_1$ and $\Delta\gamma_1$ the Gaussian and Lorentzian strain broadening parameters.

The integral breadth of a Bragg peak is calculated according to [48]:

$$\beta = \frac{1}{2} \frac{\Gamma}{\eta/\pi + (1-\eta)\sqrt{\pi/\ln 2}}$$

where Γ is the FWHM according to the TCH Pseudo-Voigt equation expressed in reciprocal lattice units \AA^{-1} (in the microstructure analysis window a factor 1000 is applied). The apparent size is calculated as $1/\beta_{size}$ and is given in \AA , while the maximum (upper limit) strain is given by $0.5 \cdot \beta_{strain} \cdot d$ (a factor 10000 is applied in the table of the microstructure analysis window).

7.8 Local susceptibility tensor

In analogy to the implementation in the CCSL, the local susceptibility tensor is defined by its main axes x , y and z with $x \parallel a^*$, $y \parallel b$ and $z \parallel c$. The six coefficients which can be entered by the user construct the symmetric anisotropic tensor χ :

$$\chi = \begin{pmatrix} \chi_{11} & \chi_{12} & \chi_{13} \\ \chi_{12} & \chi_{22} & \chi_{23} \\ \chi_{13} & \chi_{23} & \chi_{33} \end{pmatrix}$$

and the magnetic moment (in the xyz reference frame) at position i is calculated by

$$\boldsymbol{\mu}_i = \mathbf{R}_i \boldsymbol{\chi} \mathbf{R}_i^{-1} \mathbf{H}$$

with \mathbf{R}_i being the rotational part of the the symmetry operator acting on the atomic position and susceptibility tensor. Here, the magnetic field vector \mathbf{H} is also expressed in the xyz basis, i.e. the field direction (unit vector) given by the vertical diffractometer axis in reciprocal lattice units and the multiplication factor H is transformed internally before calculating the magnetic moment in the xyz basis. The magnetic moment $\boldsymbol{\mu}_i$ is then transformed back into the usual crystallographic frame in order to use the same equations as given in Secs. 7.1, 7.2 and 7.3. The same site symmetry constraints as for the anisotropic temperature factors [7] are applied to the local susceptibility tensors, however, transformed into the xyz basis.

Finally, the bulk magnetization is given by

$$\chi_{\text{bulk}} = \sum_j \sum_i \mathbf{R}_i \boldsymbol{\chi} \mathbf{R}_i^{-1} \cdot \text{mult}_j \cdot \text{occ}_j$$

where the sum is taken over all symmetry operators \mathbf{R}_i of the crystallographic space group and over all magnetic sites j with mult and occ being the site multiplicity and the occupation factor, respectively.

7.9 Standard deviations and agreement factors

The standard deviations σ are obtained by taking the square root of the diagonal of the covariance matrix \mathbf{C} :

$$\mathbf{C} = \boldsymbol{\alpha}^{-1} \cdot \chi_r^2$$

The correlation matrix is obtained by dividing the elements $C_{i,j}$ by the standard deviations $\sigma_i \cdot \sigma_j$. $\boldsymbol{\alpha}$ is a $n \times n$ square matrix with n the number of refined parameters x_j :

$$\boldsymbol{\alpha} = \mathbf{D}^T \cdot \mathbf{D}$$

with \mathbf{D} being a $m \times n$ matrix (m is the number of observations $y_{\text{obs},i}$ or calculated values $y_{\text{cal},i}$) where the j^{th} column is given by:

$$\mathbf{D}^{(j)} = \frac{y_{\text{cal},i}(x_j + \Delta) - y_{\text{cal},i}(x_j - \Delta)}{2\Delta\sigma_i}$$

The reduced χ_r^2 value is defined as

$$\chi_r^2 = \frac{\chi^2}{(m - n)}.$$

and χ^2 is expressed by

$$\chi^2 = \sum_i \left(\frac{y_{obs,i} - y_{cal,i}}{\sigma_i} \right)^2.$$

The observed and calculated values, $y_{obs,i}$ and $y_{cal,i}$, can be integrated intensities, polarization matrix elements or a point in a diffraction pattern.

The crystallographic R_F factor is given by

$$R_F = 100 \cdot \frac{\sum_Q |F_{obs,Q} - F_{cal,Q}|}{\sum_Q F_{obs,Q}}$$

and is calculated when integrated intensities or powder patterns are refined. In the case of powder data refinement the observed quantities $F_{obs,i}$ are calculated from the Rietveld formula:

$$I_{obs,Q} = I_{cal,Q} \cdot \frac{\sum_i w_i \cdot \frac{y_{obs,i} - b_i}{y_{cal,i} - b_i}}{\sum_i w_i}$$

with

$$w_i = \Lambda(2\theta_i - 2\theta_Q - \Delta 2\theta) \cdot A$$

i.e. the observed intensities are extracted based on the underlying structure model and peak clusters are proportionally decomposed depending on the calculated intensities which contribute. The weighting factors correspond to the amplitude within a specific profile function multiplied by the asymmetry function (note that the asymmetry is not included in FULLPROF, which, however does not make a difference).

For the determination of the standard deviations of the observed intensities the error propagation of the quantity $(y_{obs,i} - b_i)/(y_{cal,i} - b_i)$ is derived which results in

$$\sigma(I_{obs,Q}) = \frac{I_{cal,Q}}{\sqrt{\sum_i w_i}}$$

with

$$1/w_i = \sigma^2(y_{obs,i}) \cdot \left\{ \frac{1}{(y_{cal,i} - b_i)^2} + \left[\frac{y_{obs,i} - b_i}{(y_{cal,i} - b_i)^2} \frac{y_{cal,i}}{y_{obs,i}} \right]^2 + \left[\frac{y_{obs,i} - y_{cal,i}}{(y_{cal,i} - b_i)^2} \frac{b_i}{y_{obs,i}} \right]^2 \right\}$$

The observed structure factor is then obtained from the observed intensity corrected for the peak multiplicity and the Lorentz factor:

$$F_{obs,Q} = \sqrt{\frac{I_{obs,Q}}{m \cdot L}}.$$

Bibliography

- [1] H. T. STOKES, D. M. HATCH AND B. J. CAMPBELL. ISOTROPY.
- [2] H. T. STOKES, D. M. HATCH AND B. J. CAMPBELL. ISO-MAG. doi:iso.byu.edu/iso/magneticspacegroups.php.
- [3] H. T. STOKES, D. M. HATCH AND B. J. CAMPBELL. ISO(3+d)D. doi:iiso.byu.edu/iso/ssg.php.
- [4] H. T. STOKES, B. J. CAMPBELL AND S. VAN SMAALEN. Generation of (3+d)-Dimensional Superspace Groups for Describing the Symmetry of Modulated Crystalline Structures. *Acta Crystallogr., Sect. A: Found. Crystallogr.* **67** 45 (2011).
- [5] B. J. C. S. VAN SMAALEN AND H. T. STOKES. Equivalence of Superspace Groups. *Acta Crystallogr., Sect. A: Found. Crystallogr.* **69** 75 (2013).
- [6] H. T. STOKES AND B. J. CAMPBELL. Enumeration and tabulation of magnetic (3+d)-dimensional superspace groups. *Acta Crystallogr., Sect. A: Found. Crystallogr.* **78** 364 (2022).
- [7] W. J. A. M. PETERSE AND J. H. PALM. The anisotropic temperature factor of atoms in special positions. *Acta Crystallogr.* **20** 147 (1966).
- [8] T. HAHN, ed. International Tables for Crystallography, Volume A: Space Group Symmetry (D. Reidel Publishing Company, 1983).
- [9] W. C. HAMILTON. On the isotropic temperature factor equivalent to a given anisotropic temperature factor. *Acta Crystallogr.* **12** 609 (1959).
- [10] A. GUKASOV AND P. J. BROWN. Determination of atomic site susceptibility tensors from polarized neutron diffraction data. *J. Phys.: Condens. Matter* **14** 8831 (2002).
- [11] J. SCHWINGER. On the Polarization of Fast Neutrons. *Phys. Rev.* **73** 407 (1948).
- [12] C. G. SHULL. Neutron Spin-Neutron Orbit Interaction with Slow Neutrons. *Phys. Rev. Lett.* **10** 297 (1963).
- [13] C. G. SHULL. *Trans. Amer. Cryst. Assoc.* **3** 1 (1967).

- [14] G. P. FELCHER AND S. W. PETERSON. Schwinger and Anomalous Scattering of Neutrons from CdS. *Acta Crystallogr., Sect. A: Found. Crystallogr.* **31** 76 (1975).
- [15] J. RODRÍGUEZ-CARVAJAL. Recent advances in magnetic structure determination by neutron powder diffraction. *Physica B* **192** 55 (1993). doi:10.1016/0921-4526(93)90108-I.
- [16] G. M. SHELDRICK. A short history of *SHELX*. *Acta Crystallogr., Sect. A: Found. Crystallogr.* **64** 112 (2008). doi:10.1107/S0108767307043930.
- [17] P. J. BECKER AND P. COPPENS. Extinction within the Limit of Validity of the Darwin Transfer Equations. I. General Formalisms for Primary and Secondary Extinction and Their Application to Spherical Crystals. *Acta Crystallogr., Sect. A: Found. Crystallogr.* **30** 129 (1974).
- [18] P. J. BECKER AND P. COPPENS. Extinction within the Limit of Validity of the Darwin Transfer Equations. II. Refinement of Extinction in Spherical Crystals of SrFz and LiF. *Acta Crystallogr., Sect. A: Found. Crystallogr.* **30** 148 (1974).
- [19] P. J. BECKER AND P. COPPENS. Extinction within the Limit of Validity of the Darwin Transfer Equations. III. Non-Spherical Crystals and Anisotropy of Extinction. *Acta Crystallogr., Sect. A: Found. Crystallogr.* **31** 417 (1975).
- [20] P. J. BROWN. Spherical Neutron Polarimetry. *In* Neutron Scattering from Magnetic Materials, edited by T. CHATTERJI, chap. 5, p. 215 (Elsevier, 2006).
- [21] A. HOLLADAY, P. LEUNG AND P. COPPENS. Generalized Relations Between d-Orbital Occupancies of Transition-Metal Atoms and Electron-Density Multipole Population Parameters from X-ray Diffraction Data. *Acta Crystallogr., Sect. A: Found. Crystallogr.* **39** 377 (1983).
- [22] W. R. BUSING AND H. A. LEVY. Angle Calculations for 3- and 4-Circle X-ray and Neutron Diffractometers. *Acta Crystallogr., Sect. A: Found. Crystallogr.* **22** 457 (1967).
- [23] C. WILKINSON, H. W. KHAMIS, R. F. D. STANSFIELD AND G. J. MCINTYRE. Integration of single-crystal reflections using area multidetectors. *J. Appl. Cryst.* **21** 471 (1988).
- [24] H.-C. HU, C. YANG AND K. ZHAO. Absorption correction A^* for cylindrical and spherical samples with extended range and high accuracy calculated by the Thorkildsen and Larsen analytical method. *Acta Crystallogr., Sect. A: Found. Crystallogr.* **68** 778 (2012).

-
- [25] J. A. K. HOWARD, O. JOHNSON, A. J. SCHULTZ AND A. M. STRINGER. Determination of the Neutron Absorption Cross Section for Hydrogen as a function of Wavelength with a Pulsed Neutron Source. *J. Appl. Cryst.* **20** 120 (1987).
- [26] W. R. BUSING AND H. A. LEVY. High-Speed Computation of the Absorption Correction for Single Crystal Diffraction Measurements. *Acta. Crystallogr.* **10** 180 (1957).
- [27] A. N. LOWAN, N. DAVIDS AND A. LEVENSON. Table of the zeros of the Legendre polynomials of order 1-16 and the weight coefficients for Gauss' mechanical quadrature formula. *Bull. Amer. Math. Soc.* **48** 739 (1942).
- [28] K. MOMMA AND F. IZUMI. VESTA 3 for three-dimensional visualization of crystal, volumetric and morphology data. *J. Appl. Cryst.* **44** 1272 (2011).
- [29] J. M. PEREZ-MATO, J. L. RIBEIRO, V. PETRICEK AND M. I. AROYO. Magnetic superspace groups and symmetry constraints in incommensurate magnetic phases. *J. Phys.: Condens. Matter* **24** 163 (2012). doi:10.1088/0953-8984/24/16/163201.
- [30] J. M. PEREZ-MATO, S. V. GALLEGO, E. S. TASCI, L. ELCORO, G. DE LA FLOR AND M. I. AROYO. Symmetry-Based Computational Tools for Magnetic Crystallography. *Annu. Rev. Mater. Res.* **45** 217 (2015). doi:10.1146/annurev-matsci-070214-021008.
- [31] N. NETO. Irreducible Representations of Space Groups. *Acta Crystallogr., Sect. A: Found. Crystallogr.* **29** 464 (1973).
- [32] H. T. STOKES, B. J. CAMPBELL AND R. CORDES. Tabulation of Irreducible Representations of the Crystallographic Space Groups and Their Superspace Extensions. *Acta Crystallogr., Sect. A: Found. Crystallogr.* **69** 388 (2013).
- [33] A. P. CRACKNELL, B. L. DAVIES, S. C. MILLER AND W. F. LOVE. General Introduction and Tables of Irreducible Representations of Space Groups. *In* Kronecker Product Tables. Vol. 1 (New York:IFI/Plenum, 1979).
- [34] J. A. M. PADDISON, J. R. STEWART AND A. L. GOODWIN. Spinvert: A program for refinement of paramagnetic diffuse scattering data. *J. Phys.: Condens. Matter* **25** 454220 (2013).
- [35] D. LOUËR AND R. VARGAS. Indexation Automatique des Diagrammes de Poudre par Dichotomies Successives. *J. Appl. Cryst.* **15** 542 (1982).
- [36] A. BOULTIF AND D. LOUËR. Indexing of Powder Diffraction Patterns for Low-Symmetry Lattices by the Successive Dichotomy Method. *J. Appl. Cryst.* **24** 987 (1991).

- [37] A. BOULTIF AND D. LOUËR. Powder pattern indexing with the dichotomy method. *J. Appl. Cryst.* **37** 724 (2004). doi:10.1107/S0021889804014876.
- [38] I. KRIVÝ AND B. GRUBER. A Unified Algorithm for Determining the Reduced (Niggli) Cell. *Acta Crystallogr., Sect. A: Found. Crystallogr.* **32** 297 (1976).
- [39] A. ALTOMARE, C. CUOCCI, A. MOLITERNI AND R. RIZZI. Indexing a powder diffraction pattern. In *International Tables for Crystallography*, vol. H, chap. 3.4, p. 270 (2019).
- [40] O. SCHÄRPF. Polarization elements. In *Lecture Notes on Polarized Neutron Scattering*, edited by T. BRÜCKEL AND W. SCHWEIKA, vol. 12 (Schriften des Forschungszentrum Jülich, Series Matter and Materials, 2002).
- [41] N. K. HANSEN AND P. COPPENS. Testing Aspherical Atom Refinements on Small-Molecule Data Sets. *Acta Crystallogr., Sect. A: Found. Crystallogr.* **34** 909 (1978).
- [42] J. R. MICHAEL AND A. VOLKOV. Density- and wavefunction-normalized Cartesian spherical harmonics for $l \leq 20$. *Acta Crystallogr., Sect. A: Found. Crystallogr.* **71** 245 (2015).
- [43] B. A. FRANSEN, X. YANG AND S. J. L. BILLINGE. Magnetic pair distribution function analysis of local magnetic correlations. *Acta Crystallogr., Sect. A: Found. Crystallogr.* **70** 3 (2013).
- [44] N. N. LOBANOV AND L. ALTE DA VEIGA. Abstract P12-16. In *6th European Powder Diffraction Conference* (1998).
- [45] T. M. SABINE, R. B. VON DREELE AND J.-E. JØRGENSEN. Extinction in time-of-flight neutron powder diffractometry. *Acta Crystallogr., Sect. A: Found. Crystallogr.* **44** 374 (1988).
- [46] L. W. FINGER, D. E. COX AND A. P. JEPHCOAT. A Correction for Powder Diffraction Peak Asymmetry due to Axial Divergence. *J. Appl. Cryst.* **27** 892 (1994).
- [47] J. R. HESTER. Improved asymmetric peak parameter refinement. *J. Appl. Cryst.* **46** 1219 (2013).
- [48] T. H. DE KEIJSER, J. I. LANGFORD, E. J. MITTEMEIJER AND A. B. P. VOGELS. Use of the Voigt function in a single-line method for the analysis of X-ray diffraction line broadening. *J. Appl. Cryst.* **15** 308 (1982). doi:10.1107/S0021889882012035.